Local mRNA translation in the regulation of neurite outgrowth

Inauguraldissertation

zur

Erlangung der Würde eines Doktors der Philosophie

vorgelegt der

Philosophisch-Naturwissenschaftlichen Fakultät

der Universität Basel

von

Daniel Feltrin

aus Italien

Basel, 2012

Genehmigt von der Philosophisch-Naturwissenschaftlichen Fakultät auf Antrag von:

Prof. Dr. Olivier Pertz

Prof. Dr. Markus Rüegg

Prof. Dr. Gerhard Christofori

Basel, den 13.12.2011

Prof. Dr. Martin Spiess

Dekan

2. Abstract

Local mRNA translation allows to synthesize proteins in discrete subcellular locations upon induction by various stimuli, therefore contributing to the control of gene expression in space and in time. The possibility to rapidly produce big amounts of proteins from few molecules of localized transcripts makes this mechanism extremely cost-efficient, since it avoids the long-distance transport of proteins (Schuman 1999). This is important especially in neurons, where local translation has been shown to be involved in the control of synaptic plasticity and axonal guidance (Skup 2008) (Leung, van Horck et al. 2006). Nevertheless, it has never been studied during the early phases of neuronal polarization, before the axon/dendrite specification step.

In N1E-115 cells, a neuron-like cell line that mimics the early stages of differentiation, we identified 80 mRNAs that are enriched in neurites compared to cell bodies by a genome-wide gene CHIP analysis. This suggests that also at these stages, targeting of transcripts to specific subcellular regions can play a role in cell morphogenesis. One of the detected messengers encodes MKK7, a MAP kinase kinase that directly activates the c-JUN NH2-terminal kinases (JNKs). We showed that the 3'UTRs of *MKK7* mRNA target the transcript specifically to the growth cone. Here local synthesis of the protein allows the formation of a zone of activated, phosphorylated MKK7 that is confined to the neurite shaft. Depletion of MKK7 by siRNA leads to instable neurite extension, due to defects in microtubule bundling at the base of the neurites.

With a bioinformatic analysis of the published proteome of the N1E-115 cell line (Pertz, Wang et al. 2008) we built an MKK7-centered interactome, which includes MAPKKKs (the upstream kinase of MKK7), MKKs, JNKs, microtubule associated proteins (the effectors of JNKs), scaffold proteins and phosphatases. Immunofluorescence analysis for the localization of the components of the network, combined with knock down experiments allowed us to identify a specific signaling module consisting of DLK, MKK7, JNK1 and MAP1B that regulates microtubule bundling in the neurite shaft and promotes neurite extension. FRET experiments using an activity probe for JNK further confirmed the involvement of JNK in the neurite shaft. Moreover, with immunofluorescence experiments we demonstrated the localization of the JNK signaling module also in mice E15 hippocampal primary neurons.

This thesis proposes a mechanism by which local translation of *MKK7* mRNA in the growth cone enables the activation of a specific branch of the JNK signaling pathway to regulate neurite extension. Therefore, local protein synthesis allows the spatio-temporal control of gene expression during early stages of neuronal differentiation.

3. Introduction

3. Introduction

3.1. The Cytoskeleton

3.1.1. The cytoskeleton: Actin, Intermediate Filaments and Microtubules

The ability of eukaryotic cells to adopt a variety of shapes and to carry out coordinated and directed movements depends on the cytoskeleton, a complex network of protein filaments that extend throughout the cytoplasm. The cytoskeleton is also directly responsible for particular movements, such as crawling of cells on a substrate, muscle contraction and the many changes in shape of a developing vertebrate embryo. In addition, the cytoskeleton provides structures for the intracellular transport of organelles.

The different activities of the cytoskeleton depend on only three principal types of filaments: actin filaments (microfilaments), microtubules and intermediate filaments. These filaments are assembled from monomers in cable-like structures that, upon interaction with a number of associated proteins, can form a variety of cellular architectures and complex tridimensional networks.

3.1.1.a. Actin

The most abundant protein in many eukaryotic cells, often constituting the 5% or more of the total cell protein, is actin. Most organisms have six principal isoforms, four of which are found in different types of muscles and the other two (β and γ) in all non-muscle cells.

50% of the actin molecules in a cell is present in an unpolymerized state, as free monomers (G-actin) or in small complexes with other proteins. Actin monomers can be assembled in two different structures: microfilaments, one of the three major components of the cytoskeleton, and thin filaments, which are part of the contractile apparatus in muscle cells. Thus, actin participates in many important cellular processes including muscle contraction, cell motility, cell division and cytokinesis, vesicle and organelle movement, cell signaling, and the establishment and maintenance of cell junctions and cell shape. In solution, filament assembly starts when an actin dimer forms spontaneously, in a process called nucleation, and allows the stable addition of further monomers. The rate of assembly of actin microfilaments depends on the concentration of free monomers: once a critical threshold concentration has been exceeded, assembly of the filament is favored . Actin monomers are added to a growing filament always in the same orientation, conferring a polarity to the microfilament. Although the monomers can be added on both the plus- (the fast growing end) and the minus end of the filaments, the rate of assembly is higher at the plus end and it

depends on a conformational change that is induced after the addition of the monomers (Carlsson 2010). At the plus end, once monomers are added, an ATP cap is formed, in which all the molecules have linked ATP. But actin is an ATPase and therefore, behind the cap, there is a progressive increase in the proportion of actin-ADP toward the minus end of the filament. The hydrolysis of ATP to ADP causes the actin to be less stable in the filament and so more prone to be removed. In an ideal equilibrium it would be possible to observe the so-called treadmilling phenomenon, where the removal of an ADP-actin molecule from the minus end is perfectly balanced by the addition of an ATP-actin monomer to the plus end (Figure 1) (Carlsson 2010).

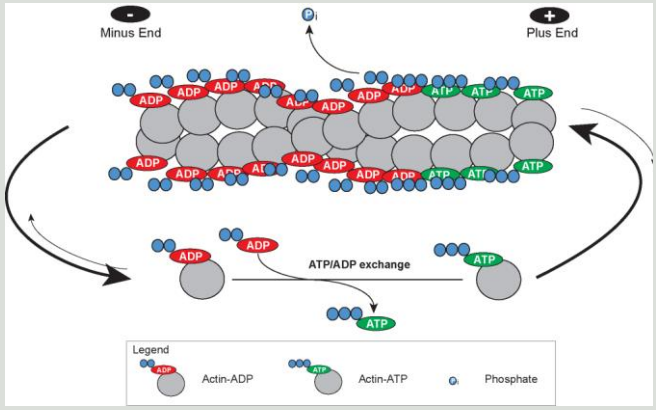

Figure 1. Actin Polymerisation process.monomeric β-Actin is sequestered by profilin in the cytosol where it gets loaded with ATP. Upon release from profiln, ATP-Actin is added at the fast growing end of the filament (Plus end). Inside the filament, ATP is hydrolized to ADP inducing the weakening of Actin binding. At the minus end ADP-actin falls off, feeding the treadmilling process. Capping proteins can block polymerisation at the plus end and induce actin filament shrinking and depolymerisation.

The functions of actin in a cell are mostly regulated by actin binding proteins. Capping proteins can bind the ends of actin filaments. Different capping proteins may either stabilize an actin filament or promote disassembly. They may have a role in determining filament length. For example: Tropomodulins cap the minus end, preventing dissociation of actin monomers (Cooper and Schafer 2000). CapZ capping protein binds to the plus end, inhibiting polymerization. If actin monomers continue to dissociate from the minus end, the actin filament will shrink (Xu, Casella et al. 1999).

Cross-linking proteins can organize actin filaments into bundles or networks. Some actin-binding proteins such as α-actinin, villin and fimbrin bind actin filaments into parallel bundles. Depending on the length of a cross-linking protein, or the distance between actin-binding domains, actin filaments in parallel bundles may be held in proximity or may be located far apart enough to allow interaction with other proteins, such as myosins. Filamins dimerize,

through antiparallel association of their C-terminal domains, to form V-shaped cross-linking proteins that have a flexible shape due to hinge regions (Cantiello 1997).

Actin can be found, polymerized, in several distinct structures: filopodia, microvilli, lamellipodia, stress fibers, cell cortex, in the contractile ring during cytokinesis and even in the nucleus where it seems to regulate transcription (Miyamoto, Pasque et al. 2011).
The regulation of assembly and disassembly of the actin cytoskeleton is very complex. Gelsolin severs actin filaments and caps them, blocking their regrowth (David J 1999). Cofilin binds to actin-ADP along the filaments and severs them and, like Twinfilin, it sequesters actin monomers in the cytoplasm, inhibiting polymerization (Cooper and Schafer 2000). Also Thymosin b4 sequesters G-actin, buffering the free G-actin in the cytosol. Finally Profilin binds the plus end of the microfilaments increasing ATP/ADP exchange and promoting depolymerization (Husson, Cantrelle et al. 2010).

3.1.1.b. Intermediate Filaments

Intermediate filaments (IF) are tough and durable protein fibers in the cytosol of most higher eukaryotic cells. Built like spinned ropes, they are typically 8-10 nm in diameter, which is “intermediate” between the thin and the thick filaments in muscle cells, where they were first discovered. In most cells IF form a basket around the nucleus and extend out, toward the cell periphery. They are particularly important in those cell types that are subjected to mechanical stress, such as in epithelia, where IF are linked intercellularly at the desmosomal junctions. They are also important in axons and throughout the cytoplasm of smooth muscle cells.

Unlike actin, the subunits of the IF are fibrous proteins that associate side by side in overlapping arrays to form long filaments with high tensile strength and they do not have an intrinsic polarity. The filaments are composed of polypeptides of a surprisingly wide range of sizes (form about 40000 to 130000 Daltons) which depend on the cell type. IF are classified in four broad classes, depending on their amino acid sequence (Figure 2) (Hermann H 1998).

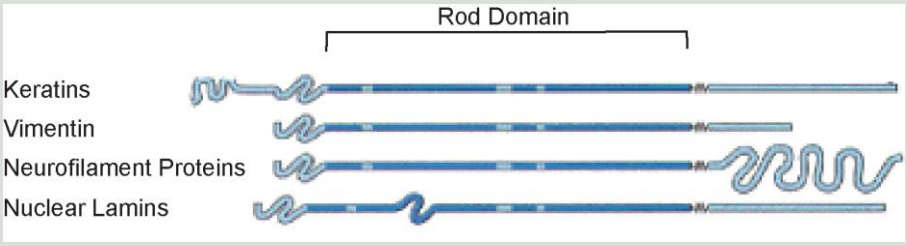

Figure 2. Classes of intermediate filamentsv(IF) proteins.IF proteins are divided in four classes and can form homo- or heteropolymers. Adapted from "The Cell: a Molecular Approach", 2nd edition, Cooper GM, 2000

The first stage of filament assembly is the formation of dimers in which the central rod domains of two polypeptide chains are wound around each other in a coiled-coil structure (Figure 3). The dimers then associate in an antiparallel fashion to form tetramers, which can assemble end to end to form protofilaments. The final intermediate filament contains approximately eight protofilaments wound around each other in a rope-like structure. Because they are assembled from antiparallel tetramers, both ends of IF are equivalent (Robert G 2007). Filament assembly requires interactions between specific types of intermediate filament proteins. IF are generally more stable than actin filaments or microtubules and do not exhibit the dynamic behavior associated with these other elements of the cytoskeleton. However, intermediate filament proteins are frequently modified by phosphorylation, which can regulate their assembly and disassembly within the cell. The clearest example is phosphorylation of the nuclear lamins, which results in disassembly of the nuclear lamina and breakdown of the nuclear envelope during mitosis (Pierre 2002). Cytoplasmic IF, such as vimentin, are also phosphorylated at mitosis, which can lead to their disassembly and reorganization in dividing cells (Pierre 2002).

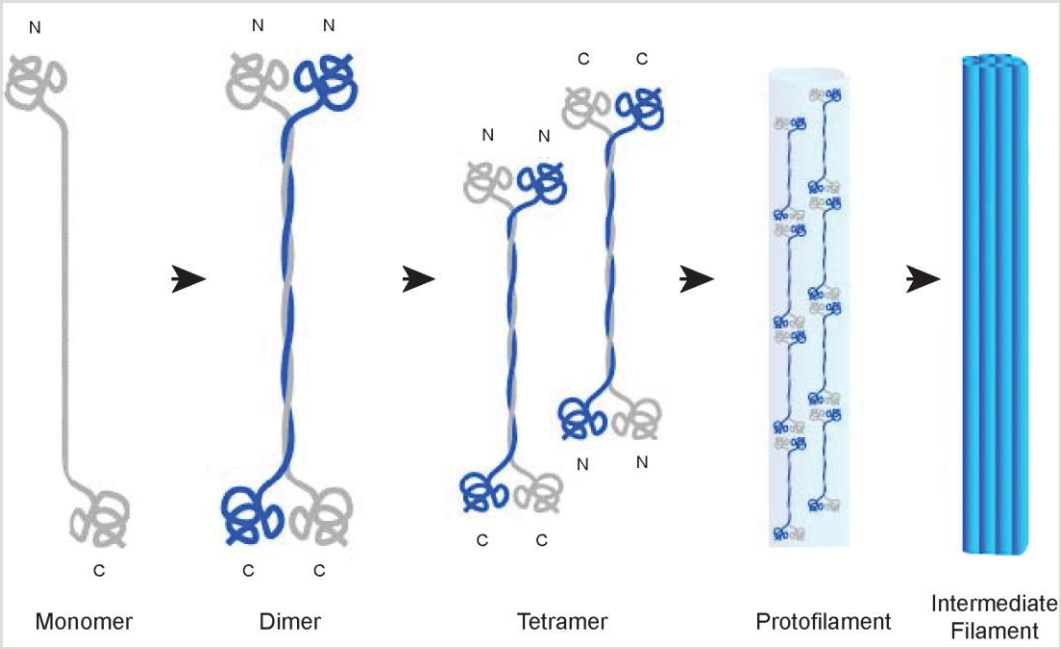

Figure 3. IF polymerization. Two IF interact through their central rod domain, wounding around each other in rope-like structure. Two dimers can associate in an antiparallel manner to form tetramers. Tetramers interact end to end and form a protofilament. Approximately eight protofilaments get assembled in an intermediate filament. Adapted from: wikispaces.psu.edu/display/Biol230WCE/The+Cytoskeleton

Although IF have for long been thought to provide structural support to the cell, direct evidence for their function has only recently been obtained. Some cells in culture make no intermediate filament proteins, indicating that these proteins are not required for the growth of cells *in vitro*. Similarly, injection of cultured cells with antibody against vimentin disrupts intermediate filament networks without affecting cell growth or movement. Therefore, it has been thought that IF are most needed to strengthen the cytoskeleton of cells in the tissues of multicellular organisms, where they are subjected to a variety of mechanical stresses that do not affect cells in the isolated environment of a culture dish (Cooper 2000).

3.1.1.c. Microtubules

Microtubules, the third principal component of the cytoskeleton, are “cables” with a diameter of about 25 nm. Like actin filaments, microtubules are dynamic structures that undergo continual assembly and disassembly within the cell. They function both to influence cell shape and are involved in a variety of cell movements, including some forms of cell locomotion, the intracellular transport of organelles and the separation of chromosomes during mitosis.

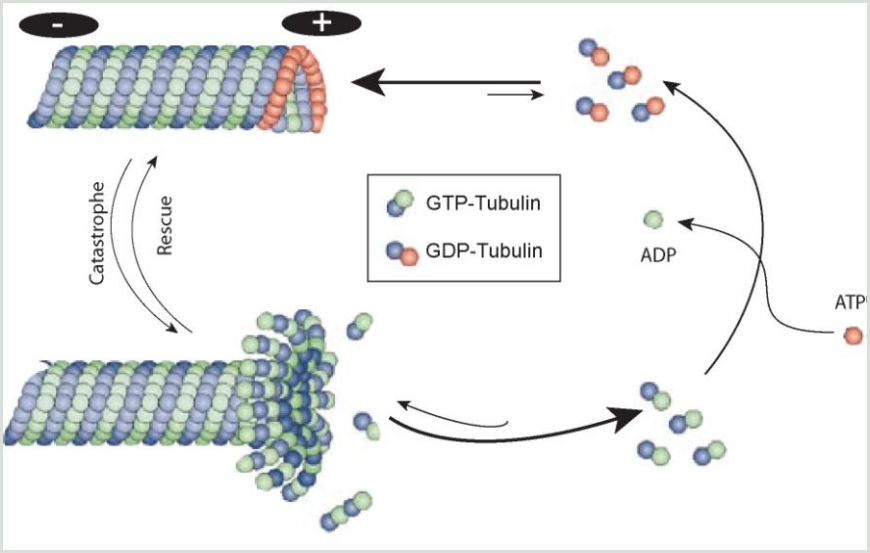

Figure 4. Microtubule dynamics. Microtubules are highly dynamic structures. α- and β-tubulin form dimers in the cytosol. When they are loaded with GTP they can be added to the fast growing end (plus end) of a microtubule. Inside the microtubule, GTP gets hydrolyzed to GDP and induces release of the dimer. This process is called treadmilling. Adapted from Cheeseman IM & Desai A (Cheeseman and Desai 2008).

In contrast to IF, which are composed of a variety of different fibrous proteins, microtubules are composed of a single type of globular protein, called tubulin. Tubulin is a dimer consisting of two closely related 55-kd polypeptides, α-tubulin and β-tubulin that have intrinsic GTPase activity (Wang, Cormier et al. 2007). Both α- and β-tubulin are encoded by small families of related genes. In addition, a third type of tubulin (γ-tubulin) is specifically localized at the centrosome, where it plays a critical role in initiating microtubule assembly.

Tubulin dimers polymerize to form microtubules, which generally consist of 13 linear protofilaments assembled around a hollow core. The protofilaments, which are composed of head-to-tail arrays of tubulin dimers, are arranged in parallel. Consequently, microtubules (like actin filaments) are polar structures with two distinct ends: a fast-growing plus end and a slow-growing minus end (Figure 4). This polarity is an important consideration in determining the direction of movement along microtubules, just as the polarity of actin filaments defines the direction of myosin movement (Heald and Nogales 2002).

Tubulin dimers can depolymerize as well as polymerize, and microtubules can undergo rapid cycles of assembly and disassembly. Both α- and β-tubulin bind GTP, which functions analogously to the ATP bound to actin to regulate polymerization. In particular, the GTP bound to β-tubulin (though not to be bound to α-tubulin) is hydrolyzed to GDP during or shortly after polymerization. This GTP hydrolysis weakens the binding affinity of tubulin for adjacent molecules, thereby favoring depolymerization and resulting in the dynamic behavior

of microtubules. Like actin filaments, microtubules undergo treadmilling, a dynamic behavior in which tubulin molecules bound to GDP are continually lost from the minus end and replaced by the addition of tubulin molecules bound to GTP to the plus end of the same microtubule. Therefore, in microtubules, GTP hydrolysis results in the behavior known as dynamic instability, in which individual microtubules alternate between cycles of growth and shrinkage. Whether a microtubule grows or shrinks is determined by the rate of tubulin addition relative to the rate of GTP hydrolysis. As long as new GTP-bound tubulin molecules are added more rapidly than GTP is hydrolyzed, the microtubule retains a GTP cap at its plus end and microtubule growth continues. However, if the rate of polymerization slows down, the GTP bound to tubulin at the plus end of the microtubule will be hydrolyzed to GDP. If this occurs, the GDP-bound tubulin will dissociate, resulting in rapid depolymerization and shrinkage of the microtubule (Heald and Nogales 2002).

Dynamic instability, described by Tim Mitchison and Marc Kirschner in 1984, results in the continual and rapid turnover of most microtubules, which have half-lives of only several minutes within the cell (Mitchison and Kirschner 1984). As discussed later, this rapid turnover of microtubules is particularly critical for the remodeling of the cytoskeleton that occurs during mitosis. Because of the central role of microtubules in mitosis, drugs that affect microtubule assembly are useful not only as experimental tools in cell biology but also in the treatment of cancer. Colchicine and colcemid are examples of commonly used experimental drugs that bind tubulin and inhibit microtubule polymerization, which in turn blocks mitosis.

3.1.2. Regulation of microtubules: the microtubule-associated proteins (MAPs)

The dynamic instability of the microtubules can be influenced during several cell actions by different kinds of proteins that are found all along the microtubules and are called microtubule-associated proteins (MAPs) (Figure 5). These molecules, that can stabilize or destabilize microtubules, have repeated domains that allow each MAP to associate with more than one tubulin dimer. The binding of MAPs to several dimers, allows both to stabilize the subunits inside the same structure and also to crosslink different microtubules. Their binding and their activity are generally controlled by phosphorylation/dephosphorylation of MAPs by kinases and phosphatases respectively (Cassimeris L 2001). Beside microtubule stabilizers, destabilizers are required for the disassembly of microtubules in particular cell states. Typical examples of processes that require microtubule stabilization or destabilization

are the interphase during mitosis, axonal guidance and dendrites formation during neuronal development and synaptic plasticity in mature neurons.

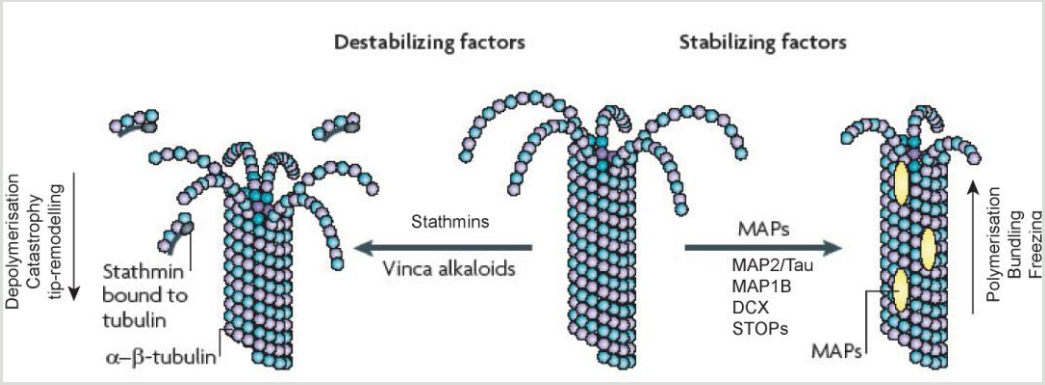

Figure 5. MAPs regulate microtubule dynamics. Stabilizing factors can bind α- β tubulin dimers inside the same structure, stabilizing microtubules, or in 2 different microtubules acting as bridges and inducing bundling. Stathmins, Katanins and other regulators can induces the collapse of the microtubules, important for the remodeling of the cytoskeleton. Adapted from Kavallaris M, 2010 (Kavallaris 2010).

Several MAPs have been identified and they have been grouped in three different classes: (1) structural MAPs; (2) microtubule destabilizers, (3) proteins that control microtubule location (Amos and Schlieper 2005).

3.1.2.a. Structural MAPs

The proteins that are part of the structural MAPs are: the Tau family, MAP1A and MAP1B, the STOPs, and Doublecortin (DCX).

The Tau family

Four main proteins are part of this family. MAP2 is concentrated in dendrites, whereas Tau is axonal; MAP4 is a high molecular weight protein present in many non neuronal mammalian cells; XMAP230 is similar to MAP4 and has been found in *Xenopous Laevis*. In addition, many homologous proteins have been found in invertebrates. All these proteins are apparently lacking a well defined secondary structure, but are unusually heat-stable; they all have a microtubule binding site that contains one to five semiconserved motifs, followed by an N-terminal projection domain that extends from the microtubules, when they are bound to them. This projecting domain seems to be a repellent agent for other microtubules, rather than a cross-linking factor; however the domain can bind other proteins, including actin for a cross-talk of actin and microtubule cytoskeleton. It seems that these MAPs favour the

movement of motors (Chen, Kanai et al. 1992) and overexpression leads to a saturation of the microtubules and inhibits motor movements (Ackmann, Wiech et al. 2000).

The proteins belonging to this class of MAPs seem to be able to stabilize microtubule in several ways. The primary stabilization way consists in the filling of β-tubulin pockets. This filling allows the stabilization of lateral contacts between protofilaments (Nogales, Whittaker et al. 1999) (Li, Finley et al. 2002), but also the straight protofilament conformation, inhibiting the GTP hydrolysis (Amos and Löwe 1999). In addition to this mechanism, thanks to loops that are repeated in the repeat domain and that occupy the β-tubulin pockets, these MAPs can bind three to four tubulin dimers at the same time, probably in adjacent filaments (Kar, Fan et al. 2003). Moreover, the molecules have other domains that almost certainly bind well to the outer surface of the microtubule and probably run along a protofilament covering several tubulin dimers (Kar, Florence et al. 2003).

In conclusion the proteins belonging to this class of MAPs favor the straight heterodimer confirmation and hold microtubules together (Amos and Schlieper 2005).

MAP1A and MAP1B

The two closely related neuronal MAPs, MAP1A and MAP1B are highly extended and appear to be unstructured in solution. Only little has been published about their structure, but it seems evident that the several short basic repeated motifs in their microtubule-binding domain interact with the negatively charged outer surface of the microtubules. MAP1A has been shown to increase nucleation and to stimulate microtubule elongation, but it's less effective than other MAPs in stabilizing the structure (Vaillant, Müller et al. 1998). MAP1B can apparently replace Tau *in vivo*, since knockout mice for one or the other gene are viable. However, mice die if both MAPs are missing (Takei, Teng et al. 2000). No obvious relationship has been shown between the microtubule binding site of MAP1A/B and MAP2/Tau and the mechanism of microtubule stabilization of these two MAPs has not been described.

STOPs

The class of MAPs called Stable tubules only polypeptides (STOPs) is responsible for the resistance of microtubules to cold. These proteins are calmodulin-binding and calmodulin-regulated proteins that use the same binding site for the binding of microtubules and of calmodulin. This binding site is different from the one of MAP2 and Tau but seems to be able to fold up as a sharp loop and bind the pocket in the β-tubulin. The synaptic defects and the

abnormal behavior of *stop* knockout mice suggests an additional role than only microtubules stabilization for these proteins in neuronal cells (Bosc, Andrieux et al. 2003).

Doublecortin (DCX)

Mutations in the *dcx* gene lead to brain development disorders that can include the formation in the brain of a "double cortex", due to an additional band of ectopic, aberrant neurons. DCX has a 30 kDa N-terminal domain that can bind microtubules and stabilize them *in vitro*. It is able to enhance tubulin polymerization and it seems also to induce microtubules bundling, due to the presence of a tandem repeat of DCX-domains in the microtubule binding site. This results in the cross-link of two tubulin subunits either in the same or in different microtubules. DCX is the only MAP, together with Tau and MAP2c, to have been studied by 3D analysis of electron microscopy images (Kar, Fan et al. 2003). The two DCX-domains of doublecortin seem to have different properties: whereas the N-terminal DCX domain can only bind to microtubules, the C-terminal one binds to both microtubules and soluble tubulin dimers, suggesting a dual role of DCX, along the microtubules and at the microtubule end (Kim, Cierpicki et al. 2003).

3.1.2.b. Microtubule Destabilizers

In contrast to structural MAPS, microtubule destabilizers favor microtubule catastrophe. Member of this class of MAPs are: Stathmins, Katanin, Kinesins and regulators, and MINUS.

Stathmins

The stathmins are tubulin-sequestering proteins that have been crystallized with tubulin (Gigant, Curmi et al. 2000) (Ravelli, Gigant et al. 2004). Stathmin interacts with two molecules of dimeric α,β-tubulin to form a ternary complex called the T2S complex. Thus, tubulin gets sequestered and becomes non-polymerizable. Without polymerization, the microtubules cannot be further assembled and are prone to disassemble. Phosphorylation of Stathmins causes weakened stathmin-tubulin binding and therefore microtubules stabilization (V Doye 1992).

Katanin

Katanin is a member of the AAA superfamily (ATPases associated with different cellular activities) and is a heterodimer of 60 and 80 kDa subunits. In the presence of ATP and

microtubules, Katanin can form a transient hexadimer that is capable of destroying contacts between αβ-tubulin heterodimers. As a result, the microtubules are severed in small pieces (Baas and Buster 2004). Katanin might be regulated by different mechanisms, one of which would involve the competition of other MAPs for the same binding sites on the microtubules (McNally, Buster et al. 2002).

Kinesins and regulators

Kinesins are mainly known as motors that are able to transport cargos along the microtubules. Nevertheless, many members of this family of proteins are able to regulate microtubule dynamics. The kinesin-13 (Kin-I) subfamily uses energy provided by ATP to depolymerize microtubules at their end (Desai, Verma et al. 1999). The binding of ATP to Kin-I attached to a tubulin dimer causes the tip of the microtubule to bend and the protofilament to roll up. After ATP hydrolysis to ADP, the motor domain of the kinesin dissociate from the filament. Also other kinesins that act as normal motor proteins seem to be involved in the control of the length of the microtubules. The minus-end-directed kinesin Ncd has been shown to shorten microtubules *in vitro* (S A Endow 1994). Finally, several kinesin members have microtubule binding sites that are separated from the motor domain and lead to cross-bridging of microtubules. MKLP1, for example, can bundle and slide antiparallel microtubules apart. MLKP1 has been proposed to be an important component of the mitotic spindle during anaphase, when microtubules get cross-bridged at the midzone and are pushed apart to form the spindle (Inoue, Savoian et al. 2004)

MINUS

Microtubule nucleation suppressor (MINUS) is a small acidic polypeptide that has been shown to suppress nucleation *in vitro*. Minus has been shown to be able to suppress taxol- and tau-mediated microtubule assembly in vitro and is inactivated by phosphorylation. MINUS appears to be able to control microtubule length by blocking nucleation, rather than inducing depolimerization or microtubule collapse (Fanara, Oback et al. 1999).

3.1.2.c. Proteins that control microtubule location

Apart from the classical MAPs described above, many other proteins can affect the behavior of microtubules, for example by guiding the plus end towards other proteins and structures and/or allowing the assembly of higher-order structures.

Growing microtubules use their dynamic instability to look for structures they can bind to, such as chromosomes or specialized membrane domains, and they are guided by the so

called plus-end tracking proteins (APC and EB1). CLIPs and CLASPs are two further plus-end tracking proteins that have first been demonstrated to be microtubule-membrane linkers (Kreis 1991), but they seem to be also able to bind along the microtubule.

To conclude, MAPs are directly responsible for the modulation of microtubule stability in cells. The problem of the extremely short half life of these cytoskeletal structures can be overtaken by the action of these proteins so that cellular structures can be formed and preserved. Nevertheless, the possibility to activate/deactivate MAPs and the concomitant action of MAPs with opposite functions can allow for a rapid disassembly of microtubules and a remodeling of the cytoskeleton.

3.1.2. Roles of MAPs in the regulation of neurite outgrowth

The early phases of neuronal differentiation are characterized by a process, called neurite outgrowth, which allows the generation of protrusions (the neurites) that are the precursors of axon and dendrites. These dynamic structures undergo cycles of protrusion-retraction before getting stabilized. It's only during axon specification that dendrites and axon mature and acquire the features that allow them to exert their functions. There is no doubt that microtubules are essential for neurite outgrowth and, therefore, full neurites cannot be generated in their absence. Microtubules seem to have a role already in the initiation of neurites, when they serve as tracks for the transport of specific signaling proteins or adhesion molecules towards the forming growth cone (Dehmelt and Halpain 2004). Later during the outgrowth, microtubules form parallel and antiparallel arrays, which may act as compression resistant supports inside neurites, especially when they are stabilized (Ingber 1993).

The proteins that are directly responsible for the stabilization of microtubules, the above mentioned MAPs, have been proposed to play an important role during neurite outgrowth (Figure 6) (González-Billault, Engelke et al. 2002). MAP2 and Tau stabilize the microtubules by reducing catastrophe events and therefore by promoting prolonged growth. In addition MAP2 has been proposed to induce microtubule rigidity, through induction of bundles formation, although clear experimental evidences have never been provided. Nevertheless, overexpression of MAP2c, a MAP2 isoform, in a non-neuronal cell line induces ectopic bundle formation (Takemura, Okabe et al. 1995). Surprisingly, single *map2* or *tau* knockout mice are viable and isolated neuroblasts from these animals form neurites and axons in culture (Harada, Oguchi et al. 1994) (Harada, Teng et al. 2002). When such knockouts are

crossed with mice lacking *map1b*, the resulting double knockouts display several sever defects in neurite outgrowth and neuronal migration in vivo, suggesting that some functions of MAP2/Tau are redundant with MAP1B (Teng, Takei et al. 2001).

Another class of MAPs has been shown to have a role in neurite outgrowth: the STOP proteins stabilize microtubules by blocking both polymerization and depolymerisation of the microtubules, therefore freezing them in the state they are. Experiments in PC12 cells (a neuronal-like cell line) suggest that they are important for the stabilization of already established microtubules, rather than for newly polymerized ones (Dehmelt and Halpain 2004).

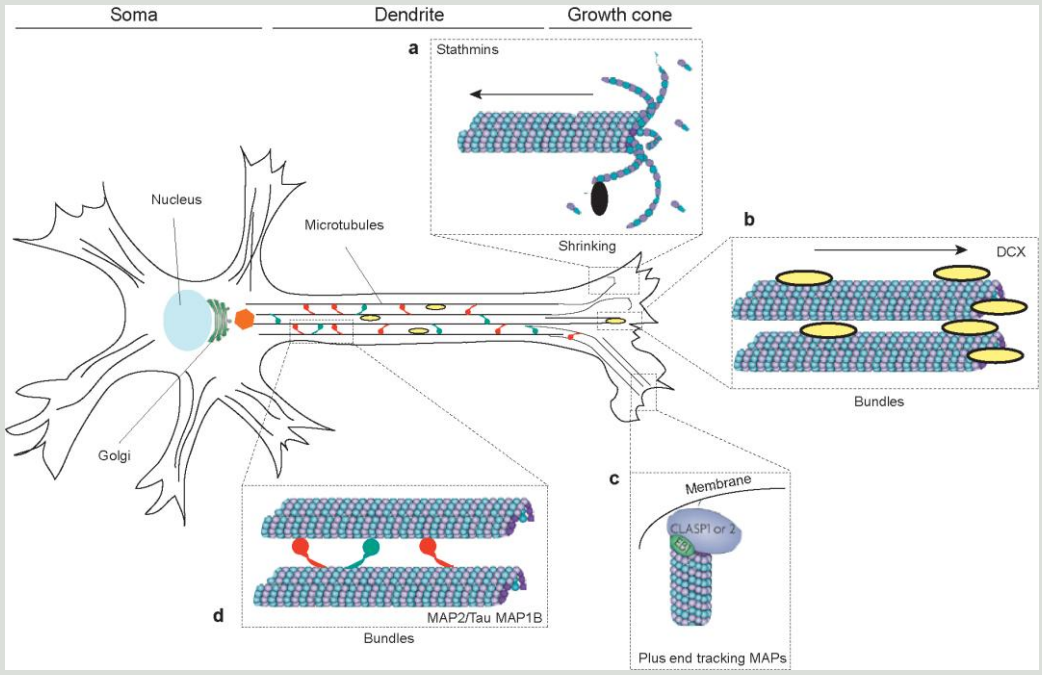

Figure 6. Roles of MAPs in neurite outgrowth. MAPs influence neurite outgrowth in different fashions; a) stathmins induce release of tubulin dimers from the plus end of the microtubules inducing them to shrink. b) DCX allows bundling of the microtubules, but can also bind at tip end of microtubules, stabilizing them. c) plus end tracking MAPs help to guide and anchor the microtubules to the membrane. d) MAP2/Tau and MAP1B bind all along the microtubules; they stabilize the filament itself and induce bundling of adjycent microtubules.

In contrast to the microtubule-stabilizing MAPs, Stathmins destabilize microtubules, favoring catastrophes. However, overepression of SCG10, a member of the stathmin family, strongly enhances neurite outgrowth (Grenningloh, Soehrman et al. 2004), whereas its down-regulation in PC12 cells inhibits NGF-induced differentiation (Di Paolo, Pellier et al. 1996).

The two studies assign a role to stathmins in remodeling of the tip of the microtubules in the growth cone rather than in the neurite shaft.

Finally, also DCX has been shown to be phosphorylated and activated mainly in the growth cone (Gdalyahu, Ghosh et al. 2004). But, unlike *scg10* knock-down cells, *dcx* depleted cells show impaired neurite outgrowth (Friocourt, Marcorelles et al. 2011). Maybe this is the result of the dual activity of DCX: in fact DCX can both bind all along the microtubules stabilizing them, and it can bind at the microtubule end, therefore in the growth cone, counteracting the activity of Stathmins.

There is no doubt that a cooperation of the different MAPs is required for a successful neurite outgrowth. Stabilization is required to confer rigidity to the body of the microtubule and destabilization, including catastrophe, is needed for the remodeling of the growth cone that is necessary for the complete maturation of the neurites and the highly dynamic behavior of growth cones.

3.2. Local mRNA translation

3.2.1. mRNA localization: biological functions

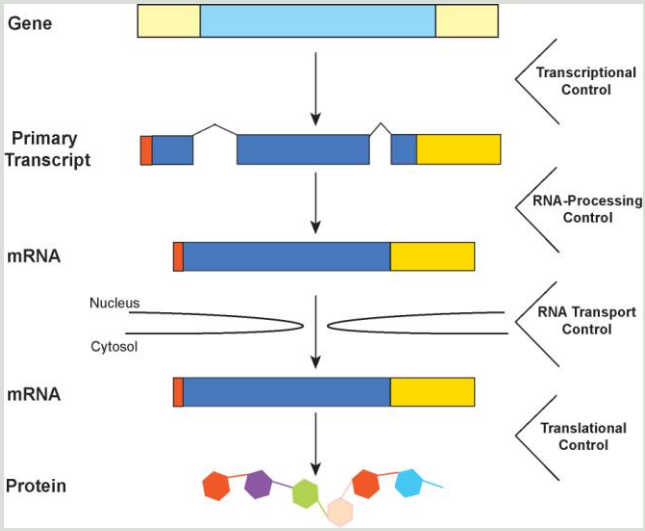

Figure 7.Regulation of gene expression. Gene expression can be regulated at different levels. Transcription, RNA processing, RNA transport and RNA translation can all be finely regulated at different subcellular locations.

Proteins constitute more than half the total dry mass of a cell and their synthesis depends on the collaboration of several classes of RNA molecules as well as of other proteins. It is a process that requires a number of preparatory steps and a fine regulation at different levels and in a fine tuned manner (Figure 7). In the nucleus the DNA has to be made accessible to the RNA polymerase. The transcription is regulated by the promoter and the participation of activators, enhancers or repressor. The primary transcript will then be processed and exported to the cytosol and its translation controlled, mostly at the level of initiation.

Over the last twenty years it became clear that also the targeting of mRNAs to specific subcellular location can contribute to the control of gene expression. But what is the purpose of localizing mRNAs?

One transcript can give rise to several proteins in a very short time, due to the capacity of several ribosomes to bind to the cap at the 5' of the mRNAs. Thus, localization and local translation of mRNA should be more cost-efficient than protein transport in case a high concentration of a protein is needed in a particular area of the cell (Du, Schmid et al. 2007).

Another reason why in some cases mRNAs rather than proteins are localized is that translation doesn't have to happen at any other place in the cell than at the target site. The most typical example is the myelin basic protein (MBP), a component of the myelin sheath of

oligodendrocytes that wraps around axons of the neurons (Boggs 2006). MBP is an intracellular molecule that interacts very strongly with membranes and causes them to compact. Unlike other components of myelin, which are exported to the myelinating cell processes by the secretory pathway, MBP is translated on free ribosomes from a localized mRNA (Trapp, Moench et al. 1987). It would be very difficult to transport the MBP from the cell body to the site of myelin formation, since MBP would stick to any membrane that it came into contact with along the way. In oligodendrocytes *MBP* mRNA, after being synthesized, is packed in granules and transported along the processes to the periphery, where it can be then again released and made available for translation (Ainger, Avossa et al. 1993). The localization of the mRNA in the periphery prevents the protein from compacting membranes in the main body of the cell.

mRNA localization might also be a useful mechanism for choosing the right isoform of a protein that can multimerize: different isoforms of a protein can be compartmentalized at different subcellular locations and the synthesis of one of them can be controlled in spatial way, allowing the translation of an already localized transcript, rather than acting on alternative splicing of the transcript in the nucleus. This might be important for example in the control of the composition of actin filaments in differentiating myoblasts: β-actin mRNA localizes to the leading lamellae at the cell periphery, whereas α- and γ-actin mRNA show a perinuclear distribution (Hill and Gunning 1993) (Kislauskis, Li et al. 1993).

Localization of mRNAs can also guarantee polarization of the cell or of a multicellular system. If the localization sequences of β-actin mRNA are mutated, both the transcript and the protein will not be correctly localized at the leading edge of lamellae anymore, causing the lamellae to collapse and inducing the cell to become symmetric. This demonstrates the importance of the localization of some transcripts for the maintenance of cell polarity (Kislauskis, Zhu et al. 1994). In addition, mRNA localization is known to preserve polarization during embryogenesis. in *Drosophila* embryos the main function of localized transcripts is to establish morphogenic gradients that guarantee the correct polarization of the embryo and allow the specification of the embryo body plans. However, localized mRNA also have other biological functions, like the segregation of cell-fate determinants (Hughes, Bullock et al. 2004) and the targeting of protein synthesis to specialized organelles or cellular domains (Adereth, Dammai et al. 2005)

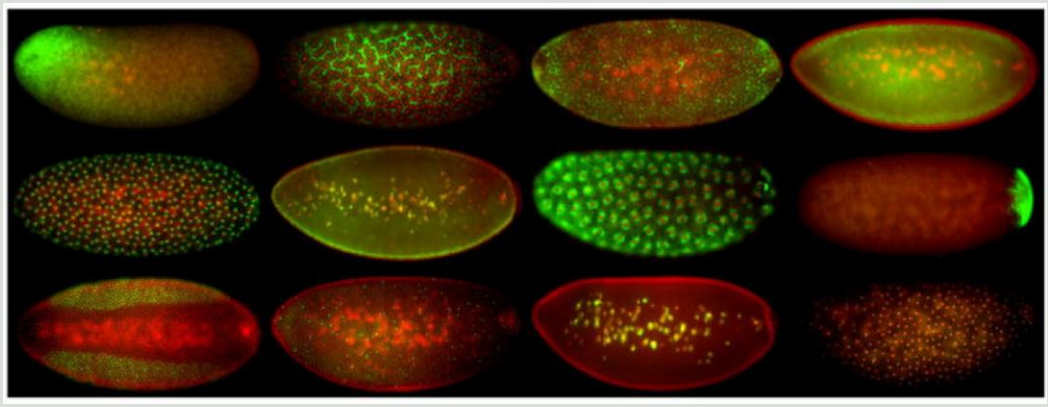

Figure 8. mRNA localization. A high-through put screening using fluorescent in-situ hybridization techniques showed that in Droshophila embryos, 71% of the analysed transcripts shows a stricking subcellular localization. Adapted from Martin KC, 2009 (Martin and Ephrussi 2009)

In a recent study involving high-throughput, high resolution fluorescent in-situ hybridizations in *Drosophila* embryos demonstrated that 71% of the over 3000 analyzed transcripts were expressed in spatially distinct patterns (Figure 8) (Lécuyer, Yoshida et al. 2007).

Finally, also neurobiologists are studying since many years the significance of mRNA localization and local translation in neurons. It looks clear that it might be very cost-efficient for a neuron to localize and locally translate an mRNA in one of its long processes, namely axon and dendrites, rather than to store big quantities of different proteins (in addition to the neurotransmitters for the transmission of an electric potential). Localization of mRNAs in dendrites and axons allows a rapid synthesis of needed proteins in response to various stimuli, avoiding transport-related delays and expenses (see sections 3.2.6 and 3.2.7) (Schuman 1999). During neuronal development, axonal growth cones are guided by external cues that induce local synthesis of cytoskeletal proteins or regulators. *β-Actin* mRNA, is locally translated in response to attractive cues (netrin-1) and allows the growth cone to turn toward the cue (Campbell and Holt 2001). C*ofilin*, instead, is locally produced in response to a repulsive stimulus (Slit-2), inducing the disassemble of actin filaments and therefore pushing the growth cone away from the cue (Wu, Hengst et al. 2005; Piper, Anderson et al. 2006). Semaphorin-3A is involved in the induction of growth cone collapse by triggering the local translation of *RhoA* mRNA (Wu, Hengst et al. 2005). Hundreds of transcripts have been shown to be enriched in the dendrites of mature neurons (Oyang, Davidson et al. 2011). Local and specific translation of a subset of these mRNAs can allow rapid and synapse-restricted response to neuronal stimulation (Sutton and Schuman 2006).

In conclusion, increasing evidence underlines more and more the importance of localization and local translation of mRNAs as a mechanism to regulate gene expression. This confirms that the control of translation in space and time is a rule rather than an exception.

3.2.2. How to localize an mRNA? The fate is in the 3'UTR

Eukaryotic mRNAs share common features that include exons, introns, a cap at the 5' and a stretch of adenines at the 3' end (polyA tail). In addition to these elements they are also characterized by the presence of 3' and 5' untranslated regions (UTRs). Most of the regulatory elements of a messenger are present in the UTRs of the transcripts, where they act as platforms for the recruitment and assembly of protein complexes to the mRNA, therefore generating the ribonucleoparticles (RNPs). In general, the two different untranslated regions have different regulatory responsibilities: if the 5'-UTR is primarly involved in the regulation of translation, the 3'-UTR regulates multiple aspects of mRNA metabolism, including nuclear export, translational efficiency, stability and cytoplasmatic localization. The discrete, asymmetrical localization of transcripts is determined, with very few exceptions, by *cis*-elements that are present in the 3'UTRs (Kislauskis and Singer 1992). In some cases only few nucleotides are sufficient to induce the right localization, in other cases, over 1 kb regions have been discovered and often clusters of elements can be detected. *Trans*-acting proteins can recognize either the nucleotidic sequence of the *cis*-elements or their secondary structure. Although many mRNAs have been extensively shown to be present in dense structures where they interact with proteins, only few *trans*-acting proteins have been identified and so also the *cis*-elements have been poorly described. The low degree of conservation between 3'UTRs and the huge variability of possible secondary structures has made the identification of localization elements very difficult. Experiments performed using vectors containing a *cis*-element cloned downstream of a transcript encoding a reporter gene, show that in most of the cases the localization elements are necessary and sufficient for the targeting of an mRNA. However, results are often difficult to interpret, considering that more localization elements can together contribute to the targeting and that also other elements in the 5'-UTRs or even in the coding sequence can have an influence on the function of the 3'-UTR. Nuclear and cytosolic remodeling of the untranslated regions can occur and can influence asymmetric mRNA localization.

One process that can lead to 3'-UTR remodeling is alternative splicing. More than 90% of human genes undergo alternative splicing (Wang, Sandberg et al. 2008) and, interestingly, the highest degree of transcript variability is in the alternative use of tandem 3'-UTRs and polyadenylation sites resulting in the generation of messengers containing either a short or a

long 3'-UTR. Several well-known splicing-related motifs were identified within untranslated regions of transcripts that also undergo polyadenylation. In 2008, *Wang et al.* (Wang, Sandberg et al. 2008), showed that consensus elements recognized by STAR splicing factors, which are splicing regulators implicated in germ line and muscle cells development, are also present in transcripts that are subject to polyadenylation. Furthermore a recent study showed that NOVA2, a member of NOVA proteins, neuron-specific splicing factors that control the alternative splicing of transcripts involved in neuronal survival, inhibitory synaptic transmission and plasticity, also seems to regulate alternative polyadenylation in the brain. 20% of the NOVA2-binding sites have been found in clusters located in 3'UTRs of messengers, where they cause promotion or inhibition of a specific polyA site. Alternative splicing is commonly considered to be a nuclear process; however, recent work shows that splicing factors can be found in isolated dendrites of hippocampal neurons (Glanzer, Miyashiro et al. 2005) indicating that this regulation also occurs in the cytosol.

Together, alternative splicing in the 3'UTR and polyadenylation seem to be directly responsible for the generation of transcripts with a long or a short 3'UTR (Timmusk, Palm et al. 1993), (Liu, Lu et al. 2006). Short or long 3'-UTRs are important for the asymmetric localization or the enrichment of transcript encoding different isoforms of the same protein (Lau, Irier et al. 2010) (An, Gharami et al. 2008).

3.2.3 Translational repression of localized mRNAs

To be localized in the cell, the mRNAs have not only to be transported, but also to be protected from translation. After nuclear export of the transcripts to the cytosol, *cis*-elements, mostly present in the untranslated regions of the mRNAs, are recognized by *trans*-acting factors, proteins that allow the formation of dense ribonucleoprotein complexes (RNPs). These complexes can be loaded on specific transport motors and at the same time sequestered from the translational machinery (Besse and Ephrussi 2008). RNPs formation starts already in the nucleus, but several dynamic remodelling steps are necessary for the completion of the assembly (Kress, Yoon et al. 2004). Proteomic analysis of RNA granules components have revealed that these structures contain a large number of proteins, including RNA-binding proteins that are known to be involved in the regulation of both the transport and the translation. Those RNA granules are well defined and specific, although they share some components with other structures, like the processing bodies (P bodies), general cytosolic sites for translational silencing. Some of the RNA-binding proteins are common in many different transport-RNPs and this suggests that often a common core for the formation of the granules is possible. Some other proteins are only able to recognize

very specific sequences that are present on a limited number of mRNAs. Biochemical purification and co-immunoprecipitation experiments revealed, in addition to RNA-binding proteins, that also components of the translational machinery are present (Kanai, Dohmae et al. 2004), (Krichevsky and Kosik 2001). However, it remains unclear whether a functional ribosome can be built starting from these components or not. Finally, short non-coding RNAs can also be found in RNA granules and can repress the translation of the carried mRNAs (e.g. the non-coding BC1 RNA and the micro-RNA miR-134) (Schratt, Tuebing et al. 2006).

Until now it has not been convincingly shown that transported mRNA are translationally repressed, but several lines of evidence support this hypothesis. 1) proteins that are encoded by transported transcripts are accumulated at their final site of destination; 2) translational repressors are associated with RNPs and their loss of function has resulted in the ectopic production of the protein (Paquin, Ménade et al. 2007); 3) in some cases localizing mRNAs seem to co-sediment poorly with fractions that contain actively translated mRNAs (Chekulaeva, Hentze et al. 2006).

One of the ways translation can be repressed is through the binding of repressors to the cap-binding protein eIF4E. This protein allows the initiation of translation when the complex between eIF4G and the RNA helicase (eIF4A) is formed. Indeed, eIF4E binding proteins (eIF4E-BP) compete with eIF4G for the binding and inhibit the assembly of the complex. In *Drosophila*, for example, the eIF4E-BP Cup has been found in RNPs, bound to Bruno, a repressor that binds *Oskar* mRNA in its 3'-UTR. Disruption of Cup- eIF4E interaction leads to ectopic translation of Oskar (Nakamura, Sato et al. 2004). In yeast, the *ASH1* mRNA binding protein Khd1, has been proposed to block directly eIF4G, by binding it on the C-terminal domain (Paquin, Ménade et al. 2007). In neurons, the RNA helicase eIF4A can be bound and inhibited by BC1; as a finally result, the recruitment of the ribosomal subunit S40 is blocked (Figure 9a) (Lin, Pestova et al. 2008).

Translational repressors can also inhibit the assembly of the ribosomes, by blocking the recruitment of the 60S subunit. This is the mechanism of action of the Zip Code Binding Protein 1 (ZBP1), a protein that binds the Zip Code sequences in the 3'-UTR of β-Actin (Figure 9b) (Huttelmaier, Zenklusen et al. 2005).

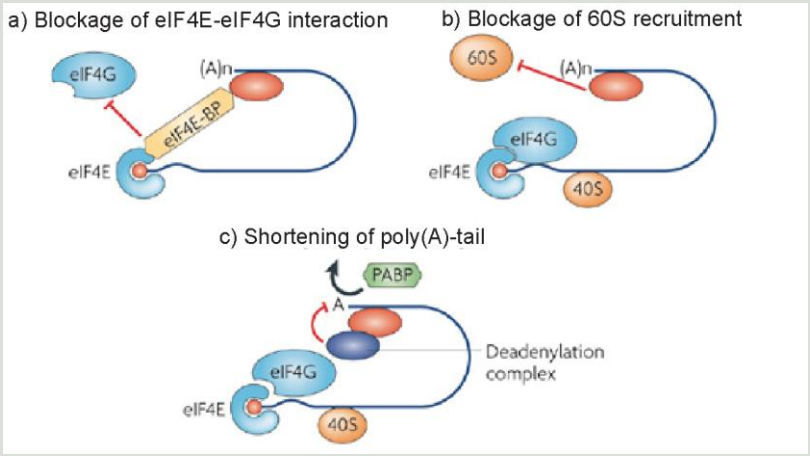

Figure 9. Mechanisms for translational inhibition. ***a)*** *In an RNP, eIF4E-BP can compete with eIF4G to inhibit the formation of the translation initiation complex, thereby inhibiting translation;* ***b)*** *The recruitment of the 60S ribosomal subunit can be inhibited by the binding of RNA-binding proteins to the transcripts. As a consequence a functional ribosome cannot be assembled.* ***c)*** *A deadenylation complex can short the polyA tail of a transcript and therefore inhibit the binding of the 60S ribosomal subunit and of the translation enhancer PABP. Adapted from Besse F. 2008 (Besse and Ephrussi 2008)*

Not only the translation *in-toto* can be regulated, but also the translational efficiency: longer polyA tails increase the efficiency of the translation, allowing the binding of the polyA-binding-protein (PABP), whereas short tails are associated with repressed states. Some modulators control the balance between elongation (induced by the activity of the polyA-polymerase) and deadenylation. Smaug, for example, controls the length of the tail by recruiting CCR4-NOT, a deadenylation complex that is known to inhibit ectopic translation of *nanos* mRNA (Figure 9c) (Zaessinger, Busseau et al. 2006).

Most of the mechanisms proposed for mRNA-specific translational derepressors involve the inhibition of the cap-dependent translation initiation process. However, translation initiation can be controlled also in a cap-independent manner, through the oligomerization of mRNAs and there package into dense RNPs. This mechanism inhibits the exposure of the eventual initiation sites to the initiation complexes and to the ribosomes (Chekulaeva, Hentze et al. 2006).

In conclusion, it looks clear that a cell can adopt a number of different mechanisms for the inhibition of translation during the transport of RNPs, including the blockage of the translation initiator complexes, the inhibition of the recruitment of the ribosomes and the reduction of translational efficiency.

3.2.4. Release of translational repression after mRNA localization

For most of the localized mRNAs, translational repression is released as soon as the transcripts reach their final subcellular destination. The best characterized mechanisms of derepression involve the kinase-mediated release of RNA-binding repressors or the competitive binding with locally produced proteins.

ZBP1 is a well characterized protein that is known to interact with the 3'-UTR of *β-actin* mRNA. It accompanies the transcript from the nucleus to its final destination, promoting its transport and translational repression the same time. The function of ZBP1 has to be therefore silenced, once the mRNA reaches its final destination. Phosphorylation by the kinase Src decreases the affinity of ZBP1 for the transcript and induces its release from the RNPs to promote translation. *In vivo* experiments show that the expression of a non-phosphorylatable form of ZBP1 leads to reduced amount of locally produced β-actin protein (Huttelmaier, Zenklusen et al. 2005). Interestingly, FRET experiments demonstrated that there is interaction between ZBP1 and β-actin only at β-actin translational sites, therefore only where the protein is synthesized (Figure 10a).

An analogous regulatory mechanism has been described in yeast for the two *ASH1* mRNA translational repressors Khd1 and Puf6. Khd1 and Puf6 can be phosphorylated by the casein kinase II (CK2) and by the type I casein kinase Yck1 respectively and the phosphorylation decreases the affinity of the two proteins for *ASH1* mRNA. In addition CK2 has been shown to accumulate at the yeast bud cortex, where it colocalizes with the pool of translated ASH1 (Deng, Singer et al. 2008). Overexpression of a non phosphorylatable form of Khd1 leads to a decrease in local protein synthesis. Once more, colocalization of ASH1 and Khd1 could only be observed at the plasma membrane in vivo (Paquin, Ménade et al. 2007). Taken all together these evidence strongly suggests that *ASH1* translational derepression requires the phosphorylation of repressing proteins that are associated with the transcript.

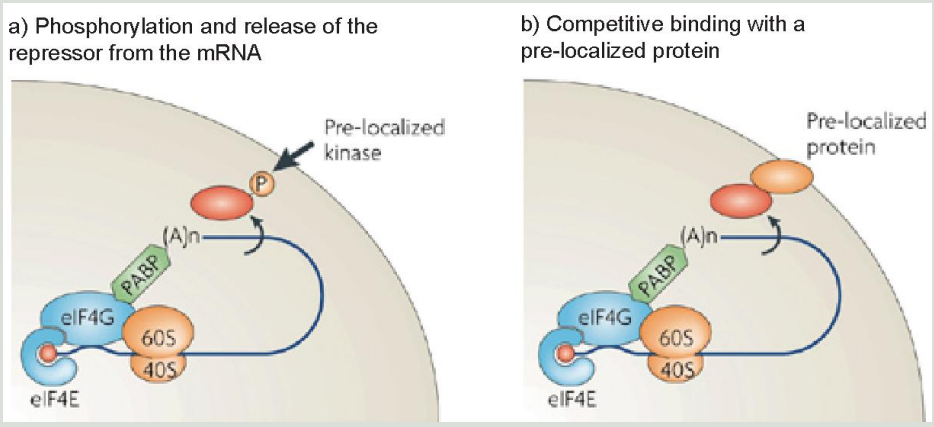

Figure 10. Release of translation inhibition. ***a)*** *Pre-localized kinase at the final destination of a transport RNA can phosphorylate the RNA-binding proteins and cause the release of the transcript and its translation;* ***b)*** *pre-localized proteins can compete with RNA for the interaction with RNA-binding proteins, causing their release and allowing the mRNA to be translated. Adapted from Besse F. 2008 (Besse and Ephrussi 2008)*

The second mechanism of translation derepression consists in the competitive interaction of the repressors with locally expressed proteins. Such an interaction sequesters the repressors from the RNPs allowing the release of the transcript. For example Oskar protein is specifically localized at the posterior pole of *Drosophila* oocytes, where it binds to Smaug, a translation-repressor of the *Nanos* mRNA allowing the messenger to be translated (Dahanukar, Walker et al. 1999). In addition, ectopic expression of Oskar leads to ectopic synthesis of Nanos (Figure 10b) (Zaessinger, Busseau et al. 2006).

In some cases mRNA*s* remain kept in a repressed state also when they reach their final destination and their translation is activated by external cues. This is a phenomenon mainly occuring in neuronal cells, where mRNA*s* get translated in the dendrites following synaptic activation or in growth cones in response to axonal guidance cues. However, such a mechanism is not exclusively neuronal, but has also been observed in *Xenopous laevis* oocytes, in which local translation of several spindle-localized mRNAs is induced by progesterone-induced meiotic maturation (Eliscovich, Peset et al. 2008).

3.2.5. Local mRNA translation in dendrites

What can be a rationale for local protein synthesis in dendrites? Theoretically, local mRNA translation could serve as a fast control of synaptic strength (Skup 2008). Local protein production allows the cell to avoid a multistep mechanism to ensure synaptic plasticity

(Schuman 1999): (1) an enriched pool of localized proteins would have to be moved from the synapse to the cell body upon activation by an external cue; (2) a pool of newly synthesized proteins would then have to be moved back to the synapse where it could be again available for a new stimulation. This multistep mechanism doesn't allow a fast, efficient and convenient communication between the synapses and the cell body. Indeed, a neuron would rather produce proteins in-situ without expenditure of energy, related to long distance transport, and of time. In addition, the protection from ectopic translation can allow a rigorous regulation of gene expression in space and time, indicating some autonomy of the dendritic compartment (from the nucleus).

To ensure local protein production in the dendrites, several elements have to be in place: the messenger RNA, polyribosomes, transfer RNAs and all the enzymes that assure translation initiation and elongation of the peptide chains. Already in 1965 *David Bodian* was the first to find ribosomes in dendrites. But it was only in 1982 that *Stewart and Levy* reported the presence of synaptic-associated polyribosomal complexes (SPRCs) in hippocampal pyramidal and granular neurons. SPRCs are polyribosomes that are associated with endoplasmic reticulum (ER) cisterns, which are localized just beneath postsynaptic sites, in the dendrites. Their localization makes them perfectly situated to be influenced by electrical and/or chemical stimuli from the synapse or from events within the dendrite proper. mRNA*s* and polyribosomes have also been found in the dendritic shaft, suggesting that the local translation of different, shaft-specific transcripts may occur and/or that transport of mRNAs from the shaft to the dendritic spine in response to electrical stimulation may occur (Ostroff, Fiala et al. 2002). In addition to long term potentiation (LTP)-dependent re-distribution of mRNA*s* in the dendrites, electron microscopy experiments demonstrated that spines of different morphology differ in polyribosomal content. Further studies showed the presence of cisternae of Golgi apparatus (Tiedge and Brosius 1996), (Gardiol, Racca et al. 1999), (Pierce, van Leyen et al. 2000), (Wang, Iacoangeli et al. 2002). *Gardiol et al*. also demonstrated the presence of protein synthesis macrocomplexes (ribosomes and eukaryotic elongation factor-2, eIF-2) and that this system is implicated in co-translational and post-translational modifications in rat ventromedial horn neurons *in vivo*. In the same work also the presence of components of the secretary pathway is demonstrated. These elements are necessary for the transport and the assembly of integral membrane protein, indicating that also membrane proteins can be locally translated. A recent study showed that 11% of all the proteins that are present at the post-synaptic density are the result of local mRNA translation (Peng, Kim et al. 2004). Finally, all these findings demonstrate that the synapses are equipped with all the essential elements that are crucial for protein synthesis, and that even

the machinery that allows the correct insertion of transmembrane proteins into the membrane is present.

In the last decade, many efforts have been undertaken to identify the composition of neuronal RNPs. Two recent studies addressed this question and allowed to determine the composition of some neuronal RNA granules. The first study made use of the interaction of transport RNPs with the conventional kinesin KIF5 to isolate large RNA-containing granules (Kanai, Dohmae et al. 2004). KIF5 has been chosen for this screening, because kinesins have previously been shown to be implicated in the transport of RNPs along microtubules in dendrites (Kiebler and Bassell 2006). The isolated granules demonstrated the presence of at least two dendritically targeted mRNAs: one encoding the α-subunit of calcium/calmodulin-dependent protein kinase II (CamKIIα) and the other encoding the immediate early gene Arc. Together with the two transcripts, 42 proteins that are known to be implicated in the regulation of mRNA transport and translation have been found (e.g. eEF1A, Staufen1, Pur-α). In addition other mRNA-binding proteins have been detected: mRNA stabilizing proteins (synaptotagmin-binding cytoplasmic-RNA-interacting protein (SYNCRIP)), translocators (TLS) and translation regulators (Fragile-X mental retardation protein, FMRP). Interestingly β-actin mRNA and its binding partner ZBP-1 have not been found in the particle, suggesting that RNPs differ in composition.

The second study used biochemical fractionation to isolate a fraction that was enriched in RNPs from developing rat-brains (Elvira, Wasiak et al. 2006). This fraction underwent then proteomic analysis. With a series of additional biochemistry experiments, the authors showed that the identified granules contained β-actin mRNA and the RNA-binding protein ZBP-1, but not CamKIIα mRNA. However, the two different preparations showed many common protein components, like hnRNPs, SYNCRIP, FMRP, Staufen. Most likely, some core-elements are indeed always required for the correct localization of transcripts, whereas other ones are added based on the brain region and developmental stage.

Many studies tried to visualize the RNPs movement by fluorescently labeling of mRNAs and/or of mRNA-binding proteins. The majority of the particles are stationary, but some have been shown to be extremely motile and can move in a retrograde or an anterograde manner. The number of RNPs containing CamKIIα mRNA increases in dendrites due to neuronal activity, thanks to the conversion of the stationary state into an anterograde transport (Rook, Lu et al. 2000). A well documented signal-dependent induction of movement of RNPs is the one of ZBP1-containing granules. These granules move into dendrites upon stimulation by depolarization, induced by NMDA receptor activation (Tiruchinapalli, Oleynikov et al. 2003). Also the translocation of Arc mRNA is NMDA-dependent: *in-situ* hybridization histochemistry

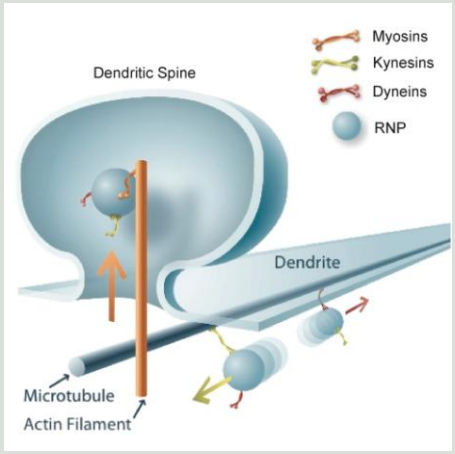

Figure 11. Motors allow the transport of mRNA granules in dendrites. Kinesins and dyneins can specifically travel along microtubules. They are the responsible for anterograde and retrograde transport of mRNAs along the dendrites, respectively. Myosins can travel on actin microfilaments and deliver the granules to the dendritic spines. Adapted from www.maths.ox.ac.uk/groups/occam/research/biosciences-and-bioengineering/bb10

experiments showed that the transcripts co-localize with NMDA receptors at the synapses *in vivo* (Steward and Worley 2001). NMDA is not the only receptor that can induce mRNA relocalization. Indeed activation of the metabotropic glutamate receptor mGluRs promotes the localization of AMPA receptor subunits GluR1 and GluR2 mRNAs into dendrites (Grooms, Noh et al. 2006). But it remains largely unclear how the granules can be transported into the dendrites. In 2006 *Yoshimura et al.* demonstrated that Myosin-Va facilitates the accumulation of TLS, an RNA-binding protein, and of its target RNA *Nd1-L*, an actin stabilizer, in neuronal dendrites an spines (Yoshimura, Fujii et al. 2006). The authors suggest that actin fibers can be the tracks used for the transport of granules with these components. On the other hand, the RNA-binding protein TLC and its target have been found associated also to the conventional kinesin KIF5, a motor that is known to surf on microtubules, suggesting that a cross-talk between actin and tubulin cytoskeleton is likely to occur (Figure 11). RNPs bind the C-terminal tail of KIF5 on a 59 amino acids binding site, which is conserved in KIF5A, KIF5B and KIF5C. It's not absolutely sure yet, which proteins of the RNA-granules bind to the motor, but a recent study suggest that Purα, an RNA-binding protein isolated from RNPs, could be a valid candidate (Kanai, Dohmae et al. 2004). Experiments performed overexpressing CFP-labelled KIF5 together with GFP-labelled Purα, demonstrated a specific localization of the RNPs in the dendrites of cultured hippocampal neurons. Interestingly, when CFP-KIF5 was contransfected only with GFP, the RNA-containing granules have been observed to be localized both in dendrites and in axons. The stationary nature of some of the RNPs that have been discovered and described implies that the action of KIF5 has to be counteract by motors that drive a retrograde transport along the microtubules. Various dyneins have been suggested to play at a tug-of-war in the RNA transport with their counterpart Kinesins (Carson, Cui et al. 2001).

Until now several mRNAs have been shown to be localized throughout the dendrites and many others have been shown to be concentrated in the very proximal part of those protrusion. The proteins that are encoded by these transcripts are involved in several different dendritic functions: microtubules regulators (MAP2, MAP1b), actin-cytoskeleton interactors (Arc/Arg3.1), neurofilaments (Neurofilament protein 6), kinases (CamKIIα), receptors or receptor-subunits (G-protein γ subunit, NR1 subunit of NMDA receptors, α-subunit of Gly receptors, Receptor IP3, GluR1 and GluR2, TrkB receptor, Rho subunit of GABA C receptor), Ca^{2+}-dependent signaling proteins (Calmodulin, CamKIIα, NR1, Receptor IP3), PDGF-dependent signaling (L7), the matrix metallo-proteinase MMP-9, the neurotrophin BDNF, FMR1 (a binding protein for FMRP), vasopressin, tissue palsminogen (tPa), proteins with unknown function (Dendrin) and of course β-actin. These transcripts show various kinds of localization inside the dendrites. They can be localized throughout the whole dendrite (CamKIIα, Dendrin, L7, IP3) or in the proximal part of the dendrite (MAP2, calmodulin, NR1, vasopressin, neurofilament). Some others reach the dendrites only during particular neuronal processes (calmoduilin reaches the dendrites during synaptogenesis) or when induced (Arc/Arg3.1) (Skup 2008).

More and more evidence suggests an implication of local protein synthesis in the control of synaptic plasticity and memory (Sutton and Schuman 2006). Given that transcriptional activation in the soma is required for late-phase long-term potentiation (LTP) , all the initial ideas regarding the sites of translation control naturally focused on the cell soma (Nguyen, Abel et al. 1994). Recent studies suggested, however, that dendritic translation is critical and that somatic translation might even be dispensable. For example, it has been shown that CA3-CA1 synaptic transmission can be potentiated after stimulation with the neurotrophin BDNF in hippocampal slices, even when CA1 dendrites are isolated from their cell bodies (Kang, Jia et al. 1996). In the same way, in similar slice preparations, activation of group 1 metabotropic glutamate receptors (mGluRs) or paired-pulse low-frequency stimulation can induce a form of long-term depression (LTD), a long-lasting weakening in signal transmission between neurons, requiring dendritic and not somatic protein synthesis (Huber, Kayser et al. 2000). Hippocampal slices prepared from the CamKIIα 3'-UTR deletion exhibit diminished late-phase LTP (Miller, Yasuda et al. 2002). In addition, dendritic local application of protein inhibitors in intact slices inhibits late LTP (Bradshaw, Emptage et al. 2003). Application of a dopamine D1/D5 agonist to isolated dendrites from cultured hippocampal neurons showed a rapid increase in the frequency of spontaneous miniature excitatory post-synaptic currents (also called "minis" or mEPSCs). This happens most likely through an increase in the number and size of synaptic GluR1 particles. This last evidence shows that local translation is important for synaptic activation. Local protein synthesis seems not only

to be important in the hippocampus but also in serotoninergic neurons (Martin, Casadio et al. 1997).

Synaptic plasticity requires that local protein synthesis gets coupled to protein degradation for its control. *Steward and Schuman* (2003) and *Bingol and Schuman* (2006) provided evidences that there is a local protein degradation and that synaptic stimulation via NMDA receptor causes redistribution of proteasomes form dendritic shafts to dendritic spines (Steward and Schuman 2003), (Bingol and Schuman 2006). Thus, these large multi-unit cellular machines that recognize, unfold and degrade ubiquinated proteins become subsynaptically available.

Although local protein synthesis in dendrites is now a well documented phenomenon and available data suggest that it is involved in plasticity, many questions remain unanswered. A crucial question concerns the translation limiting factors: not many ribosomes have been found at synapses, indicating that this might be one of the limiting factors for the translation. How are the polyribosomes localized and how is their recruitment modulated? And how do locally synthesize proteins cooperate in the modulation of synaptic transmission?

3.2.6. Local mRNA translation in axons

Although dendritic local mRNA translation has been studied for many years, the role of local axonal translation has gained attention more recently (Lin and Holt 2008). Over the last decade, growing evidences supported the hypothesis the local protein synthesis can occur in axons as well. Nevertheless, puzzlingly, rough ER (RER) and Golgi, necessary for the processing and secretion of proteins, have rarely been detected ultrastructurally in axons. But a recent study has provided immunocytochemical and functional evidences for RER and Golgi, not only in the axons, but even in growth cones (Merianda, Lin et al. 2009).

The number of axonally localized mRNAs has grown considerable in the last few years, thanks to more sensitive detection techniques and thanks to the improved methods for axon isolation. Recent studies have showed that over 2000 mRNA*s* are localized in the axons of murine retinal neurons, primary sensor neurons, cortical and hippocampal neurons (Zivraj, Tung et al. 2010) (Taylor, Berchtold et al. 2009; Gumy, Yeo et al. 2011), while up to 11000 transcripts have been found in sympathetic neuronal axons by Serial Analysis of Gene Expression (SAGE analysis) (Andreassi, Zimmermann et al. 2010). These findings defined that 6-10% of the total cellular transcripts are localized in the axons and many of these transcripts share similarities among several different types of neurons. mRNAs encoding proteins involved in protein synthesis, molecular transport and mitochondrial maintenance

represent the major categories that have been identified in the two independent screens cited above. Nevertheless, there are several distinct differences that confer cell-specificity to the mRNAs-repertoires that have been identified. For example *Impa1* mRNA, a transcript encoding for a key enzyme in the inositole cycle, has been defined as sympathetic-specific. Similarly, *CREB* mRNA is abundant in the axon of dorsal root ganglion (DRG) neurons, where its translation favours survival, but is completely absent in sympathetic neuronal axons. Interestingly, many axonal-located mRNAs show a great enrichment in those protrusions compared to the cell body, suggesting a specific anterograde transport of the transcripts to this location, rather than simple diffusion. In addition, laser-dissection experiments that allow separation of the axons from the cell bodies or even the growth cones from the axons, showed that some transcripts are even enriched in the growth cones over the axon shaft suggesting that mRNAs can be addresses specifically to these compartments (Zivraj, Tung et al. 2010). Moreover, like in dendrites, the repertoire of mRNA can functionally change also in axons: for example, mRNAs encoding proteins of the pre-synaptic machinery are found in growth cones of “target-arriving axons”, but not in “pathfinding” axons. This supports the idea that mRNA content in growth cones is really dynamic and changes in relation to the needs of the growth cone itself (Zivraj, Tung et al. 2010).

In addition to changing the mRNA repertoire during neuronal development, the growth cone must possess mechanisms for the regulation of local protein synthesis on a very rapid timescale in response to guidance cues. The guidance cues that have been shown to induces local mRNA translation in growth cones, can exert their function activating various signaling cascades, that, in most of the cases converge on the mTORC1-mediated activation of cap-dependent mRNA translation (Lin and Holt 2007). For example EphrinA, a well known repulsive cue, through its receptor EphA leads to the activation of Tsc2, resulting in a decrease of the activity of the downstream target mTORC1 and decreased axonal protein synthesis (Nie, Di Nardo et al. 2010). Other efforts have been made trying to understand if external signals can be coupled with the control of protein synthesis. Recently Flanagan’s group showed that DCC, a receptor for Netrin, co localizes with ribosomes at the endo-membrane of axons and of growth cones of spinal commissural neurons. DCC appears to interact with the inactive protein synthesis machinery, as DCC has been isolated together with ribosomal subunits and/or monosomes, but never with polysomes. This association seems to be negatively regulated by the binding of Netrin-1 to its receptor, suggesting that the ligand-receptor interaction induces local mRNA translation by release of ribosomal subunits from DCC itself (Figure 12A).

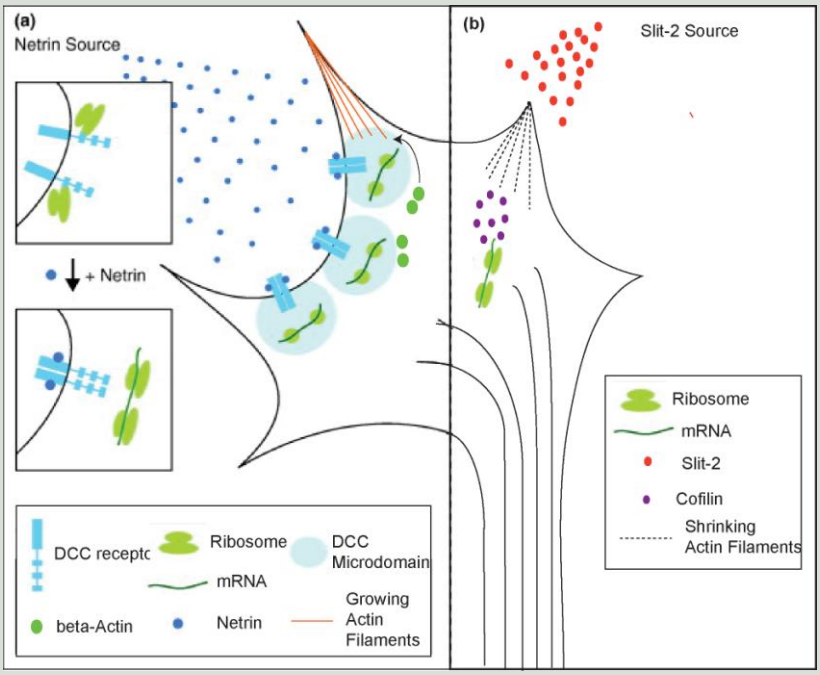

Figure 12. Local mRNA translation in axons. a) a netrin-1 (an attractive cue) source can interact with the DCC receptor and induce the release of sequestered ribosomes. Localized β-actin mRNA can be recruited and locally translated and the protein becomes available for actin polymerization. As a result, the growth cone turns in the direction of the cue. b) Slit-2 can induce local synthesis of the mRNA encoding for cofilin. As a result, actin microfilaments get disassembled and the protrusion retracts. Adapted from Jung H 2011 and Lin AC 2008 (Jung, O'Hare et al. 2011) (Lin and Holt 2008)

Different translation-inducing cues regulate the synthesis of distinct sets of mRNAs: the attractive cues netrin-1 and BDNF induce local β-Actin synthesis (Leung, van Horck et al. 2006) (Zhang, Eom et al. 2001), whereas repulsive cues like Slit2 and Sema3A induce local production of acting depolymerizing molecules, such as Cofilin and RhoA (Figure 12B) (Wu, Hengst et al. 2005) (Piper, Anderson et al. 2006). However, all these cues lead to increased translational activity in the growth cones, but how is than specific mRNA-translational control achieved? Up to now, there is no strong evidence that can provide a convincing explanation for this matter; but the most likely candidates as targets for the control of specific translation are the RNA binding proteins. FMRP for example is an RNA-binding protein that has been very well characterized in dendrites and has recently also been found to be present in axons and in growth cones, suggesting that it could play a role there. Indeed, experiments in cultured hippocampal neurons of *fmrp* knockout mice showed defects in Sema3A-induced axonal proteins synthesis and growth cone collapse (Li, Bassell et al. 2009).

But the best example for RNA-binding protein control is once more provided by ZBP: like in fibroblasts, also in neurons the release of ZBP-inhibition, via phosphorylation by Src, can

induces local translation of β-Actin in response to the attractive cue BDNF (Sasaki, Welshhans et al. 2010). Bassell's group showed that Src can phosphorylate ZBP-1 at Y396, thereby inducing the release and the translation of ***β-Actin*** mRNA. Upon overexpression of a non-phosphorylatable version of ZBP-1, both local translation of ***β-Actin*** mRNA and growth cone turning in the direction of BDNF source were reduced (Sasaki, Welshhans et al. 2010).

Another example of the regulation of local protein synthesis through the regulation of RNA-binding proteins has been provided by *Kuwako et al* (Kuwako, Kakumoto et al. 2010). *Kuwako* showed that the RNA-binding protein Musashi (Msi1) can control the translation of *robo3* mRNA. In particular they showed that precerebellar inferior olivary neurons in *msi1* knockout mice show a midline crossing defect similar to *robo3* knockout mice (Marillat, Sabatier et al. 2004). Moreover, Msi1 binds to and increases the translation of *robo3* mRNA in axons. It is very interesting to notice that the *cis*-element responsible for this regulation is located in the coding sequence of *Robo3* transcript, rather than in the predicted Msi1-binding motif in the 3'UTR. In another study, Msi1 has been shown to repress the translation of other mRNA*s* such as *m-numbm RNA* (Okabe, Imai et al. 2001)*,* providing an example of an RNA-binding protein with dual specificity.

In any case, further studies for a better understanding of the control of local mRNA translation are needed; in fact, very recently Riccio's group identified a novel 150 nt *cis-element* in the 3'-UTR of *impa-1* mRNA. They showed that the presence of this region is necessary and sufficient for axonal localization and local synthesis in response to Nerve growth factor (NGF) stimulation, but they couldn't identify the eventual binding protein that might control its transport and translation (Andreassi, Zimmermann et al. 2010). Even more interestingly, the authors showed that from the same genes, from alternative transcriptional initiation and termination, NGF-responsive and NGF-nonresponsive *impa* mRNA*s* are generated, confirming once more the importance of *cis-elements* that can be present in different parts of the transcripts.

Finally, local protein synthesis is also involved in long-range retrograde signaling. A recent study shows that the mRNA encoding the transcription factor cAMP Response Element Binding Protein (CREB) is locally translated in axons and is retrogradely transported to the cell body in response to NGF (Figure 13) (Cox, Hengst et al. 2008). Axon-specific application of anti-CREB siRNA, revealed that axonally synthesized CREB is locally phosphorylated in the axons, recognized and retrogradely transported to the cell body and then imported into the nucleus. In the nucleus CREB-mediated transcription favors cell-survival. This work shows that the locally synthesized CREB is the source of the phosphorylated and therefore active CREB in the nucleus.

But already some years before, in 2003, *Hanz et al*. showed that injured DRG axons locally synthesize Importin β, a protein that transports nuclear localization signal bearing proteins inside the nucleus, suggesting that transcription factors might be retrogradely transported from the axons until inside the nucleus (Hanz, Perlson et al. 2003).

In conclusion, in the last decade many efforts have been undertaken to demonstrate, not

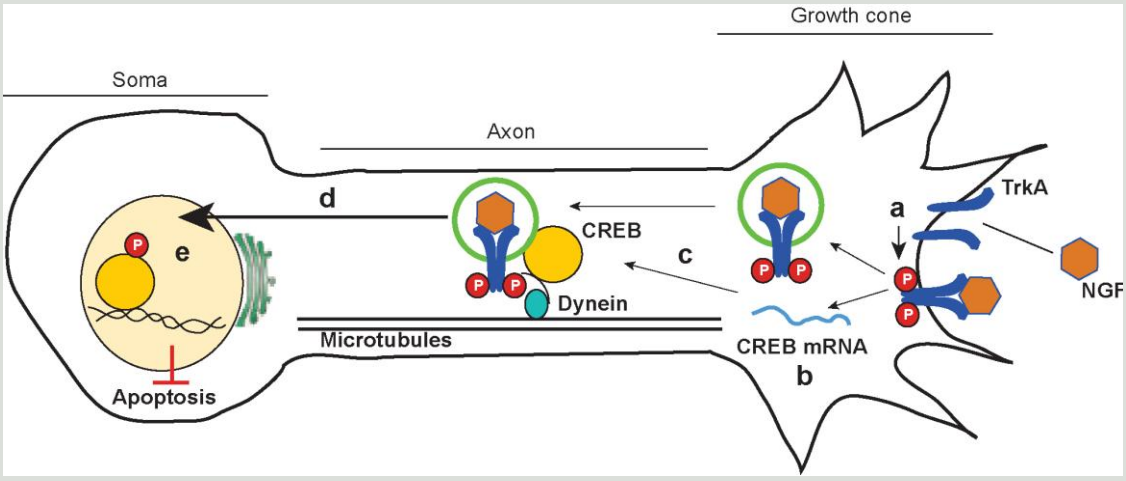

Figure 13. local translation of CREB mRNA promotes cell survival. **a)** NGF binds to TrkA receptors causing dimerization and autophosphorylation. **b, c)** TrkA activation leads to translation of axonal *CREB* mRNA **(b)** and the production of CREB protein **(c)**. NGF-bound, activated TrkA receptors are internalized into endosomes and initiate formation of a signalling complex containing downstream effectors and the motor protein dynein. Axonally translated CREB protein associates with this NGF–pTrkA signalling endosome, which is required for downstream activation of CREB signalling in the cell body. **d)** CREB is retrogradely transported to the nucleus via microtubules and is phosphorylated at Ser 133 downstream of internalized TrkA signalling endosomes, via a kinase cascade including Mek5–Erk5. **e**) Axonally derived pCREB initiates the transcription of anti-apoptotic genes in the nucleus, leading to neuronal cell survival. Adapted from Cox LJ 2008 (Cox, Hengst et al. 2008)

only that proteins can be synthesized locally in axons or dendrites, but also that the resulting molecules have specific roles in particular cell contexts. Local mRNA translation has been demonstrated to be important for the regulation of synaptic plasticity and memory in dendrites and for the control of axonal guidance, sinaptogenesis as well as neuronal survival

in axons. Nevertheless local protein synthesis has never been studied in those protrusions that are considered to be the precursors of dendrites and the axon: the neurites. In fact it is still unclear whether or not local mRNA translation can play a role in the establishment of stable protrusion that will later on result in axon- or dendrite-specification.

3.3. The JNK signaling pathway

3.3.1 The bases of signal transduction by the JNK group of Mitogen-activated protein kinases

Changes in physical and chemical properties of the environment necessitate cells to respond and adapt. These changes include alterations in the amount of nutrients, growth factors, cytokines and the adhesion to cell matrix. In addition, cells also respond to stimulations mediated by changes in the pH, osmolarity, heat, redox, radiation and chemical stress. Those entire physical and chemical cues determine the state of the cell and can have an impact on several cell functions, such as cell migration, proliferation, differentiation and death. Many signaling pathways in the cell cooperate to carry out adequate responses. Studies over the last couple of decades have established that mitogen-activated protein kinases (MAPKs) play an important regulatory role in most of these processes (Davis 2000). Genetic studies have identified five MAPK pathways in *Saccharomyces cerevisiae* (Schaeffer and Weber 1999). These are essential for mating (Fus3p), osmoregulation (Hog1p), sporulation (Smk1p), cell wall synthesis (Smk1p) and filamentation (Kss1p) and these enzymes show similarities in their structures and biochemical properties. Each MAPK is activated by dual phosphorylation of a tripeptide motif (Thr-Xaa-Tyr) located in the activation loop (T-loop). This activation is mediated by an upstream kinase, called MAPK kinase (MAPKK) that is itself activated by another upstream kinase, the MAPKK kinase (MAPKKK), resulting in a kinase signaling cascade.

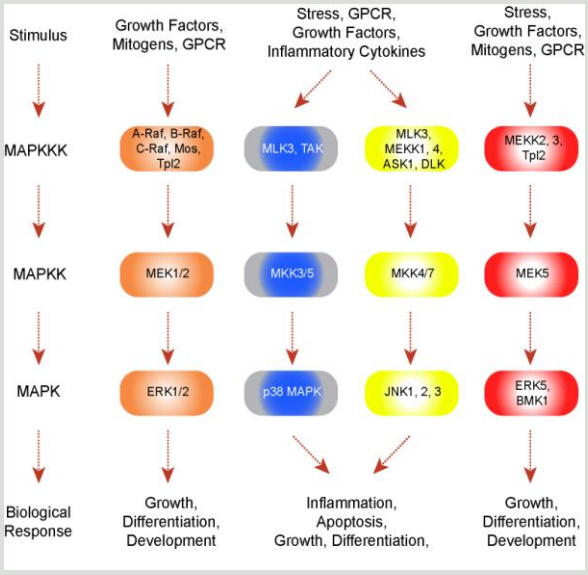

Figure 14. Mitogen-Activated Kinase pathways. A stimulus can activate a MAPKKK that phosphorylates and activates a MAPKK. Downstream a MAPK gets activated and through effectors exerts biological functions. Four distinct MAPK pathways have been identified in mammalians. Adapted from www.cellsignal.com/reference/pathway/MAPK_Cascades.html

MAPK pathways have been identified also in higher organisms. In mammalians 4 major groups of MAPK have been identified and each of these groups is activated by a protein kinase cascade (Figure 14). The

ERK and p38 groups of MAPK are related to the enzymes found in budding yeast and contain the dual phosphorylation motifs Thr-Glu-Tyr and Thr-Gly-Tyr respectively. A third group is represented by the c-JUN NH2-terminal kinases (JNKs), also known as stress-activated MAP kinases (SAPK). The dual phosphorylation motif of JNK is: Thr-Pro-Tyr (Figure 15). ERK5, also called BMK1 (Big-MAPK1) is the most recently discovered member of the MAPK family and has a 66% homology with ERK1/2 and contains the same Thr-Glu-Tyr dual phosphorylation motif as ERK1/2.

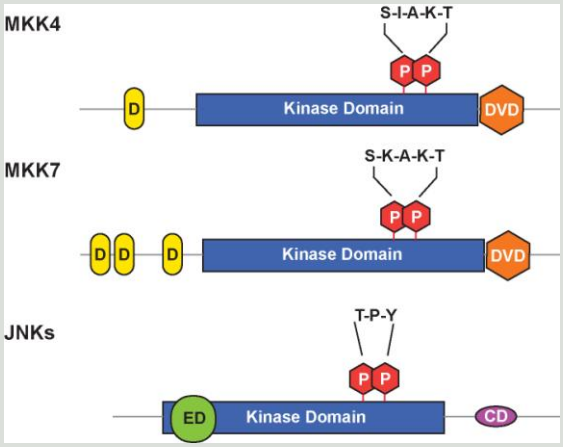

Figure 15. Schematic illustration of the MKK4, MKK7 and JNK structures. All the kinases are activated by phosphorylation of two residues in their catalytic domain (Ser-Thr for MKKs and Thr-Tyr for JNKs). D: Docking domain; CD: Common Docking Domain; ED: Glu/Asp domain; P. Phosphorylation sites. Adapted from Haeusgen 2011 and Wang 2007 (Haeusgen, Herdegen et al. 2011) (Wang, Destrument et al. 2007).

The JNK protein kinases are encoded by three genes: *JNK1* and *JNK2* are ubiquitously expressed, whereas *JNK3* gene has a more limited pattern of expression and is largely restricted to the brain, the heart and the testis. These genes undergo alternative splicing to produce, in total, ten JNK isoforms (S Gupta 1996). The transcripts that derive from all three genes encode proteins with and without a COOH-terminal extension to create both 46 KDa and 55 kDa isoforms; it remains unclear whether or not these isoforms have different functional significance. A second form of alternative splicing is limited to JNK1 and JNK2 and involves the selection of one of two alternative exons that encode part of the kinase domain, conferring substrate specificity to the JNK isoforms, by altering the ability to bind to the docking site on the substrates. The hypothesis that JNK1 could recognize preferentially the docking site of some substrates, such as c-Jun, whereas JNK2 could preferentially recognize and phosphorylate ATF2, has been overtaken after the discovery of the huge variety of isoforms of JNKs. Different tissues express different repertoires of isoforms and the particular spliced isoform that targets preferentially one or the other substrate might be encoded either by JNK1 or by JNK2. Indeed, gene disruption experiments of JNKs show that there is extensive complementation between the three *JNK* genes (Tournier, Hess et al. 2000). JNK1 or JNK2 deficient animals appear to be

morphologically normal, although they display severe immunodeficiency due to defects in T cell function.

Insights into the function of JNK protein kinases has been achieved through the determination of the atomic structure of JNK3 (Xie X 1998). The structure of the inactive complex of JNK3 with an ATP analog is similar to other MAPKs and consists of two domains with an inactive site cleft. But, differently from other MAPKs, the ATP binding site is well ordered in the inactive structure; the low activity seems to be the result of a misalignment of the active site residues and the location of the T-loop, which blocks the access of the substrate to the T-loop itself. The mechanism of JNK activation by dual phosphorylation is unclear, but it is likely that this phosphorylation may alter the structure of the T-loop and cause realignment of the NH2- and COOH-terminal domains to create a functional active site.

Biochemical studies led to the identification and purification of JNK as a “p54 microtubule-associated protein kinase” that was activated by cycloheximide (Kyriakis and Avruch 1990). JNK was found to be able to bind the C-terminus of c-JUN through its common docking domain and phosphorylate it on Ser-63 and Ser-73 (Pulverer, Kyriakis et al. 1991). JNK is known to be activated by treatment of cells with cytokines, such as TNF and IL-1 and by exposure of cells to many different forms of environmental stress (e.g.osmotic stress, redox stress, radiations) (Ip and Davis 1998). The main effect that the specific phosphorylation of Ser-63 and Ser-73 by JNK achieves, is an increased transcriptional activity of the Activation Protein 1 (AP-1), a transcription factor which is a heterodimeric protein composed of proteins belonging to the c-Fos, c-Jun, ATF and JDP families (Pulverer, Kyriakis et al. 1991). In addition, JNK can activate also other transcription factors, including JunB, JunD and ATF2, via phosphorylation of a common Ser/Thr-Pro motif located in the activation motif of these transcription factors (Ip and Davis 1998). The regulation of AP-1 transcriptional activity appears to be a critical role of JNK; in fact, in murine systems, the disruption of genes that encode components of the JNK pathway causes defects in the activation of AP-1 in response to stress and some cytokines (Yang, Tournier et al. 1997). But the activity of AP-1 is most likely modulated also by other pathways and by the interaction with other transcription factors.

JNK protein kinases are activated by phosphorylation on Thr and Tyr by the upstream, dual specific kinases MAPK kinase 4 (MKK4) and MAPK kinase 7 (MKK7) (see Figure 14 p40). These MAPKKs interact with the glutamate/aspartate domain (ED domain) of JNKs. MKK4 and MKK7 are expressed as groups of alternative isoforms of two genes. The mechanism

that creates the different MKK4 isoforms has not clearly been understood yet. In contrast, detailed studies on the *Mkk7* gene suggested that the different isoforms derive from both alternative splicing and utilization of different promoters. The two distinct MAPKK have different biochemical properties, can be activated by different upstream kinases and can activate distinct pathways (see section 3.3.2). Although MKK4 and MKK7 are dual specific kinases and do phosphorylate JNK on both Thr and Tyr, MKK4 seems to preferentially phosphorylate JNKs on Tyr, whereas MKK7 acts on Thr (Lawler, Fleming et al. 1998).

The MKK4 and MKK7 protein kinases are activated by dual phosphorylation at two sites in the T-loop by MAPKKKs (see Figure 14 p40). Several MAPKKK have been reported to activate the JNK signaling pathway, including members of the MEKK group (MEKK1-4), the mixed lineage protein kinase group (MLK1, MLK2, MLK3, DLK and LZK), the ASK group (ASK1 and ASK2), TAK1 and TPL2. Not much is known about the way these kinases act. Most of the evidences are based on overexpression and experiments using dominant-negative as well as on *in-vitro* phosphorylation assays that demonstrate phosphorylation and activation of MAPKKs. However these data don't provide evidence that these molecules can physiologically regulate the JNK cascade. Moreover it is not really clear, which MAPKKK is relevant for specific physiological stimuli because of possible functional redundancy and because of the promiscuity of functions observed in overexpression and *in vitro* assays. Important steps towards understanding the function of MAPKKK in the JNK pathway have been provided by gene disruption studies. But only some of the kinases have been taken in consideration for such studies so far. Mice deficient of *Mekk1* don't show gross morphological defects except for an eyelid closure distability (Yujiri, Ware et al. 2000); in contrast *Mekk3* deficiency causes embryonic lethality (Yang, Boerm et al. 2000). It remains unclear whether or not those defects are due to alterations in JNK signaling or changes in other pathways. Mice deficient of *Mekk2* has not yet been reported, whereas MEKK4 has been more carefully investigated in the last couple of years. MEKK4 consists of two isoforms, α and β, that seem to be able to regulate both the JNK and the p38 MAPK signaling pathways resulting in the regulation of a various number of cell-functions, including the regulation of actin cytoskelekton (Bettinger and Amberg 2007).

In the last few years one study has been carried out to characterize the role of the dual leucine zipper-bearing kinase (DLK) MAPKKK (Eto, Kawauchi et al. 2010). *In situ* hybridization experiments showed a strong expression of *DLK* mRNA in the cortical plate of the neocortex, piriform cortex, hippocampus and thalamus, while being weakly expressed in the intermediate zone (IZ) of the neocortex on E16 and E18. As development proceeds, *DLK* mRNA decreases and gets barely detectable after birth, suggesting that DLK might be very important during neuronal development. However, the functions of DLK have not been

defined *in vivo* yet, but experiments conducted on dissociated neurons in culture suggest an involvement in axonal development. Dissociated neurons, transfected with DLK shRNA, show defects in axonal development. In addition, lower levels of phosphorylated JNK1 and 2 have been observe in knock down cells confirming an involvement of the JNK cascade.

Not much is known about what is upstream of MAPKKKs. Some lines of evidence indicate that Rho family GTPases mediate the activation of JNK pathway through G-protein coupled receptors activation by unknown stimuli (Coso, Chiariello et al. 1995) (Minden, Lin et al. 1995). Potential targets of Rho family GTPases are several members of the mixed-lineage protein kinase group and MEKK groups of MAPKKK (G.R Fanger 2000). GTPases seem to mediate the activation of JNK downstream of receptor tyrosine kinases. However, alternative mechanisms of JNK activation may also contribute, e.g. the adaptor protein Nck and the Ste20-like protein kinase NIK may mediate activation of JNK by Ephrin receptors (Becker, Huynh-Do et al. 2000).

The activation of JNKs by cytokine receptors seems to be mediated by recruitment of TRAF adaptor proteins: activation of the TNF receptor leads to the recruitment of TRAF2, which is required for JNK activation. This adaptor protein has been reported to interact with MEKK1 and ASK1(Baud, Liu et al. 1999) (Nishitoh, Saitoh et al. 1998), but the mechanism of action of one or of the other MAPKKK remains unclear and it's also unclear whether or not the two kinases serve nonredundant functions in the TRAF2 pathway.

The cytokine IL-1 favors the recruitment of the adaptor TRAF6, which is also required for JNK activation (Lomaga, Yeh et al. 1999). *Lomaga et al.* demonstrated that TRAF6 interacts with MEKK1via proteolitic processing, even though this interaction could be mediated by the adaptor protein ECSIT (Kopp, Medzhitov et al. 1999). In addition, TRAF6 has been reported to bind the MAPKKK TAK1, via the adaptor protein TAB2 that induces autophosphorylation of the T-loop and therefore activation of TAK1. More recently it became clear the TAK1 can also be activated by the toll-like receptors TLR-3, TLR-4 and TLR-5 as well as by the T-cell receptor and the B-cell receptor (Wan, Chi et al. 2006) (Sato, Sanjo et al. 2005).

Inhibition of the JNK signaling pathway is achieved mainly by phosphatases, but, to date, the knowledge about these proteins is rather fragmentary and confusing. The dual specificity MKPs, also called dual-specificity phosphatases (DUSPs) are reported JNK-inactivators and the best known of them are MKP-7 and VH5 (Alonso, Sasin et al. 2004). They both have been shown to have a MAPK-binding site, dual specificity domains that confer them the ability to dephosphorylate both tyrosines and threonines, and a C-teminal Pest sequence. The Pest sequence is a polypeptidic tract, rich in proline, glutamate, serine and threonine that act as signal for degradation, suggesting a rapid turnover for these proteins. Beside de-activating JNKs these two proteins act on the p38 pathway. Other MKPs with some reported

activity towards JNKs are DSP2, MKP6, MKP1, MKP2, MKP4 and MKP5 (Alonso, Sasin et al. 2004). If only little is known about direct regulators of JNKs, even less is known about phospohatases for upstream effectors. The phosphoserine/threonine protein phosphatase 5 (PP5) was reported to suppress hypoxia-induced ASK1/MEK4/JNK signaling (Michael 2001).

3.3.2. MKK7 vs. MKK4

3.3.2.a. MKK7

The mitogen-activated protein kinase kinase 7, also called stress-activated protein kinase/extracellular signal-regulated protein kinase kinase 2 (SEK2) or c-Jun N-terminal kinase kinase 2 (JNKK2) was first cloned from murine testis tissue (Tournier, Whitmarsh et al. 1997) and subsequentially from human and rat (Holland, Suzanne et al. 1997) (Yang, New et al. 1998). The human *MKK7* gene is located on chromosome 19 and it gives rise, thanks to alternative splicing, to a group of proteins with different N-termini (α, β and γ) and two different C-termini (1 and 2). So far, four human, six murine, two rat and three MKK7 splice variants from *Drosophila (hep)* have been identified. They encode for proteins ranging from 345 to 467 amino acids and the homology among different species is very high, reaching 99% for mouse and rat MKK7γ1. MKK7 gets phosphorylated at the serine and threonine in the so-called S-K-A-K-T motif by several MAPKKKs, which are able to interact with the domain for versatile docking (DVD) situated in the C-terminus of MKK7 (Figure 15 p41). This interaction is essential for phosphorylation and it is important for the determination of the specificity of MKKK-MKK7 interactions. Interestingly, the different isoforms can act on their downstream effectors, JNKs, with different efficiencies: MKK7α, for example, exhibits lower activity compared to the β and γ isoforms (Tournier, Whitmarsh et al. 1999), maybe due to the lack of the N-terminus that in the β and γ forms contains three JNK-docking domains (D domains) (Ho, Bardwell et al. 2006). *In vitro* studies show that the different isoforms also have different biochemical properties; unfortunately, nothing is known yet about their physiological relevance.

During embryogenesis, *MKK7* mRNA is found mainly in epithelial tissues, such as lung, skin and epithelium. Deletion of *MKK7* gene results in embryonic lethality between E11.5 and E13.5 with evident defects in liver development. Therefore, most of the studies were done with *mkk7*$^{-/-}$ mouse embryonic fibroblasts (MEFs) or chimeric mouse models. *MKK7*-deficient MEFs show a decreased proliferation and premature cellular senescence, beginning with passage 4-5 and G2/M cell cycle arrest. The loss of *mkk7* could not be compensated by the

overexpression of *mkk4* (Wada, Joza et al. 2004). Correspondingly, loss of *Jnk1*, has also an anti-proliferative effect on MEFs, and inactivation of c-Jun leads to premature senescence. Taken all together, these data demonstrate the importance of the MKK-JNK cascade for development and cell growth. However, in different models, different results have been observed, such as an antiproliferative effect induced by MKK7γ1on PC12 cells (Haeusgen, Herdegen et al. 2010). Thus, conditional and cell type specific *mkk7*$^{-/-}$ knockout approaches together with studies on single MKK7 slice variants are needed in order to elucidate functional diversity.

3.3.2.b. MKK4

The other known MAPKK that can regulate the JNK cascade together with MKK7 is MKK4 (or SEK1 or JNKK1). It has first been identified in a cDNA library form *Xenopous laevis* embryos and the gene is located in human chromosome 17 and encodes a 399 amino acids protein with 94% homology to the mouse and the rat proteins. MKK4 has a S-I-A-K-T motif that contains the two phosphorylation sites, which is similar to the one of MKK7 except for to substitution of one of the Lysines with an Isoleucine. Also MKK4 has a DVD docking site in the C-terminus (Takekawa, Tatebayashi et al. 2005), that can be recognized by the majority of MAPKKKs, such as ASK, MEKKs, MLKs and TAK (Raman, Chen et al. 2007) (Figure 15 p41). In addition, the DVD of MKK4 has been shown to allow the interaction of the protein with scaffold proteins, such as JNK-interacting protein 3 (JIP-3). The 3 D domains in the N-terminus of MKK4 is responsible for the binding of the substrates JNKs and p38 (Ho, Bardwell et al. 2003) and this ability of activating the two independent cascade is a unique characteristic that none of the other MKKs have (Ho, Bardwell et al. 2003.

MKK4 is involved in a variety of physiological and pathophysiological processes; *mkk4* is expressed exclusively in the central nervous system until embryonic day E10 in mice (Lee JK 1999); by day E12 the mRNA can be detected in several tissues, with high levels in the embryonic liver. *mkk4* deficient mice die between E11.5 and E13.5 of anemia and anormal hepatogenesis (Ganiatsas, Kwee et al. 1998). Targeted deletion of the *mkk4* gene in the nervous system causes development defects, such as misalignment of Purkinje cells in the cerebellum and delayed radial migration in the cortex (Wang, Nadarajah et al. 2007). At birth, the mutant mice are indistinguishable from the wild type mice, but a few days later they stop growing, showing neurological defects and die at P20. Specific deletion in the heart clearly prevents hypertrophy, whereas conflicting results are obtained by studies on the immune system, carried out on *sek1*$^{-/-}$*/rag2*$^{-/-}$ chimeric mice (Swat, Fujikawa et al. 1998). Considering the proximity of *mkk4* gene to *p53* gene on chromosome 17, studies on a wide

spectrum of primary cancers, showed that mutations in *mkk4* are frequent in lung and pancreatic carcinomas (5%) and in addition, endogenous expression of MKK4 could reduce metastasis of pancreatic and ovarian tumors in mice (Yamada, Hickson et al. 2002). Injection of an mkk4-/- pancreatic cell line into mice reduced lung metastases of the primary pancreatic tumor (Cunningham, Gallmeier et al. 2006). On the other hand, other studies showed a pro-oncogenic role of MKK4, where knock down of MKK4 could increase apoptosis of breast cancer cells after serum-deprivation (Wang, Pan et al. 2004). All these data indicate that MKK4 might be important for cancerogenesis, but its exact role depends on the cancer type and on further mutations.

3.3.2.c. Regulation of JNKs by MKK4 and MKK7

MKK4 and MKK7 directly activate the downstream substrates JNKs, but they differ in their preference for one or the other phosphorylation site in the T-P-Y motif. Recent data show that MKK4 phosphorylates preferentially the Tyr, whereas MKK7 the Thr residue (Kishimoto, Nakagawa et al. 2003) (Tournier, Dong et al. 2001). Monophosphorylation of the Threonine residue is sufficient for the activation of JNKs, suggesting that MKK7 is the real trigger of JNK activation. The further phosphorylation of the tyrosine residue ensures an optimal JNK activation (Tournier, Dong et al. 2001). Data presented in the two cited works clearly show that only MKK7 is necessary for JNK activation. The previous claim that MKK4 is the main activator in response to arsenite has to be reconsidered carefully (Song, Li et al. 2006): the authors showed that arsenite can increase dramatically MKK4 activity, whereas the already high basal level of MKK7 activation does not further increase. But the transfection with dominant negative MKK4 only reduces activation of JNKs, without abolishing it, confirming once more MKK7 contribution. Both MKK4 and MKK7 synergically phosphorylate JNKs, as deficiencies in one or the other MAPKK results in reduced JNK activation (Ganiatsas, Kwee et al. 1998) (Kishimoto, Nakagawa et al. 2003) (Tournier, Dong et al. 2001). Also the availability of the activator determines the action of the other one: in $CD4^+/CD8^+$ thymocytes, for instance, mainly MKK7 activates JNK, because MKK4 has only a very low expression (Rincón, Whitmarsh et al. 1998). In general, one of the accepted hypothesis is that, if MKK4 and MKK7 are both present, they sequentially phosphorylate JNKs, with MKK7 that first acts on the Thr and MKK4 that subsequentially acts on Tyr (Lawler, Fleming et al. 1998).

MKK4 and MKK7 interact very specifically with the D-domains of JNKs; these domains cannot be bound by any other MAPKKs (Bardwell, Frankson et al. 2009). The affinity of MAPKK-JNK interaction seems to be isoform-specific, with MKK4 interacting better with JNK1 and JNK3 than with JNK2. Recent studied showed also that MAPKKs compete for

JNK binding to c-JUN and ATF-2 and can thereby inhibit the JNK-mediated phosphorylation of these substrates. Therefore the intracellular concentrations of binding partners apparently determine the inhibitory or activating effect of MAPKKs on JNKs (Mark W Kieran1 1999). Nevertheless, the formation of MKKs:JNKS signalosomes and their link to distinct cellular effects remain to be determined and need to be explored in order to understand the multiplicity of JNK-mediated functions.

The regulation of JNKs often requires scaffold proteins that assemble the activating kinases (Figure 16). The best studied group of scaffolds are the JNK-interacting protein1-4 (JIP1-4), which might confer signal specificity. JIP1 and JIP2 are thought to only bind to MKK7 (Whitmarsh, Cavanagh et al. 1998) (Yasuda, Whitmarsh et al. 1999), whereas JIP3 and JIP4 additionally bind to MKK4 (Kelkar, Gupta et al. 2000) (Lee, Onésime et al. 2002). However, all the proposed studies focus on apoptosis and control of cellular stress and leave therefore space for new interactions in additional processes. In addition, scaffold proteins interact with upstream regulators and with downstream effectors. JIP1/2, for example, can bind MLK2/3, ASK1, DLK and ZLK (Yasuda, Whitmarsh et al. 1999) (Mooney and Whitmarsh 2004), whereas JIP3 interacts with MLK3 and ASK1 and has a high affinity for JNK3 in the brain (Kelkar, Gupta et al. 2000).

The scaffold proteins β-Arrestin 1 and 2 seem to have a high affinity for ASK1, MKK4 and JNK3 and mediate, in addition to phosphorylation, also the subcellular localization of the complex in the nucleus or in the cytosol (Guo and Whitmarsh 2008).

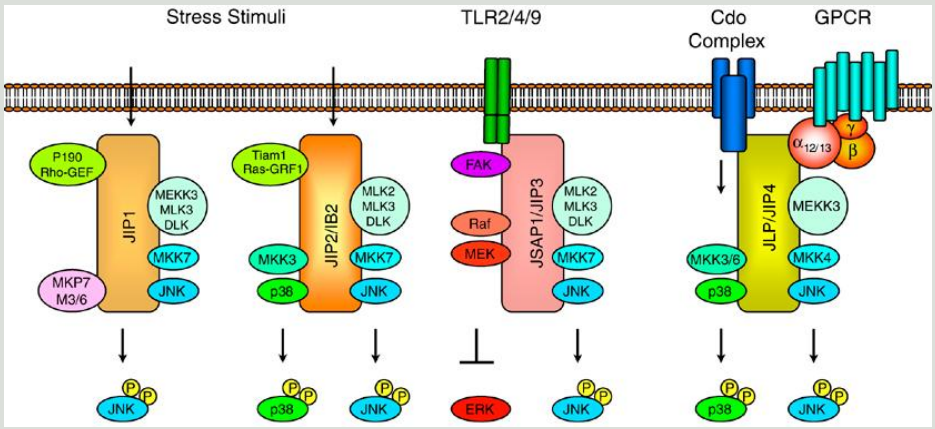

Figure 16. Scaffold proteins allow to assemble specific signalosomes. Scaffold proteins can recruit components of the JNK signaling pathway as well as other MAP Kinases allowing the regulation of cascades in space. Adapted from Dhanasekaran DN 2007 (Dhanasekaran, Kashef et al. 2007)

Plenty of SH3 (POSH) is a multidomain protein that acts as a scaffold for JNK-induced neuronal death, e.g. after NGF deprivation (Xu, Kukekov et al. 2003). Interestingly, it has been shown that it can bind also other JIPs (JIP1-3) and assemble a multiprotein complex called PJAC (POSH-JIP apoptotic complex) that mediates JNK-induced apoptosis following treatment with camptothecin (Kukekov, Xu et al. 2006).

The scaffold protein Kinase Suppressor of RAS (KSR) seems to be involved in pro-oncogenic signaling pathways and it can couple various Rho exchange factors to MLK2, MLK3 and MKK7, and provides a intriguing mechanism of JNK signaling regulation (Jaffe, Hall et al. 2005).

Finally, Filamins (A, B and C), proteins that play an important role in the organization of the cytoskeleton, have been shown to interact with various components of the JNK cascade (MKK7β, MKK7γ and MKK4) and seem to promote synergistic JNK activation through both MKK4 and MKK7 during stress and association with actin stress fibers (Nakagawa, Sugahara et al. 2010).

3.3.3. Functions of JNK in the nervous system

The components of the JNK signaling pathway are ubiquitously expressed and are involved in several cellular functions, including cell proliferation, differentiation, transformation, apoptosis, cell migration and cytoskeleton integrity (Nishina, Wada et al. 2004). Although many studies of the functions of JNK have been performed in various organs and cell systems, JNK roles have been studied extensively in the central nervous system.

3.3.3.a. JNK and neuronal cell death

Since many years it has been established that JNK is involved in the control of cell death. The involvement in apoptosis is still the mostly studied role of this signaling pathway; it is quite well accepted that JNKs have a dual function: they can induce apoptosis, but on the other hand they can also induce survival.

Activation of the JNK pathway has been examined in a variety of neuronal cell culture models with different apoptotic stimuli and the reduction or depletion of JNKs results in a protection from cell death. Initially, studies have been carried out to demonstrate a role of JNK-induced apoptosis after Nerve growth factor (NGF) withdrawal. Overexpression of dominant negative and gain-of-function components of the pathway formally showed an involvement of the pathway in the induction of apoptosis (Virdee, Bannister et al. 1997), (Zhengui Xia 1995). In addition, it has been demonstrated that the activation of survival pathways, such as ERK and Akt/PBK pathway, could suppress JNK-dependent apoptosis. The role of JNK in stressed-induced neuronal cell death has been further described in hippocampal neurons that were deficient of *Jnk3*: susceptibility to excitotoxic apoptosis, induced by kainite and glutamate has been seen to be reduced (Yang, Kuan et al. 1997).

The mechanisms by which apoptosis is induced in neurons seem to be the same that can be found in other cell types. Neurons of *jnk* deficient mice have been demonstrated to be resistant to UV-dependent apoptosis (Tournier, Hess et al. 2000). UV radiations, together with other stress factors, such as the DNA-alkylating agent methyl methanesulfate, the inhibitor of translation Anisomycin and cytokines are known to induce apoptosis through the release of Cytochrome C from the mitochondria (Figure 17). Once in the cytosol, Cytochrome C acts, together with Apaf-1 to activate Caspase 9 and consequently the caspase cascade (Tournier, Hess et al. 2000).

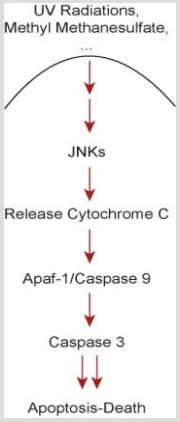

Figure 17. JNK induces apoptosis. Upon activation by stress, JNK induces apoptosis through the activation of the caspase cascade, after release of the Cytocrome C from the mitochondria. Adapted from Davis RJ 2000 (Davis 2000)

A second, nuclear, mechanism by which JNKs can induce apoptosis involves the translocation of phosphorylated JNKs to the nucleus; in the nucleus, JNKs activate the transcription of pro-apoptotic genes, such as TNF-α, Fas-L and Bak, via c-JUN phosphorylation and assembly of the transcription factor AP-1 (Fan and Chambers 2001). However, JNKs can also phosphorylate a number of other transcription factors including JunD, ATF2-3, Elk1, Elk3, p53, RXRα, RARβ, AR, NFAT4, HSF-1 and c-Myc (Johnson and Nakamura 2007). It has therefore been suggested that JNK-activity in the nucleus can increase the transcription of pro-apoptotic genes and decrease the expression of pro-survival ones (Figure 18).

Surprisingly, deprivation of ATF2 by siRNAs doesn't seem to protect the central nervous system neurons against apoptosis in response to trophic hormone withdrawal (Björkblom, Vainio et al. 2008). In fact, although a contribution of JNK to the control of cell death has been clearly defined, it seems unlikely that apoptosis represents the only functional consequence of JNK activation (Davis 2000). This might be true also considering that most forms of environmental stress don't induce apoptosis under conditions that are sufficient for JNK activation. This is partly explained by the interference of survival signaling pathways. Examples of these pathways are ERK (Zhengui Xia 1995), NF-κB and AKT/PKB. The activity of JNKs has to be seen in a coordinated concert of different signaling pathways. The absence of the apoptotic effect seems, therefore, to be rather correlated with the time course of JNK activation: sustained activation, but not transient activation of JNK seems to induce apoptosis (Y R Chen 2000). Indeed, many cytokines are able to only transiently activate the JNK-pathway, suggesting the JNK could therefore contribute to cell survival: TNFα activates the JNK-signaling pathway through TRAF2 without inducing any apoptosis (Reinhard, Shamoon et al. 1997). The strongest evidence confirming a possible role of JNK in the induction of cell survival derives from the analysis of *Jnk1*$^{-/-}$*Jnk2*$^{-/-}$ double mutants embryos that exhibit increased apoptosis in the developing forebrain (Kuan, Yang et al. 1999) (Sabapathy, Jochum et al. 1999).

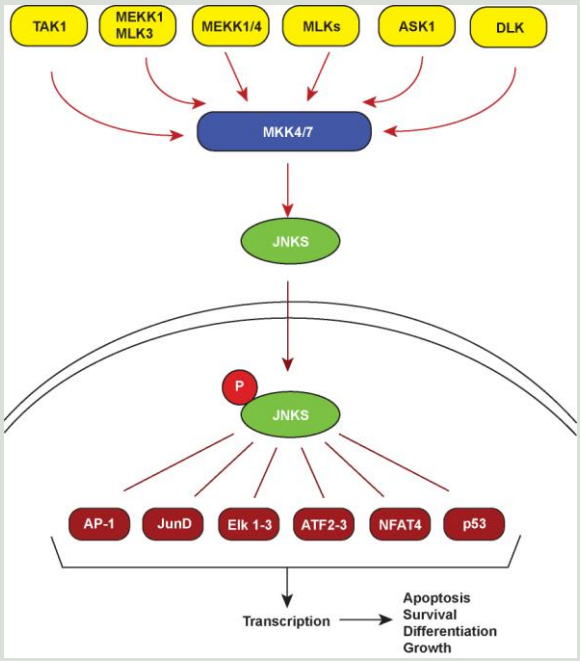

Figure 18. JNK activates a number of transcription factors. Stress factors can induce the activated JNKs to translocate in the nucleus and allow the transcription of genes that are involved in the control of apoptosis, survival, growth and differentiation. Adapted form Harper SJ and Lo Grasso P 2001 (Harper 2001)

3.3.3.b. JNK and neuronal regeneration

Traumatic injury of peripheral neurons is followed by rapid and persistent JNK activation with concomitant c-JUN phosphorylation (Waetzig, Zhao et al. 2006), (Eminel, Roemer et al. 2008). Once more JNKs show a duality and their function in neuronal regeneration is controversial. On the one hand, local application of JNK inhibitors blocksthe regeneration of explanted neurons form dorsal root ganglia, nodose ganglia and sympathetic ganglia (Lindwall, Dahlin et al. 2004). But on the other hand, inhibition of JNK prevents axotomy-induced cell death of dopaminergic neurons of the substantia nigra (Brecht, Kirchhof et al. 2005) and central extrinsic motoneurons. But the surviving motoneurons could no longer regenerate their axons (Newbern, Taylor et al. 2007).

It is now accepted that injury to adult peripheral neurons, but not to central nervous system, reactivates the intrinsic growth capacity and allows regeneration to occur (Abe and Cavalli 2008). Information about distal injury has to be communicated to the cell body to initiate a proper regenerative response. Retrograde transport of injury signals is one of the essential cellular mechanisms leading to regeneration. It has been recently shown that axonal injury induces local activation and retrograde transport of several MAPKs, including ERK (Perlson, Hanz et al. 2005), JNKs (Cavalli, Kujala et al. 2005) (Lindwall and Kanje 2005) and the protein kinase G (Sung, Chiu et al. 2006). Lindwall and Kanje showed in their work that, upon injury of the sciatic nerve, axonal transport of JNK/p-JNK, the JNK scaffolding protein JIP, and the transcription factors ATF3 and ATF2/p-ATF2 occurs. On the contrary, an increase of p-c-Jun in the nuclei of injured neurons has been observed, but without a significant translocation from the axons, indicating that nuclear, or somatic c-Jun gets phosphorylated by the retrogradely transport p-JNKs (Lindwall and Kanje 2005).

But axonal injury doesn't always leads to regeneration. Indeed, damages in the distal part of axons can result in the activation of a self-destructive program that can lead to axonal degeneration. This process, called Wallerian degeneration, can occur both in the central nervous system and in the periphery and seems to involve JNK activation through the upstream kinase DLK (Miller, Press et al. 2009). Nevertheless, the mechanisms that lead preferentially to Wallerian degeneration rather than to axon regeneration remain unclear.

3.3.3.c. JNK and the cytoskeleton

The last two decades brought more and more evidence about JNK signaling pathway involvement in the control of several cellular functions.

Recently growing evidence indicate that JNK substrates, especially the non nuclear proteins, have a wide-range of functional roles in cell migration, axonal guidance, neurite formation

and outgrowth, brain development, dendritic architecture and regeneration of nerve fibers after injury (Sun, Yang et al. 2007); but also mitosis and progression through the cell cycle (Waetzig, Zhao et al. 2006). One common feature that can be found for all the above mentioned functions is the cytoskeleton.

Many recent studies have shown a direct involvement of JNKs in the regulation of the cytoskeleton and this result is achieved via modulation of the phosphorylation of Microtubule Associated Proteins (Figure 19). MAP2 as well as other MAPs have been shown to be highly phosphorylated in the adult brain of mice (-Nido et al. 2000) and in 2003 *Chang et al*. showed that a lack of MAP2 phosphorylation is observed in the brain of *Jnk1* knockout mice. Since, unlike ERK and p38, JNKs are not known to phosphorylate substrates through subordinated kinases, it is most like the case that JNK1 directly phosphorylates MAP2. In addition JNK1 has been shown by the same authors to co-precipitate with MAP2 and to rescue the microtubule-polymerisation deficiency when overexpressed in *Jnk1*$^{-/-}$ cells *in vitro* (Chang, Jones et al. 2003).

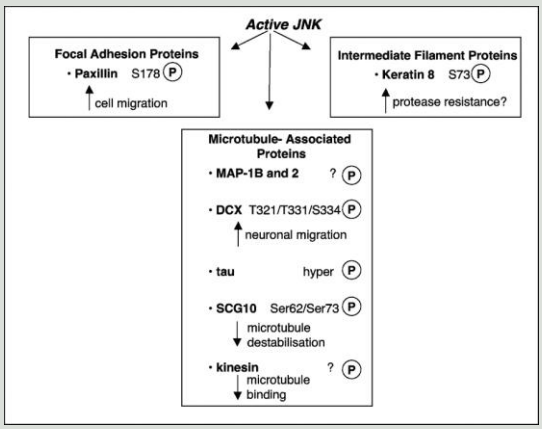

Figure 19. JNK modulates the cytoskeleton. Some of the downstream effectors of JNK are the Microtubule associated proteins. Their phosphorylation via JNK induces stabilization (MAP2, MAP1B, Tau) of the microtubules or collapse (stathmins) during a number of cell processes, such as cell migration, axonal guidance, neurite formation and outgrowth, brain development, dendritic architecture, regeneration of nerve fibers after injury, mytosis, progression through the cell cycle. Adapted from Bogoyevitsch MA 2006 (Bogoyevitch and Kobe 2006)

Further strong evidence demonstrates that MAP1B can be directly phosphorylated both *in vitro* and *in vivo* by JNKs. First, JNK1 can phosphorylate MAP1B (and MAP2) in an *in vitro* kinase assay (Huang, Jacobson et al. 2004). Second, 2D electrophoretic analysis of MAP1B (and MAP2) from *Jnk1*$^{-/-}$ brain indicated that the phosphorylation of MAP1B (and MAP2) is reduced *in vivo* in the absence of JNK1 (and it is not compensated by other JNKs) (Kawauchi, Chihama et al. 2005). Third, the phosphorylation of MAP1B can be inhibited by

the JNK inhibitor, SP600125 (Chang, Jones et al. 2003). MAP2 and MAP1B seem to be mainly involved in the maintenance of neuronal microtubules and in the promotion of neuronal migration (the mechanism that allows neurite extension toward the target destination, followed by the translocation of the nucleus and cytoplasmic components (Gdalyahu, Ghosh et al. 2004)) (Huang, Jacobson et al. 2004). *Jnk1* knockout mice exhibit disorganized neuronal microtubules and progressive degeneration of long nerve fibers (Sun, Yang et al. 2007). Moreover, treatment of neurons with SP600125 causes abnormal organization of the microtubules (Kawauchi, Chihama et al. 2003). Studies during early phases of neuronal differentiation, at the transition between the undifferentiated state to neurite bearing morphology, showed that MAP1B and MAP2 have the redundant function of forming microtubules bundles in cells (Tögel, Wiche et al. 1998).

Doublecortin (DCX) has been shown to directly interact with and be a downstream target of JNK2 (Gdalyahu, Ghosh et al. 2004). In primary hippocampal neurons in culture, DCX can interact through scaffold proteins in complexes with JNK2 and MKK7 at the tip of neurites. The consequence of the constitutive phosphorylation and therefore activation of DCX in these cells, obtained with the transfection of phospho-mimicking DCX, leads to an increased neurite length and an increased number of long neurites, confirming a role of DCX in neuronal migration. DCX contains a tandem domain that allows the interaction with more than one partner; a certain colocalization has been shown with the scaffold protein JIP-1 in growth cones and it has been suggested that DCX can bind at the same time JIP-1 and the JNK responsible for its phospohrylation (Sapir, Horesh et al. 2000).

Finally, JNKs have been shown to interact with another class of microtubule associated proteins, the microtubule destabilizers Stathmins. The protein known as superior cervical ganglion 10 (SCG10) is part of the Stathmin family, it is enriched in growth cones and it has been reported to be a direct substrate of JNKs (Bogoyevitch and Kobe 2006). Phosphorylation of SCG10 on Ser62 and Ser73 reduces its microtubule-destabilizing activity in the growth cone and provides a meaning for the control of growth cone microtubule formation. However, although a strong interaction of SCG10 with JNKs has been demonstrated, a direct activation by JNK has never been formally shown, although a lack of phosphorylates SCG10 (Ser73) has been observed in the cortex of brain tissues isolated from *Jnk1*$^{-/-}$ animals (Tararuk, Östman et al. 2006).

In conclusion, although an involvement of JNKs in the regulation of microtubules has been proposed and in some cases well demonstrated, many question remain open. A clear mechanism of action of one or the other JNK is missing. A clear identification of specific

functions of the different branches of the JNK-pathway has never been provided, due to the high cell-specificity of functions, and evidences for regulation in time and space are needed.

4. Aim of the Thesis

4. Aim of the Thesis

Local mRNA translation has been extensively shown in dendrites, where it mainly contributes to control of synaptic plasticity and in axons during axonal guidance. However, it has been never studied during the early stages of differentiation in neurites. A genome-wide screen for mRNA localization showed that 80 mRNAs are significantly enriched in neurites compared to cell bodies, suggesting that local mRNA translation in these structures may occur.

The aim of this study was to demonstrate that the mRNA encoding for the MAP kinase kinase MKK7, an upstream kinase of the c-JUN N-terminal kinase (JNK), is translated in the growth cones of extending neurites and induces a branch of the JNK pathway to stabilize microtubule and increase neurite elongation.

5. Statement of my work

5. Statement of my work

Local mRNA translation is a mechanism that allows to regulate gene expression in space and time. It has been mostly studied during axonal guidance and sinaptogenesis, but not during the initial neurite outgrowth, before the axon/dendrite specification step.

In N1E-115 cells, a neuron-like cell line that mimics the initial phases of neuronal differentiation, we identified 80 neurite-enriched mRNAs. One of them encodes the MAP kinase kinase MKK7, a kinase that directly activates JNK. We found that *MKK7* mRNA is targeted to the growth cone and there it gets locally translated.

In this work we propose a mechanism by which local translation of MKK7 allows to activate a specific branch of the JNK pathway at the base of growing neurites, regulating microtubule bundling and therefore neurite extension.

I contributed to the work by performing all the experiments except the gene-CHIP analysis in Figure 1B (performed by Prof. Olivier Pertz), part of the western blot analysis in Figure 2C-D and Figure 3C-D (performed by Mrs. Erika Fluri), and the experiment 3 of the Supplementary Figure 3A (performed by Mr. Ludovico Fusco). For the performance of FRET- and FRAP-experiments I have been assisted by Dr. Michel Letzelter and Mrs. Katrin Martin, respectively. I have been provided mice E-15 hippocampal primary neurons by Dr. Harald Witte (Post Doctoral fellow in the lab led by Prof. Peter Scheiffele at the Biozentrum, Basel). I contributed to the analysis of data; I designed all the figures and participated in the writing of the manuscript.

The manuscript in Appendix I represent chapter 13 of the book “Rho GTPases – Methods and Protocols”, of the series “Methods in Molecular Biology” Vol. 827, 2012, 2012, XIV, 407 p., Humana Press. It includes detailed experimental protocols for the performance of experiments in N1E-115 cells, some of which have been used also for the work presented in this thesis. I contributed to the writing of the experimental protocols presented in the chapter.

6. Results

6. Results

Growth cone *MKK7* mRNA translation regulates MAP1b-dependent microtubule bundling to control neurite elongation.

Daniel Feltrin[1], Ludovico Fusco[1], Katrin Martin[1], Michel Letzelter[1], Erika Fluri[1], Harald Witte[2], Peter Scheiffele[2] and Olivier Pertz[1*]

[1]Institute for Biochemistry and Genetics, Dept. Biomedicine, University of Basel, Mattenstrasse 28, 4058 Basel, Switzerland

[2]Biozentrum, University of Basel, Klingelbergstrasse 50/70, 4056 Basel, Switzerland

[*]To whom correspondence should be addressed:

Olivier Pertz, Dept. of Biomedicine, University of Basel, Mattenstrasse 28, 4058 Basel, Switzerland

Phone: +41 61 267 22 03; Fax: +41 61 267 35 66; E-mail : olivier.pertz@unibas.ch

Running title: Growth cone local *MKK7* mRNA translation

Abstract

Local mRNA translation in neurons has been mostly studied during axon guidance and synapse formation but not during initial neurite outgrowth. We performed a genome-wide screen for neurite-enriched mRNAs and identified an mRNA that encodes MKK7, a MAP kinase kinase (MAPKK) for Jun kinase (JNK). We show that *MKK7* mRNA is locally translated in the growth cone. MKK7 is then specifically phosphorylated in the neurite shaft, where it is part of a MAP kinase signaling module consisting of DLK, MKK7 and JNK1. This triggers Map1b phosphorylation to regulate microtubule bundling leading to neurite elongation. We propose a model in which *MKK7* mRNA local translation in the growth cone allows for a cell autonomous mechanism to position JNK signaling in the neurite shaft and to specifically pair it to microtubule bundling. At the same time, this allows to uncouple activated JNK from its functions relevant to nuclear translocation and transcriptional activation.

Introduction

Local mRNA translation is an important aspect of the regulation of axonal guidance and the formation of synapses in the nervous system. In axons, local translation of □-actin mRNA has been implicated in growth cone turning (Holt and Bullock 2009). Local translation of *RhoA* mRNA regulates axonal growth cone collapse (Wu, Hengst et al. 2005). Local translation of the transcription factor ELK at the synapse (Barrett, Sul et al. 2006) allows for retrograde signaling with the nucleus. A combination of gene expression profiling and neuronal process purification techniques, have unveiled complex local transcriptomes that depend on the neurite identity (axon/dendrite) (Martin and Zukin 2006; Jung, O'Hare et al. 2011), the differentiation state (young versus old axons (Zivraj, Tung et al. 2010)) and upon neurite injury (Gumy, Yeo et al. 2011). This suggests that a large variety of local translational programs can regulate distinct neuronal functions depending of specific cellular states. However, local mRNA translation has not been explored during the initial process of neurite outgrowth, before axon-dendrite specification.

Jun N-terminal kinases (JNKs) are a subgroup of mitogen-activated kinases (MAPKs) that control cell survival or death through regulation of transcriptional programs in response to a variety of pro-inflammatory cytokines or environmental insults (Weston and Davis 2007). While JNKs were originally considered to mediate neuronal degeneration in response to stress and injury, relatively high JNK activity is maintained in neurons even in absence of stress (Coffey, Hongisto et al. 2000). Consistently, it recently become clear that JNKs are essential regulators of neurite growth and regeneration (Waetzig, Zhao et al. 2006). In this context, JNKs have been implicated in the regulation of microtubule (mt) dynamics through phosphorylation of a variety of proteins such as the mt associated proteins (Chang, Jones et al. 2003) (MAPs), catastrophe promoting factors stathmins (Ng, Zhao et al. 2010), SCG10 (Tararuk, Ostman et al. 2006) and doublecortins (Gdalyahu, Ghosh et al. 2004). An important question is how JNKs can be spatio-temporally regulated to selectively phosphorylate distinct targets that are relevant for the control of nuclear, transcriptional programs versus cytoskeletal dynamics.

Here we perform a genome-wide screen and identify 80 mRNAs that are significantly enriched in neurites of N1E-115 neuronal-like cells. We study an mRNA encoding mitogen-activated protein kinase kinase 7 (MKK7), a MAPKK for JNK (Tournier, Whitmarsh et al. 1997). *MKK7* mRNA is locally translated in growth cones and its protein product is activated in the neurite shaft. We propose a model in which local translation of MKK7 triggers a spatio-temporal JNK signaling module in the neurite to specifically regulate mt bundling and neurite elongation.

Results

Genome-wide screen identifies *MKK7* mRNA in the growth cone

To identify on a genome wide scale neurite-localized mRNAs during neuronal outgrowth, we used our previously described microporous filter technology (Pertz, Wang et al. 2008) to fractionate neurites from the soma of N1E-115 neuronal-like cells (Figure 1A). In this model system, differentiated N1E-115 cells are plated on a 3 µm microporous filter that has been coated with laminin on the bottom part. This leads to neurite outgrowth to the bottom filter surface, allowing biochemical separation of neurites from the soma. Total RNA from purified neurite and soma equivalents were analyzed by Affymetrix gene chip technology to quantitate relative mRNA abundance. This revealed 80 mRNAs that are significantly enriched in the neurite fraction (Table S1), which encode a wide variety of different functions (Figure 1B). In contrast, transcripts enriched in the soma consisted mostly of small nucleolar RNAs (e.g. that are concentrated in the nucleolus). To validate the enrichment of mRNAs in the neurite, we used quantitative polymerase chain reaction coupled with reverse transcription (RT-qPCR) to compare relative mRNA abundance in both fractions and observed similar results as for the gene chip experiment (Figure 1C). We explored the localization of one of these neurite-enriched mRNAs, *MKK7*, using fluorescence in situ hybridization (FISH) experiments in N1E-115 cells. While some *MKK7* mRNA was found in the soma, it predominantly localized to bright punctate structures in growth cones (Figure 1D), suggesting association with ribonucleoprotein particles (Kiebler and Bassell 2006) (RNPs). The control sense FISH probe exhibited very little signal (Figure 1E). Because *β-actin* mRNA was previously documented to be localized in neuronal growth cones (Holt and Bullock 2009), but was not found in our genome-wide screen, we also evaluated its subcellular localization in N1E-115 cells (Figure 1F and G). While *β-actin* mRNA was obvious in growth cones, unlike *MKK7* mRNA, a large pool also localized to the soma. This explains why our purification approach, which relies on relative comparison of mRNA levels in purified neurite and soma equivalents, will only detect transcripts that are robustly enriched in the neurite.

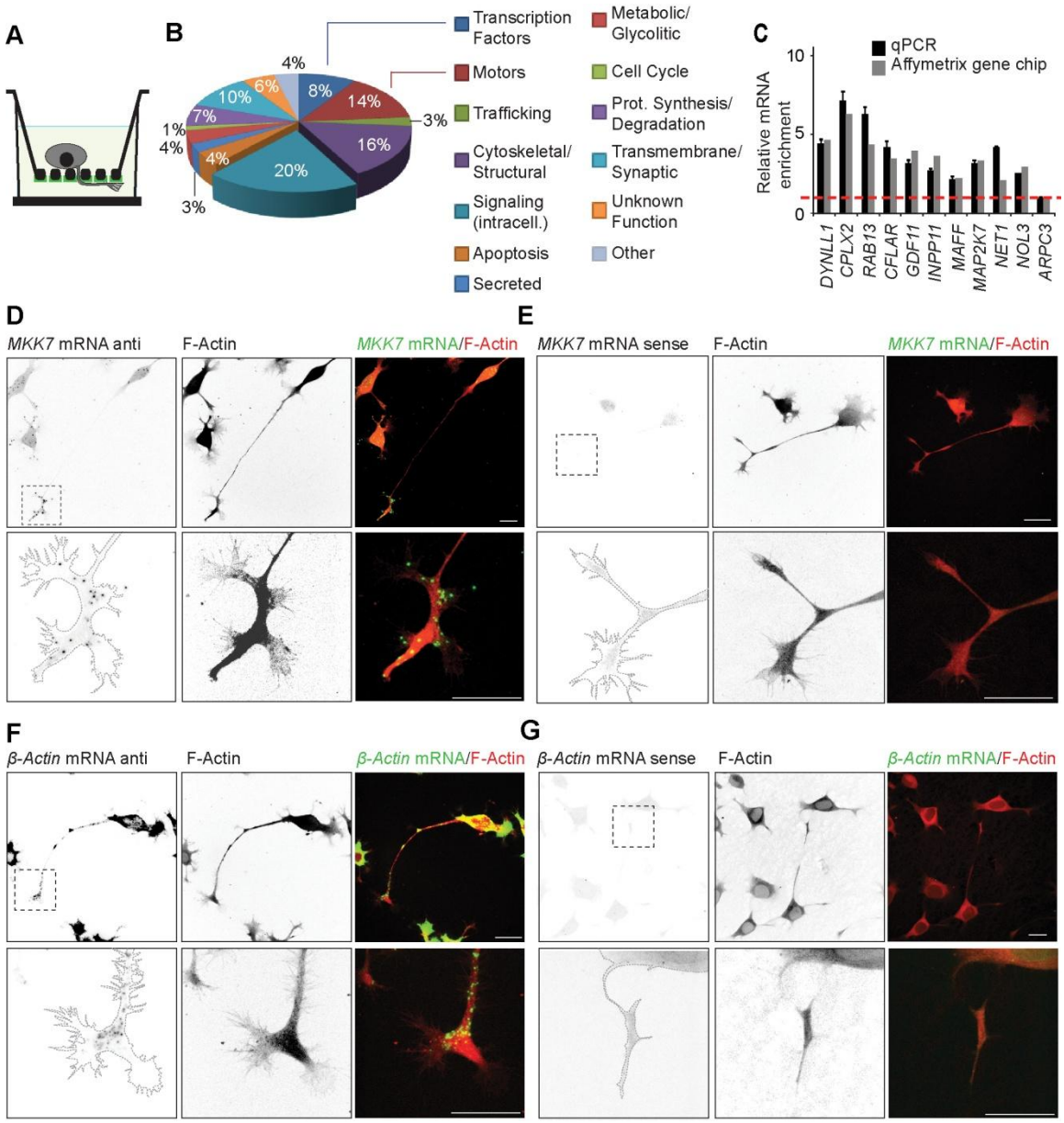

Figure 1. Genome-wide screen for mRNAs that are enriched in neurites identifies *MKK7* mRNA in growth cones. (A) Schematics of microporous filter technology that allows for neurite purification. Asymmetric LM coating allows to drive neurite to the filter bottom. 3 µm pore size restricts somata to the filter top. (B) Gene ontology analysis of classes of mRNAs identified. (C) Validation of mRNA neurite enrichment of selected genes. Equal amounts of neurite and soma mRNA fractions were subjected to RT-qPCR using specific primers for each gene. n=2 experiments, error bars represent s.e.m. (D) *MKK7* mRNA growth cone localization. Confocal fluorescence micrographs of *MKK7* mRNA FISH in differentiated N1E-115 cells. *MKK7* mRNA is found in punctuate structures that most likely represent RNP particles. Left and middle panels: FISH (Left panel) and phalloidin-staining (middle panel) signals in inverted black and white (ibw) contrast, right panels: overlay MKK7 mRNA (green) / phalloidin-staining (red). Lower panels show magnification of the growth cone re-acquired using higher magnification. (E) MKK7 mRNA sense probe signal. Fluorescence intensity signals were scaled as in (D). (F) *β-actin* mRNA FISH antisense probe signal. Note clear dotted signals indicative of *β-actin* RNP particles in the growth cone. Also note strong *β-actin* mRNA signal in the soma. This explains why the neurite purification procedure, because it takes advantage of neurite/soma equivalents cannot resolve *β-actin* mRNA in the neurite. (G) *β-actin* mRNA FISH sense probe signal. Fluorescence intensity signals have been scaled as in (F). Scale bars: 25 µm.

A spatio-temporal JNK signaling module in the neurite shaft

To understand the functional significance of the *MKK7* mRNA pool in the growth cone, we evaluated the subcellular localization of total MKK7 protein (tMKK7) and its activated, phosphorylated form (pMKK7). In N1E-115 cells, tMKK7 displayed a cytosolic subcellular location and was excluded from the nucleus (Figure 2A, upper row). In contrast, pMKK7 was observed predominantly in the neurite shaft and exhibited a decreasing gradient from the base of the neurite to the growth cone. Strikingly, a very sharp loss of pMKK7 at the base of the neurite was observed (Figure 2A, middle row, quantitated in Figure 2B). While pMKK7 levels were globally lower in the growth cone than in the neurite shaft, pMKK7 was also significantly enriched in filopodia ((Figure 2A, bottom row). Western blot analysis of biochemically purified neurite and soma fractions also revealed an increase of pMKK7 in the neurite, while tMKK7 was higher in the soma (Figure 2C). In contrast, the phosphorylated form of the other JNK-specific MAPKK MKK4 (pMKK4) was found to display a distinct distribution than pMKK7, being high in the soma and the growth cone and decreasing in the neurite (Figure S1A).

To further understand the role of MKK7 in neurite outgrowth, we also compared pMKK7, tMKK7 and *MKK7* mRNA levels and subcellular localization in non-differentiated (e.g. cells without neurites) and differentiated N1E-115 cells. Western blot analysis revealed an increase in pMKK7 level concomitant with differentiation while tMKK7 remained constant (Figure 2D). Immunostaining revealed that this raise in pMKK7 resulted exclusively from the neurite localized pMKK7 pool (Figure 2E). In both cases, tMKK7 was excluded from the nucleus. At the transcript level, *MKK7* mRNA was found throughout the cytosol of non-differentiated cells (Figure 2F). During differentiation, 53±3 % (n=23 cells) of *MKK7* mRNA RNPs relocalized to the growth cone (Figure 2F). RT-qPCR revealed that *MKK7* mRNA level remained unchanged in both cellular states (Figure 2G). Globally, these results show that there is an increase of pMKK7 level associated with cell differentiation and neurite outgrowth. Rather than translocating to the nucleus to regulate transcriptional programs, this pMKK7 pool specifically localizes to the neurite. This correlates with a redistribution of MKK7 mRNA from the cytosol to the growth cone where it probably gets locally translated.

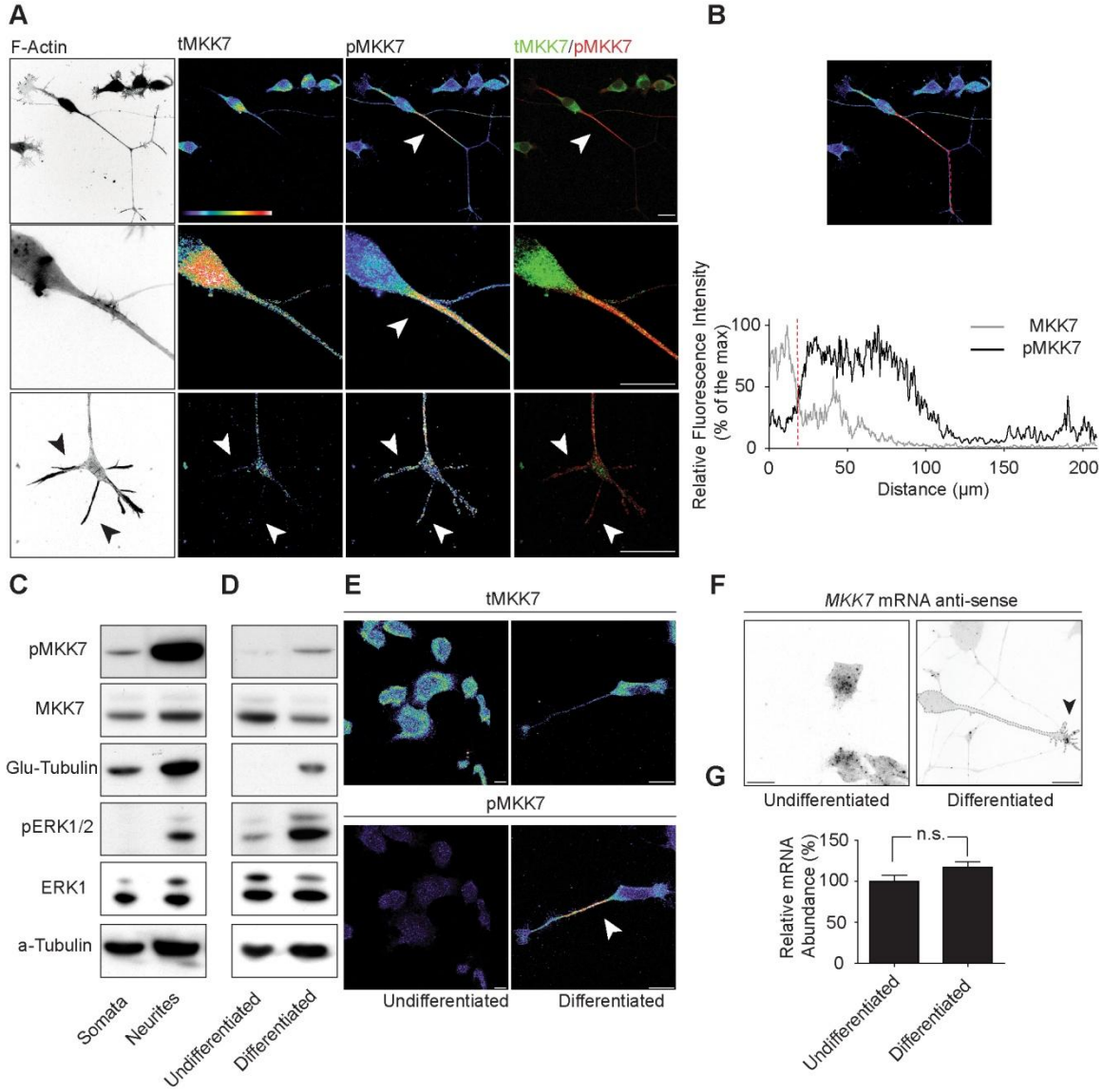

Figure 2. MKK7 is phosphorylated in the neurite in differentiated N1E-115 cells. (A) Representative confocal fluorescent micrographs of N1E-115 cells immunostained for tMKK7 and pMKK7. First row: global view, second row: closeup of neurite base, third row: closeup of neuronal growth cone. Images are shown with color-coded fluorescence intensities (warm and cold colors represent high and low fluorescence intensities respectively), ibw contrast or green/red color composites. Note that because confocal microscopy is used to image the subcellular location of pMKK7, the characteristic neurite to soma decreasing signal cannot be attributed to volume effects. Note that the closeup pictures have been acquired at a higher zoom to provide maximal resolution. (B) Fluorescence intensity profile in tMKK7 and pMKK7 micrographs along line. Red dotted line on the graph represents neurite-soma interface. (C) MKK7 phosphorylation status in purified neurite and soma lysates. Equal amount of purified neurite and soma lysates were probed with different antibodies using western blot analysis. Glu-tubulin and phospho-Erk1/2 (pERK1/2) serves as quality controls for neurite purification as previously described (Pertz, Wang et al. 2008). Total Erk1 (tERK1) and α-tubulin serve as loading controls. (D and E) MKK7 phosphorylation status in undifferentiated versus differentiated N1E-115 cells. (D) Global quantitation of tMKK7 and pMKK7. Equal amounts of cell lysates from N1E-115 cells in the undifferentiated or differentiated state were analyzed by western blot. (E) Representative confocal micrographs of non-differentiated and differentiated N1E-115 cells. Cells were probed for pMKK7 and tMKK7 by immunostaining. Images are color-coded for fluorescence intensity and scaled identically. Note that elevated pMKK7 signal occurs solely in the neurite. (F) MKK7 mRNA localization in non-differentiated and differentiated N1E-115 cells. Representative confocal micrographs of *MKK7* mRNA FISH experiments are shown. Images are shown in ibw contrast. (G) Comparison of global MKK7 mRNA levels in undifferentiated and differentiated N1E-115 cells. RT-qPCR with MKK7 specific primers were performed on equal amounts of total mRNA lysate. Error bars represent s.d., n=3 experiments. Scale bars: 25 µm.

We then evaluated the signaling events downstream of MKK7, including JNKs and its mt-regulating substrates. We found that total JNK (tJNK) was evenly distributed throughout the cell and excluded from the nucleus (Figure 3A). An antibody that detects the activated, mono-phosphorylated form of JNK isoforms 1, 2 and 3 (pJNK-T183) specifically stained the neurite in a pattern reminiscent of pMKK7 (Figure 3A and B). However, there was no activated JNK in growth cone filopodia. In contrast, an antibody that recognizes the dually-phosphorylated form of JNKs (pJNK-T183Y185) specifically labeled the growth cone (Figure S1B). Biochemical experiments showed that both phosphorylated JNK forms were also enriched in purified neurites (Figure 3C), and increased concomitantly with differentiation (Figure 3D). Beyond the ability of these JNK isoforms of being phosphorylated in the neurite, we also directly measured JNK activity in single living cells using a fluorescence resonance energy transfer (FRET)-based reporter for JNK activation (Fosbrink, Aye-Han et al. 2010) (JNKAR). We observed JNK activity throughout the neurite, including the growth cone, but not in the soma (Figure 3E). Timelapse analysis showed that this neurite-localized pool of JNK activation was stable for timescales of minutes (Movie S1). A non-phosphorylatable JNKAR T/A mutant probe did not exhibit increased FRET signal in the neurite (Figure 3E and F). The observation that the FRET activation pattern does not precisely recapitulate the striking pMKK7 and pJNK T183 patterns can be explained because JNKAR is a cytosolic probe which will rapidly diffuse upon phosphorylation, and because JNKAR can be phosphorylated by all JNK isoforms. These results formally show the existence of localized JNK activity in neurites. We then evaluated the subcellular localization of multiple mt-regulating JNK substrates in their phosphorylated form. Immunostaining for the phosphorylated forms of MAP1b and MAP2 recapitulated the subcellular distributions of pMKK7 and pJNK T183 (Figure 3G and H). In contrast, phospho-stathmin and JNK interacting proteins (JIP1 and JIP3, scaffolds for JNK signaling) recapitulated the subcellular location of pMKK4 and pJNK-T183Y185, while phospho-doublecortin was homogeneously distributed in the neurite (Figure S1C-F). This implies the existence of distinct spatio-temporal JNK signaling modules in the neurite.

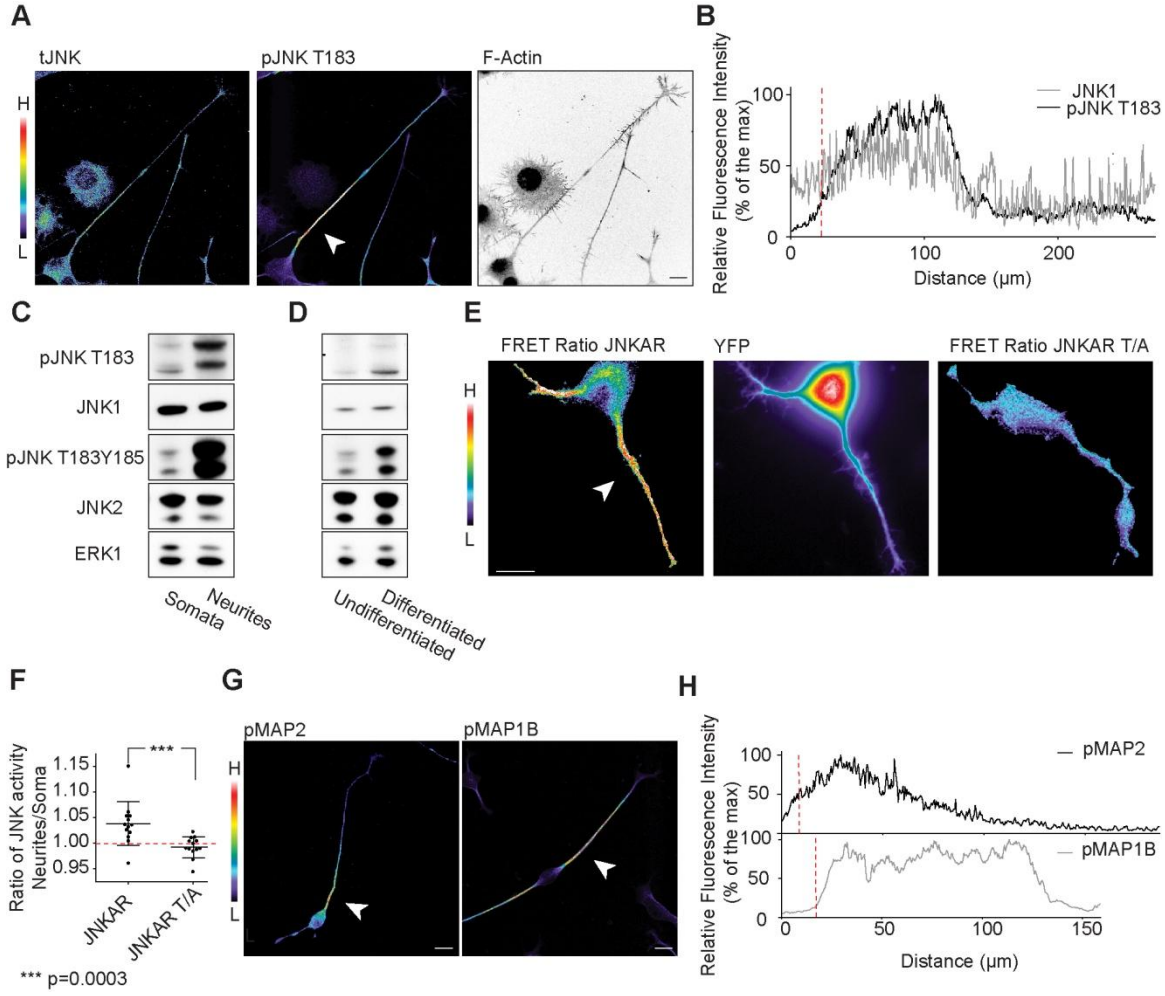

Figure 3. JNKs and its downstream effectors MAPs are phosphorylated in the neurite. (A) Representative confocal fluorescent micrographs of differentiated N1E-115 cells immunostained for tJNK and pJNK T183. Images are color coded for staining intensity so that warm and cold colors represent high (H) and low (L) signal intensity. F-actin image is shown in ibw contrast. (B) Fluorescence intensity profile in tJNK and pJNK T183 micrographs along line drawn in (A). (C and D) JNK T183 and T183Y185 phosphorylation status in purified neurite and soma lysates (C), and in non-differentiated versus differentiated N1E-115 cells (D). (C), (D) Equal amount of lysates of purified neurite and soma lysates (C) or cells in the undifferentiated and differentiated states (D) were probed with different antibodies using western blot analysis. (E) Analysis of JNK activity in single living cells using JNKAR FRET probe. Left panel: FRET emission ratio using JNKAR probe, middle panel: JNKAR probe distribution (YFP channel), right panel: emission ratio using JNKAR T/A non-phosphorylatable probe. FRET emission ratio pictures are color-coded so warm and cold colors represent high and low JNK activation or probe localization. Corresponding movie: Movie S1. (F) Ratio of mean JNK activities in the neurite versus the soma are shown for wild-type or a non-phosphorylatable T/A mutant. Mean ± s.d. is shown, n=15 cells. (G) Representative confocal fluorescent micrographs of differentiated N1E-115 cells immunostained for phospho-MAP2 (pMAP2) or phosho-MAP1b (pMAP1b). (H) Fluorescence intensity profile in pMAP2 and pMAP1b micrographs along line drawn in (G). Scale bars: 25 µm.

MKK7 controls neurite elongation by regulating mt bundling

To study the function of MKK7 during neurite outgrowth, we used RNA interference to knockdown *MKK7* mRNA (Figure 4A). This led to a potent reduction in neurite outgrowth (Figure 4B and C). To get further insights in this phenotype, we examined the dynamics of the neurite outgrowth process. Phase contrast timelapse microscopy revealed that both control and MKK7 KD cells were able to initiate neurite outgrowth. However, neurites of MKK7 KD cells were highly unstable and frequently retracted precluding the formation of long neurites (Figure 4D and E, Movie S2). This suggests that MKK7 is an essential regulator of neurite elongation. Because, the signaling events downstream of MKK7 are highly likely to involve microtubules, we evaluated the mt cytoskeleton in fixed, immunostained, as well as live cells expressing GFP-tubulin. Newly formed neurites in control cells displayed highly parrallel bundled microtubules, whereas neurites from *MKK7* KD cells displayed curly and bent microtubules that were unable to coalesce in obvious bundles (Figure 4F and G, Movies S3 and S4). We also observed that MKK7 mRNA KN only affected mt bundling but not centrosome formation or mt recruitment to the neurite tips. These results show that MKK7 specifically regulates mt bundling in the neurite, most likely to provide the rigidity necessary for outgrowth above a critical length.

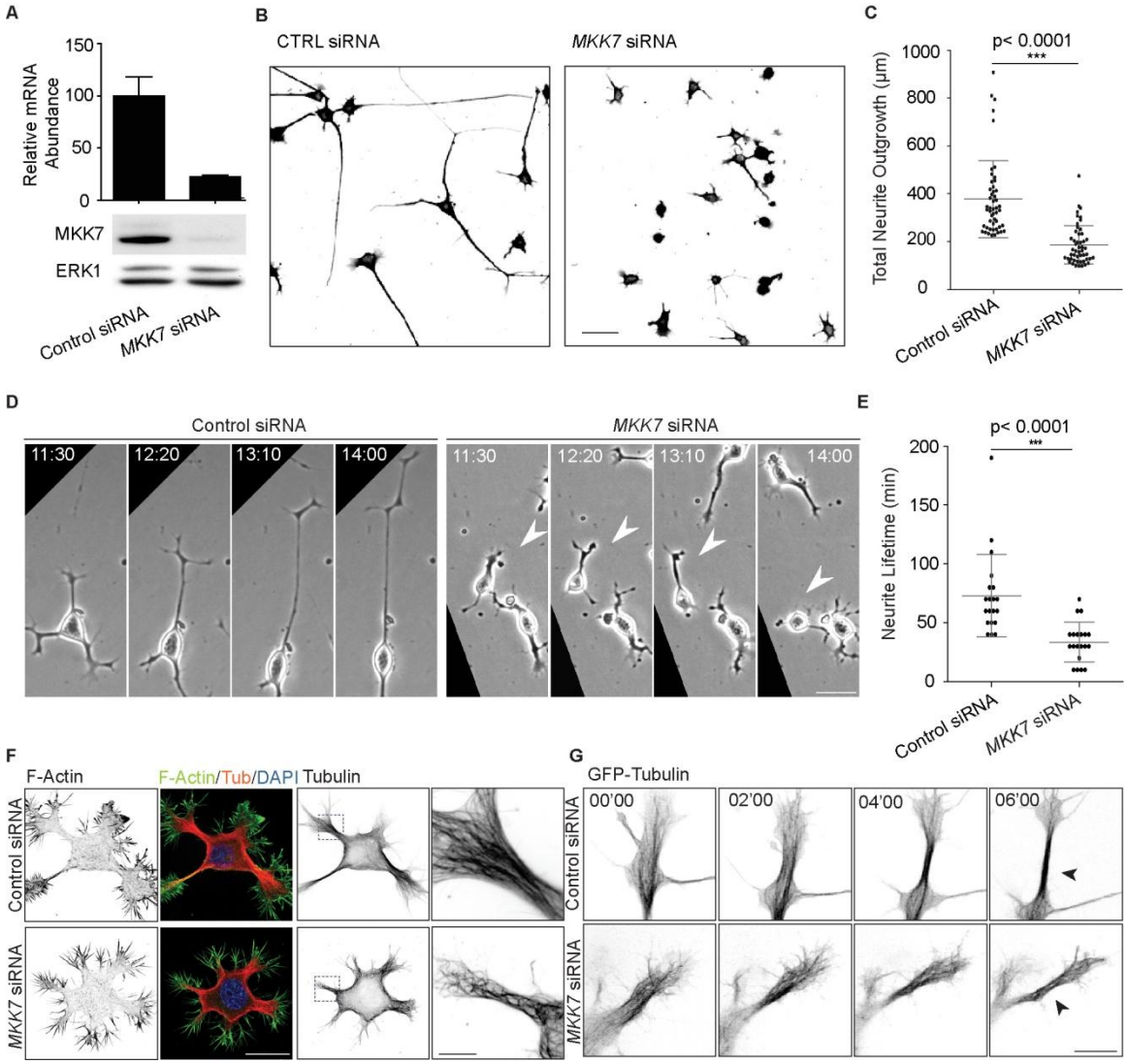

Figure 4. MKK7 controls neurite elongation through mt bundling in the neurite shaft. (A) *MKK7* KN efficiency. Equal amount of RNA or protein cell lysates of control or MKK7 siRNA-transfected cells were assessed by RT-qPCR (n=3 experiments) or western blot. (B) Representative micrographs of α-tubulin immunostained control of MKK7 siRNA-transfected cells. SiRNA-transfected N1e-115 cells were differentiated through serum starvation and replated on laminin-coated coverslips. Ibw contrast is shown. Scale bars: 50 µm. (C) Total neurite outgrowth/cell measurements of (B). Measurements of the 10% of the cells with longest neurites are shown. Error bars represent s.d., n=500 cells. (D) Neurite outgrowth dynamics of control or MKK7 siRNA transfected cells. Differentiated, siRNA-transfected N1E-115 cells were replated on laminin-coated coverslips and imaged using phase-contrast timelapse microscopy. Arrowheads point to neurite retraction events. Scale bars: 40 µm. Corresponding movie: Movie S2. (E) Quantification of neurite extension lifetime. Neurite extension lifetime was manually measured on multiple timelapse movies. Error bars represent s.d., n=20 cells. (F) Confocal fluorescent micrographs of differentiated control and *MKK7* KN N1E-115 immunostained for α-tubulin, phalloidin and DAPI. Composite images or ibw constrast are shown. Closeups (re-acquired at higher magnification) show the state of the mt cytoskeleton at high resolution. Scale bar: 25 µm, 12 µm (closeup). (G) Timelapse confocal video microscopy of control and *MKK7* KN N1E-115 cells expressing GFP-tubulin. Note the parrallel bundling of microtubules in control cells versus curly, bent microtubules that are unable to coalesce in a bundle in the *MKK7* KN cells. Scale bar: 12 µm. Corresponding movie: Movie S3. An additional example is shown in Movie S4.

Growth cone MKK7 mRNA localization is essential for neurite elongation

To explore the functional significance of *MKK7* mRNA localization, we identified the determinants, often localized in 3'-untranslated regions (3'-UTR) (Martin and Zukin 2006), that allow mRNA targeting to the growth cone. The *MKK7* locus generates multiple MKK7 isoforms which can contain two different 3'-UTRs. To evaluate the ability of these 3'-UTR sequences lo localize mRNA transcripts, we flanked these two sequences at the 3' of a chimeric human β-globin gene that was previously used to study mRNA transport to fibroblast lamellipodia (Mili, Moissoglu et al. 2008) (Figure 5A). We then exogenously expressed these constructs in N1E-115 cells, biochemically purified neurite and soma fractions, and used RT-qPCR to determine the subcellular localization of the exogenously expressed mRNAs. We found that 3'-UTR2 allowed enrichment of the β-globin gene in the neurite, while the opposite was observed with 3'-UTR1 (Figure 5B). We then took a functional approach in which we compared the ability of *MKK7* mRNAs engineered to be soma or neurite localized to rescue the *MKK7* knockdown (KN) phenotype. For that purpose, we constructed siRNA-resistant, green fluorescent protein (GFP)-tagged MKK7 constructs that were either not flanked with any sequence, or flanked at their 3' with the 3'-UTR1 or 3'-UTR2 (Figure 5C). Evaluation of the subcellular localization of the mRNAs encoded by these constructs using the neurite purification assay recapitulated our results with the □-globin constructs (Figure 5D). FISH experiments revealed that while the majority of the 3'-UTR1 flanked construct was observed in the soma, a small pool of mRNA still localized to the growth cone (Figure 5E and S2). In contrast, the 3'-UTR2 sequence conferred robust growth cone mRNA enrichment. 3'-UTR1 and 3'-UTR2 MKK7-GFP flanked constructs were significantly more potent to rescue MKK7 KN cells than unflanked alleles when neurite outgrowth (Figure 5F and G), or neurite outgrowth dynamics were evaluated (Movies S5 and S6). Simple overexpression of a 3'-UTR 1 or 2 flanked MKK7 allele also led to longer neurites compared to an MKK7 allele without 3'-UTR (Figure 5H). Western blot analysis (Figure 5I), and assessment of GFP fluorescence intensities (Figure S2B and C) revealed that exogenously expressed MKK7-GFP 3'-UTR2 flanked constructs were expressed to a lower level that those of MKK7-GFP, further emphasizing the functional importance of the 3'-UTR. These results show that growth cone localization of the MKK7 mRNA is essential for its ability to regulate neurite elongation.

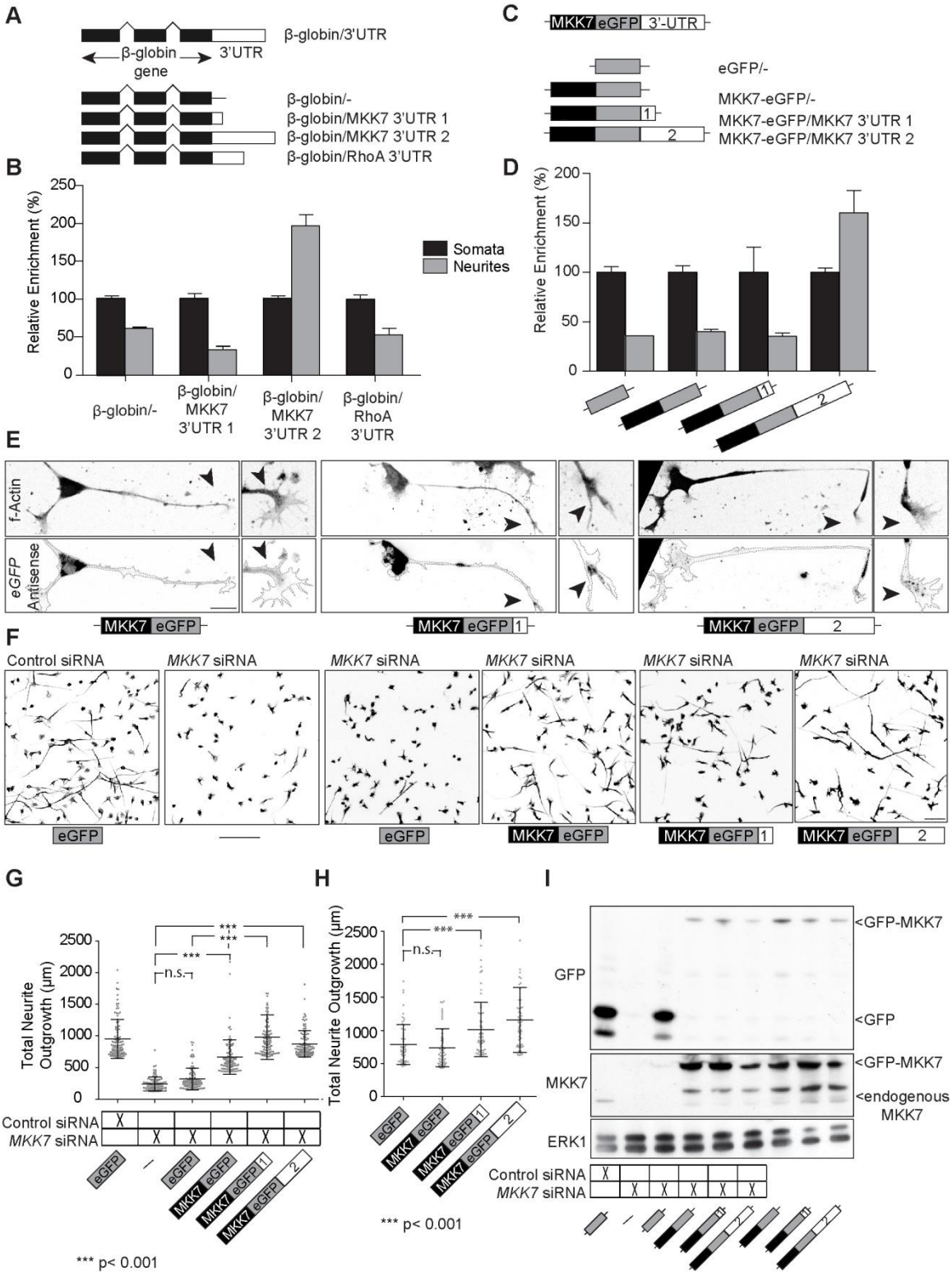
A
β-globin/3'UTR
β-globin gene
3'UTR
β-globin/-
β-globin/MKK7 3'UTR 1
β-globin/MKK7 3'UTR 2
β-globin/RhoA 3'UTR
B
Relative Enrichment (%)
Somata
Neurites
β-globin/-
β-globin/ MKK7 3'UTR 1
β-globin/ MKK7 3'UTR 2
β-globin/ RhoA 3'UTR
C
MKK7 eGFP 3'-UTR
eGFP/-
MKK7-eGFP/-
MKK7-eGFP/MKK7 3'UTR 1
MKK7-eGFP/MKK7 3'UTR 2
D
Relative Enrichment (%)
E
f-Actin
eGFP Antisense
MKK7 eGFP
MKK7 eGFP 1
MKK7 eGFP 2
F
Control siRNA
MKK7 siRNA
eGFP
MKK7 eGFP
MKK7 eGFP 1
MKK7 eGFP 2
G
Total Neurite Outgrowth (µm)
n.s.
Control siRNA
MKK7 siRNA
*** p< 0.001
H
Total Neurite Outgrowth (µm)
n.s.
*** p< 0.001
I
GFP
<GFP-MKK7
<GFP
MKK7
<endogenous MKK7
ERK1
Control siRNA
MKK7 siRNA

Figure 5. Identification and functional assessment of determinants that allow *MKK7* mRNA localization and function. (A) Human β-globin chimeric constructs schematics. Black boxes: exons, black lines: introns, white boxes: 3'-UTR. (B) Subcellular localization of exogenously expressed constructs. The different constructs were transiently transfected in N1E-115 cells of which neurite and soma fractions were purified. Equal neurite and soma mRNA amounts were then probed by RT-qPCR to determine relative enrichment in each fraction using human β-globin-specific primers. Note that a 3'-UTR sequence of the *RhoA* mRNA, which our genome-wide assay was not identified to be neurite-enriched, did not lead to β-globin mRNA neurite enrichment. n=3 experiments. (C) Schematic of MKK7-GFP expression constructs engineered to be locally translated in the soma or in the neurite. (D) Subcellular localization of exogenously expressed mRNAs determined as performed in (B). n=2 experiments. (E) Representative FISH micrographs of exogenously expressed GFP-MKK7 constructs. Images are in ibw contrast. Arrow points to growth cone. Note mRNA growth cone localization of MKK7-GFP constructs flanked with 3'-UTR 1 or 2. Scale bar: 25 µm. (F) Representative micrographs of differentiated N1E-115 *MKK7* KN cells rescued with different exogenously expressed MKK7-GFP constructs. Cells were immunostained for α-tubulin. Note that with siRNA and plasmid transfection efficiencies of 100 and 80 % respectively, average whole population measurements can be made. Scale bar: 100 µm. (G) Neurite outgrowth measurements from micrographs in (F) are shown. Measurements from 10% cells with longest neurites are shown, n=1000 cells. (H) Neurite outgrowth measurements of differentiated N1E-115 cells overexpressing different MKK7-GFP alleles. Measurements from 10% cells with longest neurites are shown, n=600 cells. (I) Western blot analysis of expression of endogenous MKK7 (anti-MKK7 antibody) and exogenously expressed MKK7-GFP (anti-GFP). ERK1 serves as loading control. In all the experiments mean ± s.d. is shown.

MKK7 mRNA is locally translated in neuronal growth cones

To address local *MKK7* mRNA translation in the growth cone, we took advantage of a recently described sensor for local translation, which consists of a membrane-targeted, photoconvertible Dendra2 fluorophore, PalX2-Dendra2 (Welshhans and Bassell 2011). This sensor was flanked at its 3' with *MKK7* mRNA 3'-UTR1 or 3'-UTR2 sequences and exogenously expressed in N1E-115 cells. Rather than using photoconversion (Welshhans and Bassell 2011), which in our hands led to poor elimination of the green fluorophore form, we illuminated the growth cone and the first 50 µm of the neurite shaft with intense green light to bleach the Dendra2 fluorophore. Because membrane targeted proteins diffuse at a rate of ~ 50 µm/hour (Fivaz and Meyer 2003), any newly green fluorescence appearing in the growth cone in a period of less than one hour should represent locally translated protein. We found that non-flanked PalX2-Dendra2 did not recover fluorescence post bleaching, whereas 3'-UTR1 or 2 flanked reporters displayed robust green fluorescence growth cone recovery (Figure 6A-C, Movie S7). Furthermore, this fluorescence recovery was sensitive to the translation inhibitor anisomycin (Figure 6D-F). These results formally show that the 3'-UTR sequence in the *MKK7* mRNA leads to growth cone translation.

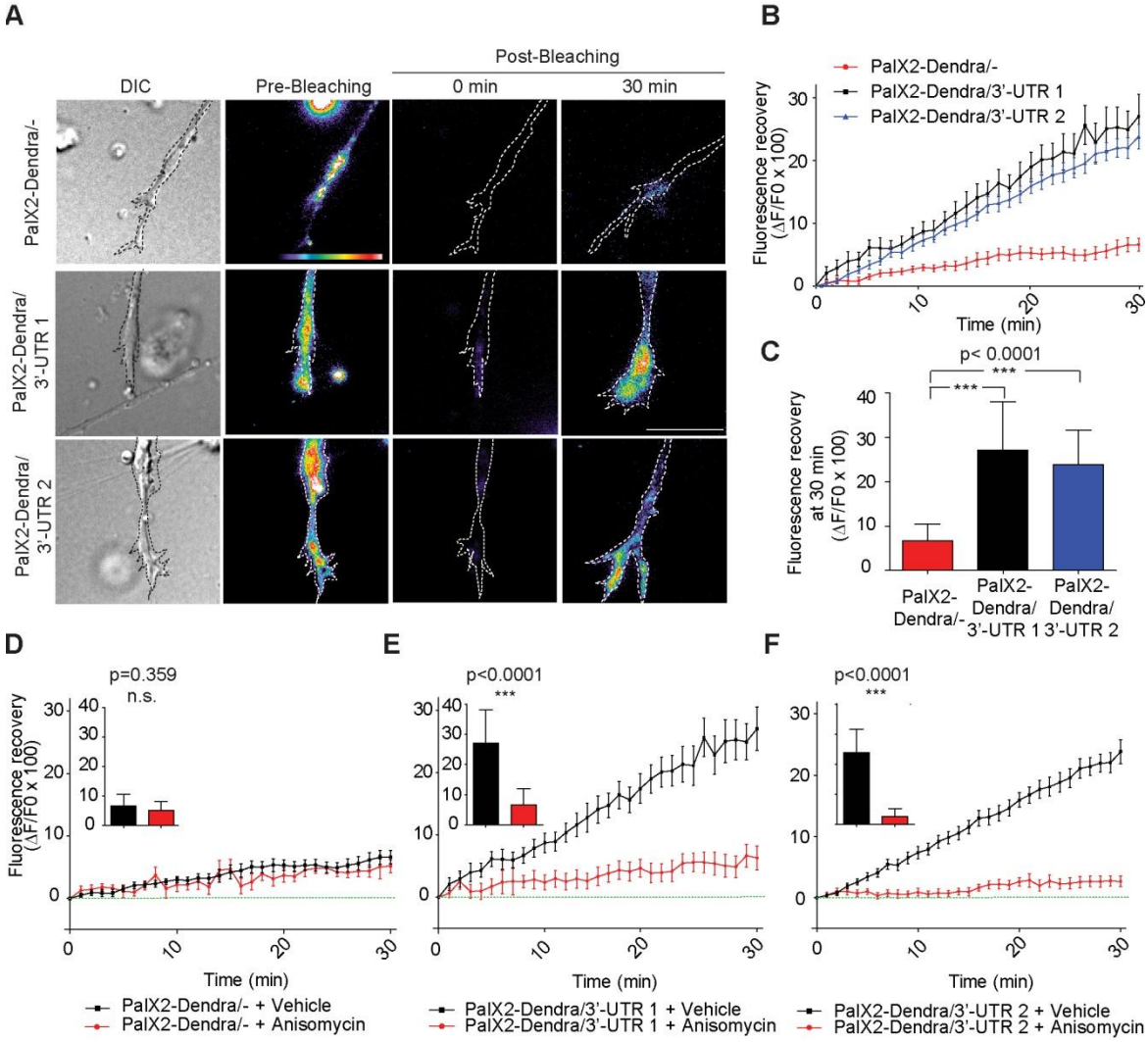

Figure 6. *MKK7* mRNA 3'-UTR sequences lead to growth cone mRNA translation. (A) Representative micrographs of PalX2-Dendra2/-, 3'-UTR1, 3'-UTR2 reporters in live growth cones in the pre- and post-bleaching state at different time points (0 and 30 minutes). N1E-115 cells were transiently transfected with the PalX2-Dendra2 reporters, differentiated and replated on laminin-coated coverslips for 24 hours. One image was acquired in the pre-bleaching state, the growth cone and 50 µm of the neurite were bleached using intense 488 nm laser light, and green fluorescence recovery kinetics were then acquired using timelapse microscopy. Images are color-coded so that warm and cold colors represent high and low green fluorescence intensity. A differential interference contrast (DIC) image is also shown. Note that the pre-Bleaching image is scaled differently as the post-bleaching images because it displays higher fluorescence intensities. Results from two independent experiments were merged. Scale bar: 10 µm. (B) Fluorescence recovery kinetics in growth cones. The ratio of the increase in mean growth cone fluorescence intensity between two consecutive frames (ΔF) over the initial mean growth cone fluorescence (F_0) immediately post-bleaching times 100 is shown. Mean ± s.e.m. is shown. PalX2-Dendra2/- (n=14 cells); PalX2-Dendra/3'-UTR1 (n=10 cells); PalX2-Dendra/3'-UTR2 (n=16 cells). (C) Mean fluorescence recovery 30 min post-bleaching of the different fluorescent reporters. Error bars represent s.d. n like in (C). (D, E and F) Fluorescence recovery kinetics, and mean fluorescence recovery at 30 min of the three reporters in presence and absence of anisomycin. Cells were treated with 40 µM anisomycin 20 minutes before Dendra2 photobleaching. Error bars represent s.e.m and s.d. in the line graphs and in the bar graphs respectively. (D) Pal2X-Dendra2/- (+ vehicle n=14 cells, + anisomycin n=9 cells), (E) Pal2X-Dendra2/3'-UTR1 (+ vehicle n=10 cells, + anisomycin n=10 cells), (F) Pal2X-Dendra2/3'-UTR2 (+ vehicle n=16 cells, + anisomycin n=11 cells).

Functional characterization of a neurite-localized JNK signaling module

To get functional insights in the JNK signaling module that allows mt bundling and neurite elongation, we mined our previously published neurite and soma N1E-115 proteome dataset (Pertz, Wang et al. 2008) for neurite-localized JNK interacting proteins including MAPKKKs, MAPKKs, MAPKs, phosphatases, scaffold proteins, and mt-regulating JNK substrates (Figure 7A, Table S2). We then performed a siRNA screen for each of these genes and evaluated neurite length, dynamics, and KN efficiency when antibodies were available (Figure S3). The screen was repeated three times and some variation was observed. However, KN of the following genes: the MAPKKK DLK (MAP3K12), JNK1 (MAPK8) and MAP1b (MAP1B) always recapitulated the MKK7 KN phenotype in terms of neurite length (Figure 7B and C) and instable neurite outgrowth (Movie S8). We then observed that these phenotypes resulted from the inability of mt-bundling in the neurite (Figure 7D). KN of the other proteins did not lead to any obvious phenotype. Indeed, we cannot rule out that in some cases, we might miss some phenotypes because of low KN efficiency or penetrance. These results identify a novel linear MAPK cascade composed of at least DLK, MKK7 and JNK1 that are specifically dedicated to regulation of mt-bundling through MAP1b allowing for efficient neurite elongation. The observation that DLK displayed identical subcellular localization than pMKK7, pJNK T183 and pMAP1b (Figure 7E and F), strongly suggests that DLK regulates this MAPK signaling module in time and space.

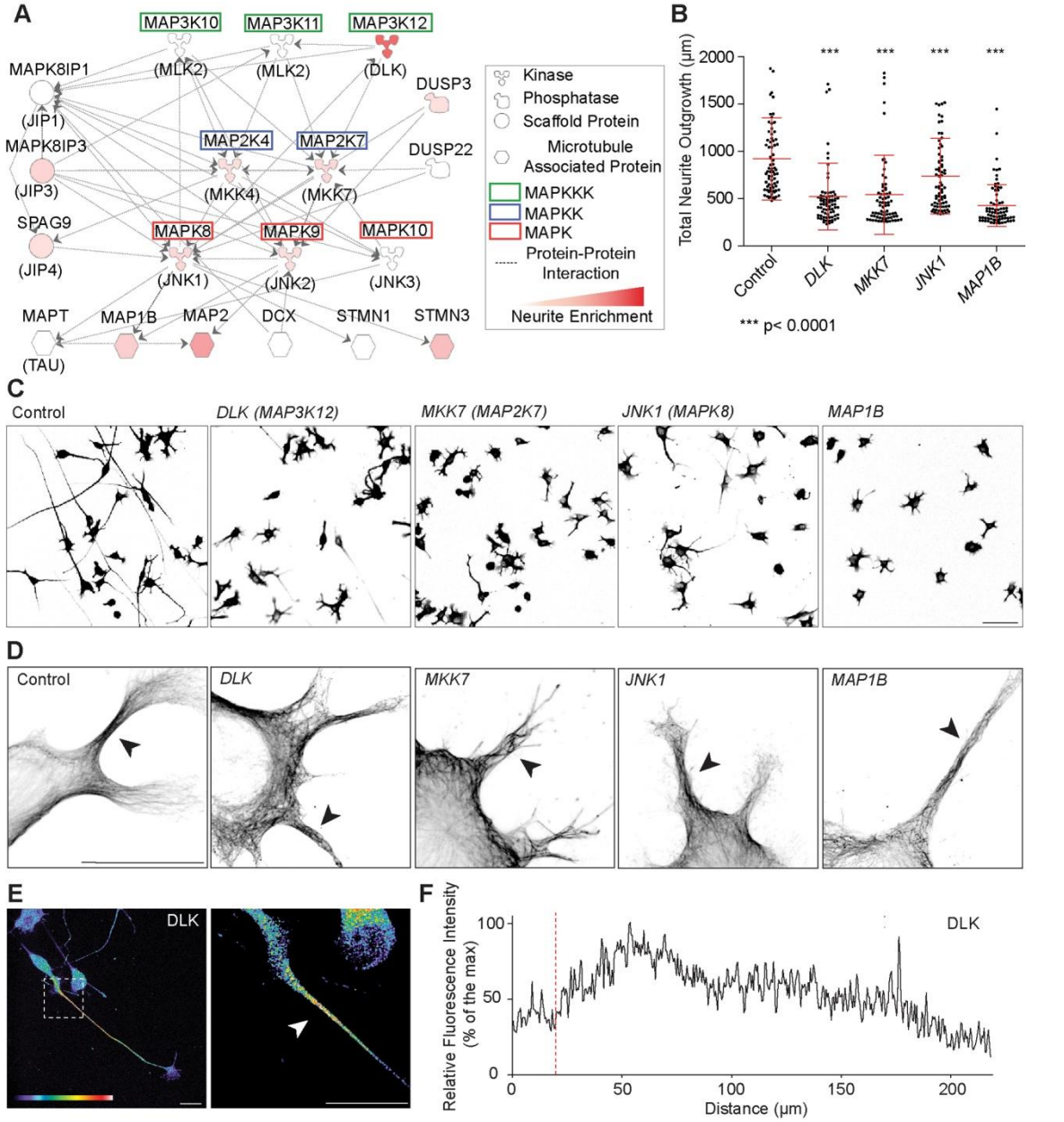

Figure 7. Characterization of a neurite-localized JNK signaling network and model for JNK signaling during neurite outgrowth. (A) JNK signaling network identified in the neurite proteome. Hugo gene (top) and common protein names (bottom, in brackets) are shown. Signaling network was built using Ingenuity Pathway software package, taking in consideration proteins from our proteomics screen that are either significantly enriched in the neurite (quantitated by red color code for the degree of enrichment) or at least present in the neurite and the soma (color-coded in white). Soma-localized proteins were ignored. Each line represents a documented direct protein-protein interaction. (B) Total neurite outgrowth length measurements in response to KN of proteins from the JNK network that phenocopy the *MKK7* KN phenotype. Measurements of the 10 % cells with longest neurites are shown. Mean ± s.d. is shown, n=700 cells for each siRNA. Full siRNA screen dataset is shown in Figure S3. (C) Representative micrographs of α-tubulin immunostained control of siRNA-transfected cells in ibw contrast. Scale bar: 100 µm. (D) Loss of mt bundling capability induced by siRNA-mediated loss of functions of these proteins. High resolution confocal micrographs of siRNA-transfected, differentiated N1E-115 cells stained for alpha-tubulin are shown. Scale bar: 25 µm. (E) Representative confocal fluorescent micrographs of differentiated N1E-115 cells immunostained for DLK. Image is color coded for staining intensity so that warm and cold colors represent high and low signal intensity. Scale bar: 25 µm. (F) Fluorescence intensity profile along line drawn in (E). Red line represents neurite/soma interface.

Validation of the JNK signaling network in primary hippocampal neurons.

Finally, we found that an identical spatio-temporal JNK signaling module is also present in primary E18 mouse hippocampal neurons. For that purpose, we used day in vitro 1 neurons, a stage at which cells mostly exhibit short neurites before the axon/dendrite specification step. *MKK7* mRNA was prominently enriched in neuronal growth cones (Figure 8A and B). DLK, pMKK7, pJNK T183, pJNK T183Y185 and Map1b were present in all neurites with identical subcellular localizations than in N1E-115 neuronal-like cells (Figure 8C and 8D). These results show that the neurite-localized spatio-temporal JNK signaling module also occurs during initial neurite outgrowth in primary hippocampal neurons.

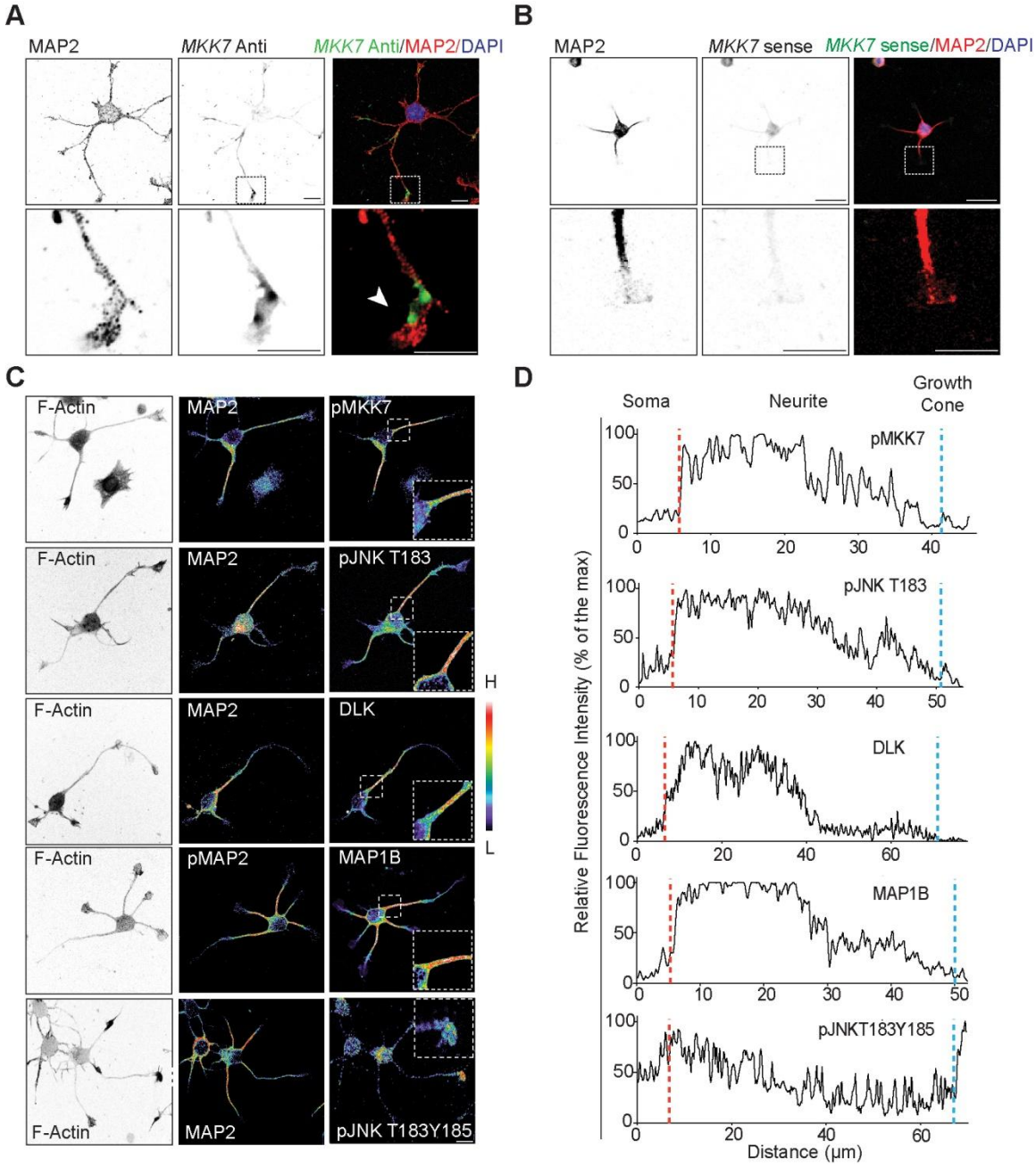

Figure 8. Validation of neurite-localized JNK network in primary neurons. E15 hippocampal neurons were plated on poly-D-Lysine–coated coverslips. Cells were fixed at day in vitro 1. (A) Confocal fluorescence micrographs of *MKK7* mRNA FISH using antisense probe. Top panels: fluorescence signal in ibw contrast. Bottom panels: composite image of FISH and MAP2 immunostain. Arrowheads point to *MKK7* mRNA. (B) Sense MKK7 mRNA FISH control. Fluorescence intensities were scaled as in (A). (C) Confocal fluorescence micrographs of neurons immunostained for different components. Images are color coded for fluorescence intensity so that warm and cold colors represent high and low signal intensity respectively. (D) Fluorescence intensity profiles along chosen neurites. Red dotted lines represent the base of the neurite whereas blue dotted line represents growth cone. Scale bars: 10 µm.

Discussion

Local mRNA translation is essential for cell morphogenesis during axon and synapse formation. Here, we identify a set of 80 mRNAs that are enriched in the neurite before the axon-dendrite specification step. This suggests that even during early stages of neuronal polarization, anchoring of mRNAs at specific subcellular regions and, possibly, their local translation plays a role in cell morphogenesis. These mRNAs encode a large variety of different signaling, cytoskeletal, motor, trafficking proteins that are consistent with local functions in the neurite. A portion of these mRNAs have also been found in fibroblast lamellipodia (Table S1) (Mili, Moissoglu et al. 2008), possibly consistent with a signature of localized mRNAs in relatively unpolarized membrane protrusions. Further work will be necessary to understand the significance of the local translation of these mRNAs.

Here, we explored the function of a growth cone localized mRNA that encodes MKK7, a MAPKK for JNKs. MKK7 functions within a novel, spatio-temporal MAPK signaling module that consists of DLK, MKK7 and JNK1 leading specifically to MAP1b phosphorylation and mt bundling necessary for elongation during initial neurite outgrowth. *MKK7* mRNA is locally translated in the growth cone, and growth cone localization is necessary for this signaling module to function. We propose a model in which growth cone *MKK7* mRNA translation allows to define a spatio-temporal JNK signaling domain specifically in the neurite (Figure 9). This mechanism allows for several important features. 1. It specifically positions MAP1b phosphorylation in the neurite for adequate localization of mt bundling. 2. It allows to uncouple active JNK from nuclear translocation and activation of transcription, which typically occurs in response to cellular stress or neuronal injury (Waetzig, Zhao et al. 2006). 3. It provides for a cell-autonomous, cell-geometry dependent mechanism to switch on this JNK pathway during neurite outgrowth. Here, simple production of a growth cone, by providing a platform for MKK7 mRNA translation, will trigger and appropriately position the specific MAPK module leading to mt bundling. In that respect, there is evidence that local mRNA translation is coupled with adhesion signaling which is specifically taking place in the growth cone. Ribosomes, RNA binding proteins and mRNAs have been shown to localize to adhesion complexes (Chicurel, Singer et al. 1998; de Hoog, Foster et al. 2004) and regulation of β-actin mRNA translation is regulated by Src-dependent phosphorylation of zipcode binding protein in neurites (Huttelmaier, Zenklusen et al. 2005). It will be important to explore the nature of the *MKK7* mRNA 3'-UTR determinants, as well as the RNA binding proteins that control MKK7 mRNA transport and local translation. Our preliminary bioinformatic analysis was however not able to pinpoint any RNA motif in the *MKK7* mRNA 3'-UTR that could bind to specific RNA binding proteins. An important consequence of a growth cone mediated adhesion signal that switches on local MKK7 mRNA translation, is

that simple growth cone removal due to neurite collapse or injury is susceptible to switch off this specific spatio-temporal JNK signaling network and MAP1b-dependent bundling of microtubules. Consistently, we observe that neurite JNK activation is lost during neurite collapse using the JNKAR FRET probe (data not shown). It will also be important to explore the mechanisms that allow to deactivate the JNK network at the base of the neurite so that activated JNKs do not leak to the soma and the nucleus. One possibility is that this is specified at the level of DLK, of which the subcellular localization of the total protein recapitulates the location of pMKK7, pJNK T183 and pMAP1b. It will therefore be important to study the determinants that allow DLK neurite localization.

Evaluation of the subcellular location of the signaling components, as well as our functional data, identifies a DLK-MKK7-JNK1 spatio-temporal module that leads to mono-phosphorylated pJNK on T183. This signaling module is highly activated at the base of the neurite, decreases towards the growth cone and specifically regulates MAP1b, mt bundling and neurite elongation. This is consistent with documented functional and biochemical interactions: 1. DLK regulates mt stabilization during neuronal outgrowth (Hirai, Banba et al. 2011); 2. DLK preferentially phosphorylates MKK7 (versus MKK4) in vitro (Merritt, Mata et al. 1999); 3. MKK7 preferentially phosphorylate T183 (versus Y185) on JNKs (Fleming, Armstrong et al. 2000); and 4. JNK1 has specifically been linked to mt regulation through MAP phosphorylation in the brain (Chang, Jones et al. 2003). Importantly, our results also suggest the existence of a second spatio-temporal JNK signaling module that leads to dually-phosphorylated JNK T183Y185 specifically in the growth cone, where it co-localizes with pMKK4, JIP1 and pStathmin. Consistently, MKK4 preferentially phosphorylates Y185 (versus T183) on JNKs (Fleming, Armstrong et al. 2000). The findings that JNK T183Y185 (Oliva, Atkins et al. 2006) and JIP1 (Dajas-Bailador, Jones et al. 2008) later become selectively enriched in axons, suggest that the function of this distinct JNK signaling module is the regulation of axonal specification, which is not accessible in our N1E-115 cell system. Finally, our results might also explain some controversial findings about DLK. Depending on the cellular context, DLK regulates outgrowth (Hirai, Banba et al. 2011), but also axon regeneration (Yan, Wu et al. 2009) as well degeneration upon neuronal injury (Miller, Press et al. 2009; Xiong, Wang et al. 2010; Sengupta Ghosh, Wang et al. 2011). In the latter context, DLK regulates both Wallerian degeneration (Miller, Press et al. 2009) and retrograde shuttling of JNK signaling complexes to the nucleus (Xiong, Wang et al. 2010; Sengupta Ghosh, Wang et al. 2011). Consistently with a cell autonomous switch, an interesting possibility is that growth cone elimination through injury, and loss of MKK7 local translation, might allow DLK to be coupled with distinct JNK signaling complexes that

regulate the latter functions. In this context, the regeneration function of DLK is known to occur through MKK4 (Yan, Wu et al. 2009).

In short, our results suggest a cell-autonomous, cell-geometry dependent mechanism that involves localized mRNA translation to modulate a specific spatio-temporal JNK signaling module that regulates neurite elongation. Further work will be needed in the future to explore how this integrates with the multiple spatio-temporal JNK signaling modules that regulate neuronal growth, axonal specification, regeneration and degeneration.

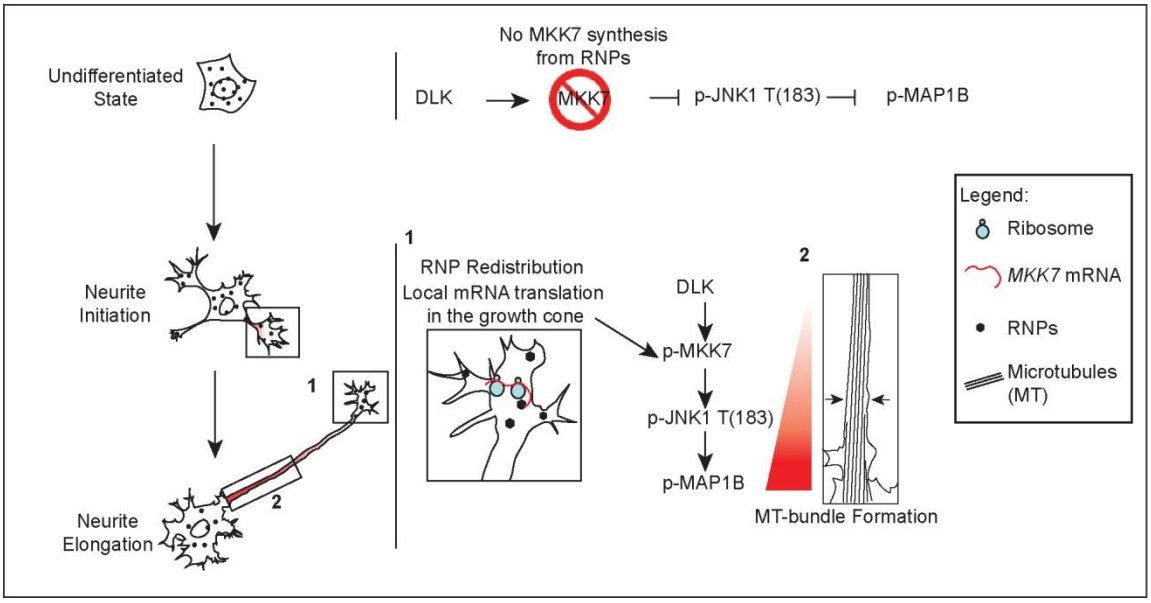

Figure 9. Model of localized JNK signaling during neurite elongation. In the undifferentiated state, in the absence of growth cones, *MKK7* mRNAs remain in RNPs in a translation incompetent state. During neurite initiation, *MKK7* mRNA containing RNPs are transported to the growth cone where local translation occurs. Local MKK7 synthesis and its phosphorylation by DLK allows to switch on JNK1, MAP1b phosphorylation and mt bundling to ultimately allow neurite elongation.

Material and Methods

Cell culture, transfection and immunofluorescence

N1E-115 neuroblastoma cells (American Tissue Culture Collection) were cultured in Dulbecco's modified Eagle's medium (DMEM) supplemented with 10% FBS, 1% L-Glutamine and 1% penicillin/streptomycin. For differentiation, N1E-115 cells were starved for 24h in serum-free Neurobasal medium (Invitrogen) supplemented with 1% L-Glutamine and 1% penicillin/streptomycin. Cells were detached with PUCK's saline and replated on coverslips previously coated with 10 ug/ml laminin (Millipore-Chemicon). For experiments with primary cells, E18 hippocampal neurons were isolated and plated on coverslips coated

with poly-D-Lysine. For plasmid transfection, N1E-115 cells were transfected as previously described (Chong, Lee et al. 2006). For siRNA-mediated KN experiments, $3x10^5$ N1E-115 cells were transfected with 100 pmol of siRNA (Dharmacon siRNA Smartpool Plus) with 6 µl of Dharmafect-2 transfection reagent (Dharmacon) per well (6-well plate) in presence of serum. 48 hours post-transfection cells were starved in neurobasal medium. 72 hours post-transfection cells were used in the different assays. For combinations of siRNA-mediated KN and plasmid transfection, cells were transfected as previously described (Chong, Lee et al. 2006) and 100 pmol of siRNA were added to the transfection mix. In the MKK7 rescue experiments, a single MKK7-specific siRNA (Invitrogen Stealth Select) was used for KN.

Neurite purification, Genechip and RT-qPCR analysis

Neurite purification was performed as described elsewhere (Pertz, Wang et al. 2008). For RNA extraction, the Nucleospin RNA II kit (Macherey–Nagel) was used according to manufacturer's protocol. For western blot analysis, a 1% SDS buffer containing protease inhibitors and 2 mM Vanadate was used. Genechip analysis of soma and neurite total RNA was performed in duplicate. CRNA target synthesis was done starting from 200 ng total RNA using the WT Expression kit (Ambion, In Vitrogen Life Sciences)) following standard recommendations. The further steps were performed according to manufacturer's protocol (Affymetrix). To select differently expressed genes a one-way ANOVA model was applied. Genes were filtered on the basis of an adjusted p-value lower than 0.01. For RT-qPCR analysis, 1 ug of total mRNA lysate was retrotranscribed to cDNA using the ImProm-II Reverse Transcription System (Promega). RT-qPCR analysis was performed using a SYBR green mix (Applied Biosystems), appropriate primers and RPL19 primers for normalization.

Immunofluorescence

N1E-115 cells were washed with phosphate buffered saline (PBS), fixed in 80 mM PIPES, 1 mM MgCl2, 1 mM EGTA, pH 6.8 containing 0.25% glutaraldehyde for 45 seconds and permeabilized in the same buffer containing 0.1% Triton-X for 10 minutes. Coverslips were incubated with 0.2% sodium borohydride in PBS for 20 min, and blocked in 2% BSA, 0.1% Triton-X in PBS for 15 minutes. Cells were stained with primary antibodies for 1 hour, and then with secondary antibodies for 30 min (alexa-fluor 488 labeled phalloidin, Alexa-fluor 546 secondary antibody, and DAPI for 30 minutes (all Invitrogen). For all the other immunofluorescence experiments, N1E-115 cells or day in vitro 1 mouse hippocampal neurons were washed in PBS, fixed in PBS containing 4% paraformaldehyde (Sigma Aldrich) for 20 minutes and permeabilized in PBS containing 1% of Triton-X for 2 minutes. Coverslips were then washed, blocked, stained and mounted as described above.

Fluorescent in-situ hybridization (FISH)

Labeled probes were generated by *in vitro* transcription from restriction-digested plasmids using the DIG RNA labeling mix (Roche) according to the manufacturer's protocol. The FISH protocol is described elsewhere (Vessey, Macchi et al. 2008) and was adapted with the following changes: probes (1 ng/µl) were heated to 70°C for 7 min and incubated on ice for 2 min before applying to fixed cells; after overnight hybridization at 65°C and extensive washes in PBS-0.1% Tween, cells were blocked in blocking buffer (2% BSA PBS-Tween) for 2 h; detection by TSA-Alexa488 or TSA-Alexa546 (Invitrogen) were performed according to the manufacturer's protocol.

Microscopy, image acquisition and analysis

All wide field microscope experiments were performed on an inverted Eclipse Ti microscope (Nikon). Phase contrast live imaging of neurite dynamics: N1E-115 cells were replated on laminin-coated glass-bottom multiwell plates (MatTek). Three to four hours after plating, cells were imaged in Neurobasal medium (Invitrogen) in a heated closed chamber. GFP-tubulin, JNKAR FRET and PalX2-dendra2 live cells imaging experiments: serum-starved, N1E-115 cells transfected with the different constructs were replated on laminin-coated coverslips for different times and imaged in Neurobasal medium supplemented with 10 µg/mL oxyrase reagent (Oxyrase Inc.) in a closed chamber. FRET ratio imaging was performed as described elsewhere (Hodgson, Pertz et al. 2008). In the bleaching experiments, a FRAP3D module (Roper Scientific) was used to bleach a region of interest with 488 nm laser light. Neurite outgrowth analysis: automated neurite segmentation was performed using Metamorph software. For confocal imaging of fixed, stained samples, a Leica TCS SP5 confocal microscope steered was used.

Bioinformatic and statistic analysis

The JNK signaling network was extracted from our previously published neurite proteome dataset (Pertz, Wang et al. 2008) using Ingenuity pathways software (Ingenuity Systems). Only proteins that were enriched in the neurite or found in the neurite and soma fractions were considered. MKK7, MKK4, JNK1, JNK2 and JNK3 were used as "bait" to discover proteins that can directly interact with them. Statistical analysis was performed using GraphPad Prism 5 software (Mozilla Labs). For multiple comparisons One-way anova with Dunnet test with 95% confidence intervals was used, for single comparisons a two-tail unpaired T-test was used.

Antibodies and plasmids

For western blot and immunofluorescence experiments the following antibodies were used: anti-MKK7, anti-JNK1, anti-JIP1, anti-JIP3 (all Santa Cruz Biotechnology), anti-phospho-MKK7 (S271+T275), anti-phospho-JNK (T183+Y185), anti-phospho-JNK (T183), anti-DLK, anti-phospho-MKK4 (S257+T161), anti-phospho-Doublecortin (S28), anti eEF1A1, anti-GluTubulin (all Abcam), anti-phospho-Stathmin (S38), anti-phospho-MAP2 (S136) (all Cell Signaling), anti-MAP2 (Millipore), anti-α-Tubulin, anti-MAP Kinase Activated (T183-Y185), anti-ERK1 (Sigma Aldrich), anti-GFP (Roche), Alexa Fluor350 phalloidin, Alexa Fluor488 phalloidin, Alexa Fluor555 phalloidin (all Invitrogen), DAPI (Sigma Aldrich). GFP-MKK7 (gift of Jiyan Zhang, Institute of Basic Medical Science, Beijing) was mutated to confer siRNA resistance. GFP-MKK7, β-globin (gift of Ian G. Macara, University of Virginia), and PalX2-Dendra (gift of Gary Bassell, Emory University, Atlanta) reporters in eukaryotic expression vectors were all flanked at the 3' with the *MKK7* 3'-UTR 1 and 2 sequences. JNKAR1 and JNKAR1(T/A) genetically encoded FRET probes were a kind gift of Jin Zhang (John Hopkins University School of Medicine, Baltimore). Detailed construct maps are available on request.

Acknowledgements

We are grateful to Michael Kiebler for sharing protocols, to Ian Macara, Jin Zhang, Jiyan Zhang and Gary Bassell for sharing *reagents*, and to Philippe Demougin for help with GeneChips analysis. This work was supported by grants from the Swiss National Science Foundation and from the International Research Foundation for Paraplegy.

Supporting Information figures

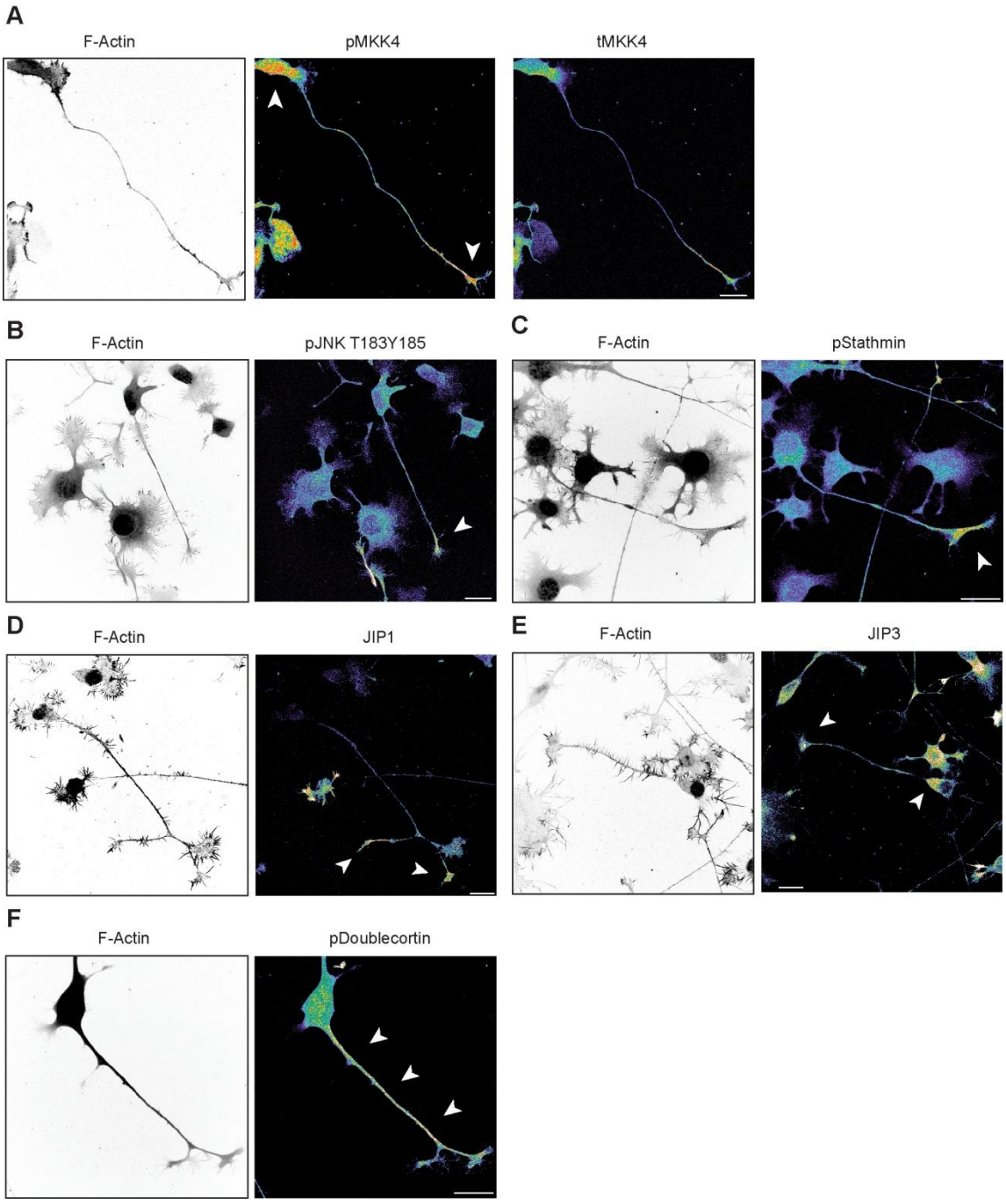

Figure S1. Subcellular localization of additional components of the neurite JNK signaling network. Representative confocal fluorescent micrographs of differentiated N1E-115 cells immunostained for different components are shown. Images are shown with color-coded fluorescence intensities (warm and cold colors represent high and low fluorescence intensities respectively). F-actin images are shown in ibw contrast. (A) pMKK4 and tMKK4. Note inverse distribution compared with pMKK7 with high signal intensity in the growth cone decreasing in the neurite. Substantial pMKK4 signal is also found in the soma. (B) pJNK T183Y185. Note high signal in the growth cone, low signal in the neurite. (C) pStathmin. Note high signal in the growth cone, low signal in the neurite. (D) JIP-1. Note high signal in the growth cone, low signal in the neurite. (E) JIP-3. Note high signal in the growth cone and the soma, low signal in the neurite. (F) pDoublecortin. Note identical signal intensity in the soma and the neurite. Scale bars: 25 µm.

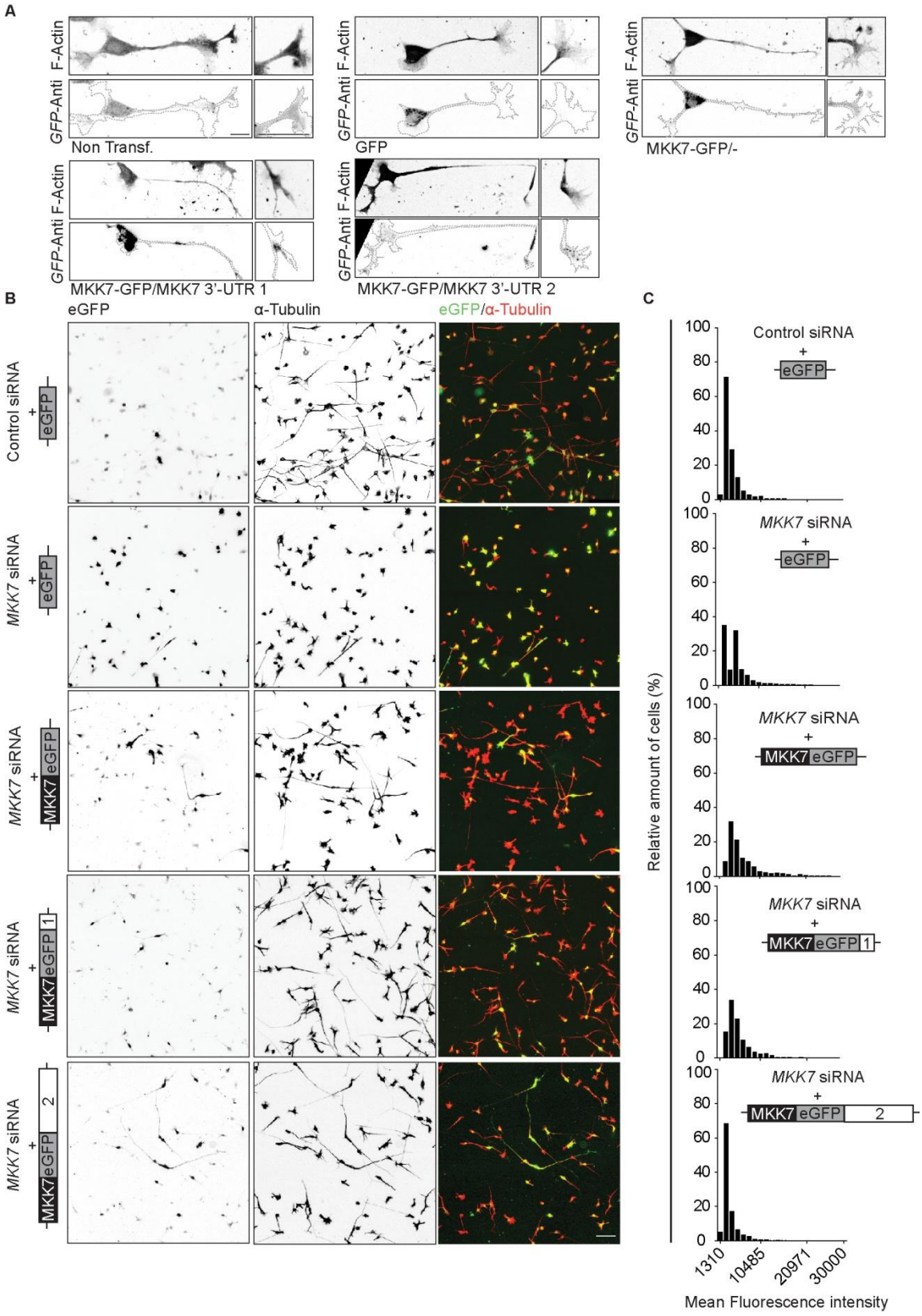
A
F-Actin
GFP-Anti
Non Transf.
GFP
MKK7-GFP/-
MKK7-GFP/MKK7 3'-UTR 1
MKK7-GFP/MKK7 3'-UTR 2
B
eGFP
α-Tubulin
eGFP/α-Tubulin
Control siRNA + eGFP
MKK7 siRNA + eGFP
MKK7 siRNA + MKK7 eGFP
MKK7 siRNA + MKK7 eGFP 1
MKK7 siRNA + MKK7 eGFP 2
C
Control siRNA + eGFP
MKK7 siRNA + eGFP
MKK7 siRNA + MKK7 eGFP
MKK7 siRNA + MKK7 eGFP 1
MKK7 siRNA + MKK7 eGFP 2
Relative amount of cells (%)
0
20
40
60
80
100
1310
10485
20971
30000
Mean Fluorescence intensity

Figure S2. MKK7 knockdown rescue control experiments. (A) FISH controls. Representative confocal fluorescence micrographs of *GFP* mRNA FISH in differentiated N1E-115 cells. Images from non–transfected or cells transfected with eGFP, eGFP-MKK7, eGFP-MKK7/3'-UTR1, eGFP-MKK7/3'-UTR2 are shown. Note that some of these images are also shown in figure 5E. Fluorescence intensity in all images are scaled identically and shown in ibw contrast. F-actin images are also shown. Note that closeup images have been acquired at higher magnification. Scale bar: 25 µm. (B) Representative confocal fluorescence micrographs of eGFP and α-tubulin signals. Fluorescence images are shown in ibw contrast or color composite. Scale bar: 50 µm. (C) Expression level of the different constructs. Occurrence plots of per cell fluorescence intensities. Note lower expression level of the MKK7-eGFP/3'-UTR2 construct.

Figure S3. Neurite-localized JNK network siRNA screen. (A) Total neurite outgrowth measurements. Total neurite outgrowth length measurements in response to knockdown of different components of the 10 % cells with longest neurites are shown. Results of three independent experiments are shown. Statistical significance is shown. In all the experiments mean ± s.d. is shown, n=400 (experiment 1), n=340 (experiment 2), n=500 cells (experiment 3). (B) Representative neurite outgrowth phenotypes. Representative micrographs of α-tubulin immunostained control of siRNA-transfected cells in ibw contrast. Example from one representative experiments is shown. Scale bar: 100 µm. (C) Assessment of knockdown efficiency. Western blot analysis of relative protein level in equal amounts of lysates of cells transfected with a non-targeting control or specific siRNA are shown. Quantification of knockdown efficiency normalized to ERK1 loading control are also shown.

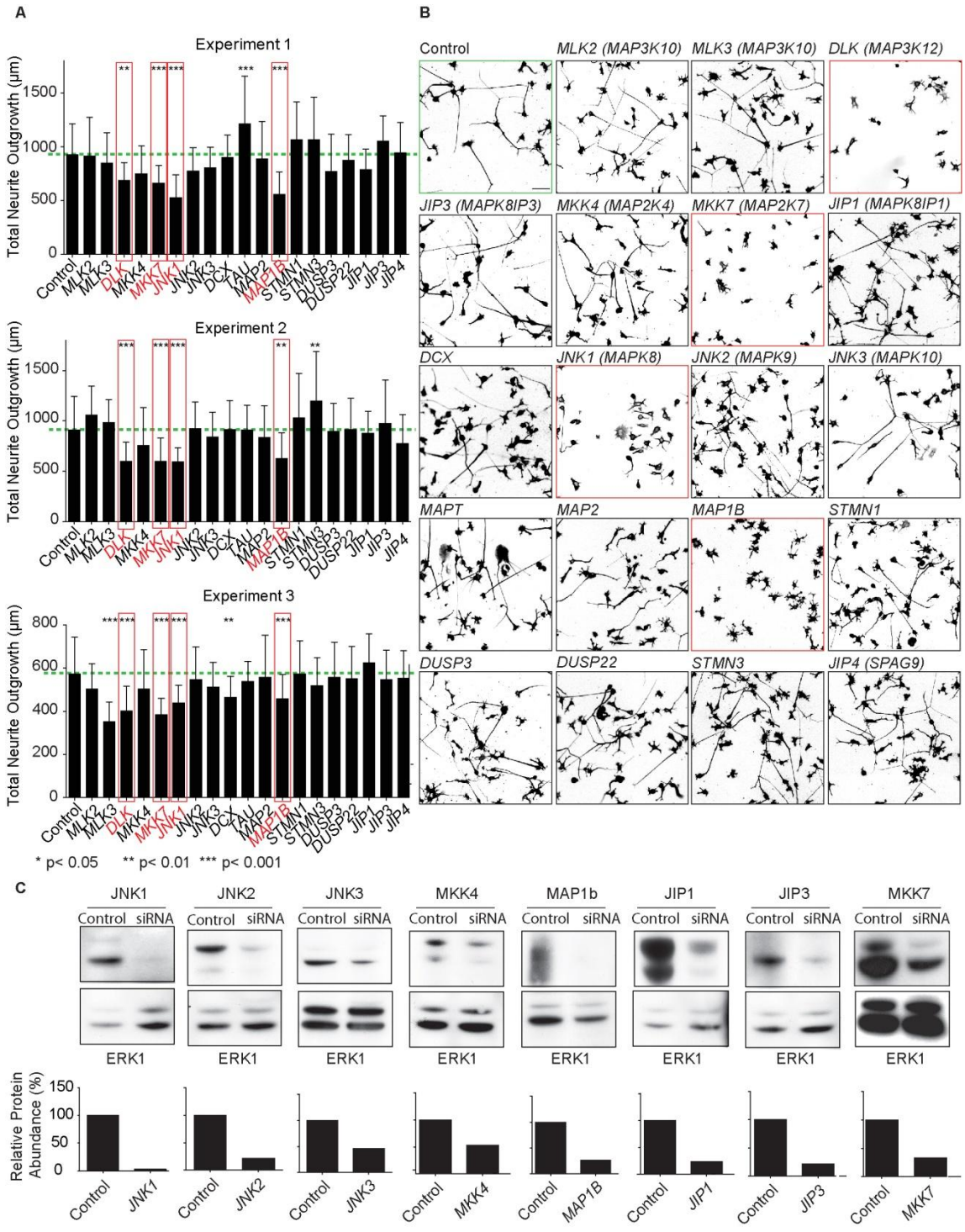
A
Experiment 1
Experiment 2
Experiment 3
Total Neurite Outgrowth (µm)
Control
MLK2
MLK3
DLK
MKK4
MKK7
JNK1
JNK2
JNK3
DCX
TAU
MAP2
MAP1B
STMN1
STMN3
DUSP3
DUSP22
JIP1
JIP3
JIP4
* p< 0.05 ** p< 0.01 *** p< 0.001
B
Control
MLK2 (MAP3K10)
MLK3 (MAP3K10)
DLK (MAP3K12)
JIP3 (MAPK8IP3)
MKK4 (MAP2K4)
MKK7 (MAP2K7)
JIP1 (MAPK8IP1)
DCX
JNK1 (MAPK8)
JNK2 (MAPK9)
JNK3 (MAPK10)
MAPT
MAP2
MAP1B
STMN1
DUSP3
DUSP22
STMN3
JIP4 (SPAG9)
C
JNK1
JNK2
JNK3
MKK4
MAP1b
JIP1
JIP3
MKK7
Control siRNA
ERK1
Relative Protein Abundance (%)

Hugo gene Symbol	Entrez Gene Name	Fold enrichment in the neurite	Location by proteomics	mRNA enriched in fibroblast lammelipod	Function
TP53INP2	tumor protein p53 inducible nuclear protein 2	8.204	n/a	yes	Unknown
CPLX2	complexin 2	6.351	n/a	no	Transmembrane/Synaptic
CYB5R3	cytochrome b5 reductase 3	5.047	n/a	no	Metabolic/Glycolitic
DYNLL2	dynein, light chain, LC8-type 2	4.692	-6	yes	Motor
RAB13	RAB13, member RAS oncogene family	4.345	n/a	yes	Signaling molecule
TRAK2	trafficking protein, kinesin binding 2	4.306	n/a	no	Trafficking Protein
GDF11	growth differentiation factor 11	3.984	n/a	no	Secreted Protein
SH3PXD2A	SH3 and PX domains 2A	3.760	n/a	no	Signaling molecule
INPP1	inositol polyphosphate-1-phosphatase	3.648	-0.1	yes	Signaling molecule
CFLAR	CASP8 and FADD-like apoptosis regulator	3.554	n/a	no	Anti-apoptotic
BCMO1	beta-carotene 15,15'-monooxygenase 1	3.418	2	no	Signaling molecule
MAP2K7	mitogen-activated protein kinase kinase 7	3.325	2	yes	Signaling molecule
VASH1	vasohibin 1	3.257	n/a	no	Secreted Protein
GLT8D3	glycosyltransferase 8 domain containing 3	3.251	-2	no	Metabolic/Glycolitic
EFCAB2	EF-hand calcium binding domain 2	3.110	n/a	no	Signaling molecule
EPM2A	epilepsy, progressive myoclonus type 2A, Lafora disease (laforin)	3.105	n/a	no	Metabolic/Glycolitic
NOL3	nucleolar protein 3 (apoptosis repressor with CARD domain)	2.989	n/a	no	Anti-apoptotic
ZBTB12	zinc finger and BTB domain containing 12	2.929	n/a	yes	Transcription factor
DYNC1LI2	dynein, cytoplasmic 1, light intermediate chain 2	2.901	1.2	no	Motor
GAB2	GRB2-associated binding protein 2	2.874	n/a	yes	Signaling molecule
RAB3C	RAB3C, member RAS oncogene family	2.815	8	no	Trafficking Protein
KCTD10	potassium channel tetramerisation domain containing 10	2.655	n/a	yes	Transmembrane/Synaptic
SYP	synaptophysin	2.567	2.1	no	Transmembrane/Synaptic
DUSP19	dual specificity phosphatase 19	2.482	n/a	no	Signaling molecule
AMMECR1	Alport syndrome, midface hypoplasia and elliptocytosis chromosomal region gene 1	2.395	n/a	no	Unknown
UHMK1	U2AF homology motif (UHM) kinase 1	2.352	n/a	no	Cell cycle
KIF1C	kinesin family member 1C	2.324	n/a	yes	Motor
MAFF	v-maf musculoaponeurotic fibrosarcoma oncogene homolog F (avian)	2.265	-2	no	Transcription factor
KIF5B	kinesin family member 5B	2.237	neurite unique	yes	Motor
KIF1A	kinesin family member 1A	2.235	4.7	no	Motor
PGGT1B	protein geranylgeranyltransferase type I, beta subunit	2.233	n/a	no	Metabolic/Glycolitic
FGD3	FYVE, RhoGEF and PH domain containing 3	2.232	n/a	no	Unknown
C19ORF68	chromosome 19 open reading frame 68	2.231	n/a	no	Unknown
RPL29	ribosomal protein L29	2.231	n/a	no	Protein Synthesis/Degradation
FYCO1	FYVE and coiled-coil domain containing 1	2.219	3	no	Other
APC	adenomatous polyposis coli	2.215	n/a	yes	Apoptosis Regulator
KIF5C	kinesin family member 5C	2.191	2.1	no	Motor
FBXO32	F-box protein 32	2.140	n/a	no	Protein Synthesis/Degradation
WASF3	WAS protein family, member 3	2.125	2.7	no	Cytoskeletal/Structural
NET1	neuroepithelial cell transforming 1	2.094	n/a	no	Signaling molecule
DDR2	discoidin domain receptor tyrosine kinase 2	2.085	3	yes	Transmembrane/Synaptic
ARHGAP11A	Rho GTPase activating protein 11A	2.051	n/a	no	Signaling molecule
KLC4	kinesin light chain 4	2.041	5.5	no	Motor
KIF5A	kinesin family member 5A	1.968	2.1	no	Motor
SYNM	synemin, intermediate filament protein	1.925	13	no	Cytoskeletal/Structural
TRIM56	tripartite motif-containing 56	1.873	n/a	no	Protein Synthesis/Degradation
CACNG4	calcium channel, voltage-dependent, gamma subunit 4	1.872	n/a	no	Transmembrane/Synaptic
KANK2	KN motif and ankyrin repeat domains 2	1.867	n/a	yes	Cytoskeletal/Structural
SAMD4A	sterile alpha motif domain containing 4A	1.856	1.5	no	Protein Synthesis/Degradation
NSBP1	nucleosomal binding protein 1	1.849	n/a	no	Transcription factor
ZEB1	zinc finger E-box binding homeobox 1	1.846	n/a	yes	Transcription factor
WNK1	WNK lysine deficient protein kinase 1	1.843	3.1	no	Signaling molecule
KSR2	kinase suppressor of ras 2	1.825	n/a	no	Signaling molecule
DNAL1	dynein, axonemal, light chain 1	1.807	n/a	no	Motor
ZC3H13	zinc finger CCCH-type containing 13	1.791	1	no	Transcription factor
MAP4	microtubule-associated protein 4	1.784	4.1	no	Cytoskeletal/Structural
TRPM2	transient receptor potential cation channel, subfamily M, member 2	1.771	n/a	no	Transmembrane/Synaptic
AKAP12	A kinase (PRKA) anchor protein 12	1.750	n/a	no	Other
KIF26B	kinesin family member 26B	1.737	n/a	no	Motor
MAPKBP1	mitogen-activated protein kinase binding protein 1	1.727	n/a	no	Signaling molecule
PKP4	plakophilin 4	1.703	n/a	yes	Cytoskeletal/Structural
BRF1	BRF1 homolog, subunit of RNA polymerase III transcription initiation factor IIIB (S. cerev	1.669	n/a	no	Other
HTATSF1	HIV-1 Tat specific factor 1	1.643	n/a	yes	Transcription factor
KLHL12	kelch-like 12 (Drosophila)	1.607	n/a	no	Protein Synthesis/Degradation
TNS1	tensin 1	1.602	n/a	no	Cytoskeletal/Structural
RHOV	ras homolog gene family, member V	1.591	n/a	no	Signaling molecule
GRAP2	GRB2-related adaptor protein 2	1.589	n/a	no	Signaling molecule
ATF5	activating transcription factor 5	1.588	n/a	no	Transcription factor
KLC1	kinesin light chain 1	1.579	4	no	Motor
BSN	bassoon (presynaptic cytomatrix protein)	1.575	n/a	no	Cytoskeletal/Structural
MYRIP	myosin VIIA and Rab interacting protein	1.571	3	no	Cytoskeletal/Structural
PTPN11	protein tyrosine phosphatase, non-receptor type 11	1.571	1	no	Signaling molecule
DST	dystonin	1.567	2	no	Cytoskeletal/Structural
ANK2	ankyrin 2, neuronal	1.545	9	no	Cytoskeletal/Structural
ISLR	immunoglobulin superfamily containing leucine-rich repeat	1.541	3	no	Cytoskeletal/Structural
C5ORF13	chromosome 5 open reading frame 13	1.533	n/a	no	Unknown
PHACTR2	phosphatase and actin regulator 2	1.529	n/a	no	Signaling molecule
UTRN	utrophin	1.514	4	no	Transmembrane/Synaptic
SYNE2	spectrin repeat containing, nuclear envelope 2	1.500	-2	no	Cytoskeletal/Structural

Table S1: Neurite-enriched mRNAs identified in genome-wide screen. Hugo Gene Symbol and Entrez gene names of mRNAs that are enriched more than 1.5 times in the neurite versus the soma fraction are shown. Neurite or soma localization of the products encoded by the different mRNAs are also shown according to our previously published N1E-115 neurite and soma proteomes (Pertz, Wang et al. 2008). Some proteins were not identified in our proteome and are marked as non-available (n/a). Otherwise, the ratio of the spectral peptide count in the neurite versus the soma is shown, with positive values showing neurite enriched and negative values showing soma enriched proteins. For one of the protein, peptides were only found in the neurite (neurite unique). MRNAs that have also been found to be enriched in fibroblast pseudopods (Mili, Moissoglu et al. 2008) are also indicated. Finally, the function of the different genes is shown.

Symbol	Entrez Gene Name	Neurite Enrichment	Entrez Gene IDMouse
DCX	doublecortin	1.00	13193
DUSP22	dual specificity phosphatase 22	1.00	105352
DUSP3	dual specificity phosphatase 3	1.09	72349
MAP1B	microtubule-associated protein 1B	2.50	17755
MAP2	microtubule-associated protein 2	5.00	17756
MAP2K4	mitogen-activated protein kinase kinase 4	1.67	26398
MAP2K7	mitogen-activated protein kinase kinase 7	2.00	26400
MAP3K10	mitogen-activated protein kinase kinase kinase 10	1.00	269881
MAP3K11	mitogen-activated protein kinase kinase kinase 11	1.00	26403
MAP3K12	mitogen-activated protein kinase kinase kinase 12	8.00	26404
MAPK10	mitogen-activated protein kinase 10	1.00	26414
MAPK8	mitogen-activated protein kinase 8	2.00	26419
MAPK8IP1	mitogen-activated protein kinase 8 interacting protein 1	1.00	19099
MAPK8IP3	mitogen-activated protein kinase 8 interacting protein 3	2.25	30957
MAPK9	mitogen-activated protein kinase 9	1.00	26420
MAPT	microtubule-associated protein tau	1.00	17762
SPAG9	sperm associated antigen 9	1.55	70834
STMN1	stathmin 1	1.00	16765
STMN3	stathmin-like 3	3.50	20262

Table S2: Description of neurite-enriched JNK signaling network genes targeted in the siRNA screen. Hugo gene symbol and Entrez Gene name and ID are shown along with protein enrichment according to our previously published N1E-115 neurite and soma proteomes (Pertz, Wang et al. 2008).

Supporting Information movies

Movie S1. JNK phosphorylation dynamics in differentiating N1E-115 cells.

FRET emission ratio is shown for JNKAR and control, non-phosphorylatable JNKAR probes. Images are color-coded so that warm and cold colors represent high and low levels of JNK activation respectively. Timescale is in hours:minutes. Scale bar: 25 µm.

Movie S2. Neurite extension dynamics of control and MKK7-siRNA transfected N1E-115 differentiating cells.

Phase contrast timelapse imaging of control and MKK7 knockdown are shown. Timescale is in hours:minutes. Scale bar: 50 µm. Note highly instable neurite outgrowth in the MKK7 knockdown cells.

Movie S3. Microtubule dynamics of control and MKK7-siRNA transfected N1E-115 differentiating cells.

Fluorescence confocal microscopy images of control and MKK7 knockdown cells expressing GFP-tubulin are shown in ibw contrast. Timescale is in hours:minutes. Scale bar: 25 µm.

Movie S4. Microtubule dynamics in control and MKK7 knockdown N1E-115 differentiating N1E-115 cells.

Epifluorescence microscopy images of control and MKK7 knockdown cells expressing GFP-tubulin are shown in ibw contrast. Timescale is in hours:minutes. Scale bar: 25 □m.

Movie S5. MKK7 knockdown rescue experiment.

Neurite extension dynamics of differentiating N1E-115 cells transfected with: 1. control siRNA and GFP, 2. *MKK7* siRNA and GFP, or 3. MKK7 siRNA and GFP-MKK7/-. Phase contrast timelapse imaging and GFP fluorescence signal in ibw contrast are shown. GFP channel was acquired every 5th frame. Timescale is in hours:minutes. Scale bar: 50 µm. Note partial rescue of neurite elongation with the GFP-MKK7/- construct.

Movie S6. MKK7 knockdown rescue experiment.

Neurite extension dynamics of differentiating N1E-115 cells transfected with: 1. control siRNA and GFP, 2. *MKK7* siRNA and GFP-MKK7/3'-UTR1, or 3. MKK7 siRNA and GFP-MKK7/3'-UTR2. Phase contrast timelapse imaging and GFP fluorescence signal in ibw contrast are shown. GFP channel was acquired every 5th frame. Timescale is in hours:minutes. Scale bar: 50 µm. Note robust rescue of neurite elongation with the GFP-MKK7/3'-UTR1 and GFP-MKK7/3'-UTR2 constructs. Also note highly unstable neurite extension in GFP-negative cells.

Movie S7. Visualization of growth cone mRNA translation dynamics using PalX2-Dendra2 reporters.

Timelapse movie of growth cones of N1E-115 cells expressing the PalX2-Dendra2/-, PalX2-dendra2/3'-UTR1 or PalX2-dendra2/3'-UTR2 reporters pre- and post-bleaching are shown. Dendra2 fluorescence signals and DIC images are shown. Fluorescence images are color-coded so that warm and cold colors represent high and low fluorescence intensities. Pre- and post-bleaching images are scaled differently so that signal is not saturated in the pre-bleached state. Note that the bleached region of interest is much larger than the growth cone portion that is shown. Note robust fluorescence recovery of PalX2-Dendra2 reporters flanked with *MKK7* mRNA 3'-UTRs. Timescale is in minutes. Scale bar: 12 µm.

Movie S8. Neurite extension dynamics of control and DLK, JNK1 or MAP1b siRNA transfected N1E-115 differentiating cells.

Phase contrast timelapse imaging of control and the different knockdown cells are shown. Timescale is in hours:minutes. Scale bar: 50 µm. Note highly instable neurite outgrowth in all knockdown cells.

7. Summarizing Conclusions

7. Summarizing Conclusions

Local mRNA translation can be described as a sophisticated mechanism that contributes to the control of gene expression in addition to the more traditionally studied control of transcription, processing of the messenger and regulation of translation initiation. This process allows the cell to tightly regulate protein function in time and space. Indeed, the function of a protein might be needed only in particular subcellular locations in defined moments, in response to a number of stimuli. One of the purposes that lead a cell to localize and locally produce a protein is merely economy-related: a neuron would produce proteins in-situ without expenditure of energy, related to long distance transport, and of time, rather than transporting a pool of proteins to the site (Schuman 1999). But this is not the only reason why local translation occurs: ectopic production of a protein, for instance, can have harmful effects on the cell. It is therefore more convenient to synthesize it at a specific subcellular location rather than producing it everywhere and maybe degrading it or inactivating it where it is not needed. (Boggs 2006)

Local mRNA translation has extensively been studied in dendrites and in axons and it has been demonstrated to be essential for synaptic plasticity and during axonal guidance (Skup 2008) (Leung, van Horck et al. 2006). Nevertheless, the attention of the neurobiologists never focused on the early phases of neuronal differentiation, before the axon/dendrite specification step.

Does local mRNA translation occur also in neurites?

We performed a genome-wide analysis for mRNA localization in an N1E-115 neuroblastoma cell line and identified 80 neurite-enriched mRNAs, transcripts encoding for proteins that are involved in a big variety of functions. We found mRNAs encoding signaling proteins, cytoskeletal regulators, motors, trafficking proteins, anti-apoptotic factors, secreted proteins and even transcription factors. Among them we found that the mRNA encoding the MAP kinase kinase 7 (MKK7), a component of the JNK-signaling pathway, is three times enriched in neurites compared to the cell body. Detection of the messenger with fluorescent *in-situ* hybridization allowed us to visualize a great proportion of mRNA packed in granules and stored in the growth cone upon induction of differentiation (Results Figure 1D, p.65). We hypothesize that these granules might be ribonucleoparticles, packed structures that contain RNA-binding proteins and ribosomal proteins in addition to the mRNA and are bound to motors for their transport. Asymmetric localization of transcripts is determined, with very few exceptions, by *cis*-elements that are present in the 3' untranslated regions of the messengers (Kislauskis and Singer 1992). Experimentally we demonstrated the validity of

this statement for *MKK7* mRNA by flanking reporters alternatively with one of the two known 3'-UTRs of MKK7 and visualizing the exogenous mRNA localization in N1E-115 cells. Only one of the two 3'-UTRs led to an enrichment of the transcript in neurites, but both allowed to localize the mRNA specifically in growth cones (Results Figure 5 A-E, p73).

Classical experiments for the visualization of local mRNA translation are performed in NGF- or BDNF-stimulated neurons using reporters that consist of a destabilized fluorophore (deGFP) that is fused to a membrane targeting sequence (that limits the diffusion of the protein) flanked with the localizing mRNA portion (generally the 3'-UTR). The 3'-UTR allows the localization of the transcript and the newly locally synthesized fluorophore will be trapped in the membrane thanks to the membrane targeting sequence (Aakalu, Smith et al. 2001). The PEST-destabilizing sequence reduces the half-life of the fluorophore, limiting the diffusion of the protein. We tried this approach, but unfortunately without success: the absence of an external cue for the induction of protein synthesis limited our chances to visualize very low amounts of newly synthesized proteins. Alternatively a photoconvertible fluorophore (EOS or Dendra) can be used instead of a classical green fluorescent protein: photoconvertible proteins can be converted from green to red upon a flash of UV light (405 nm). Kristy Welshhans and Gary Bassell observed green fluorescence recovery in growth cones of hippocampal neurons, after photoconversion of the growth cone itself and of the distal part of the axon, thus formally demonstrating local mRNA translation of the reporter (Welshhans and Bassell 2011). We tried this approach as well, once more without success: the incomplete photoconversion of Dendra, together with the absence of protein synthesis inducing cues didn't allow us to visualize newly synthesized green Dendra. We overtook these problems by modifying our approach: instead of photoconverting Dendra, we decided to simply bleach the growth cone and a big portion of the neurite and observe the recovery of the green signal in these cellular portions. The very high bleaching efficiency allowed us to visualize also small increases in green fluorescence signals. We demonstrated that the fluorescence can be recovered only when Dendra is flanked with one or the other 3'-UTR sequences of MKK7 and, in addition, that the recovery is abolished upon treatment with the translation inhibitor anisomycin.

We formally demonstrated that local mRNA translation occurs in neurites and that the localization of the mRNA encoding for MKK7 is driven by determinants that are present in the 3'-UTRs.

What is the role of MKK7 in neurite outgrowth?

The JNK signaling pathway is one of four mitogen-activated kinase cascades that have been identified in mammalians (see Figure 14 p.40). JNKs are also called stress-activated MAP

kinases (SAPKs) for their involvement in the response to stress: JNK is known to be activated by treatment of cells with cytokines, such as TNF and IL-1 and by exposure of the cells to many different forms of environmental stress (e.g. osmotic stress, red-ox stress, radiations) (Ip and Davis 1998). The main effect that the specific phosphorylation of Ser-63 and Ser-73 by JNK achieves, is an increased transcriptional activity of the Activation Factor 1 (AP-1), a transcription factor which is a heterodimeric protein composed of proteins belonging to the c-Fos, c-Jun, ATF and JDP families (Pulverer, Kyriakis et al. 1991). In addition, JNK can activate also other transcription factors, including JunB, JunD and ATF2, via phosphorylation of a common Ser/Thr-Pro motif located in the activation motif of the transcription factors. Therefore, JNK activity is to been seen preferentially in the nucleus, where it drives the transcription of pro- or anti-apoptotic genes. The non nuclear targets of JNK activate the caspase cascade leading to apoptosis.

Surprisingly, when we looked at the subcellular localization of the activated, phosphorylated form of MKK7, which is upstream of JNKs and directly activates them by phosphorylation, we saw that it was almost exclusively located in the shaft of neurites (see Results Figure 2 A-C p67) and not in the nucleus. MKK7 phosphorylates preferentially JNKs on the Threonine in their T-P-Y motif (T-loop) thereby inducing their activation. We therefore looked at the localization of the activated JNKs using an antibody that recognizes specifically the Thr-monophosphorylated form of JNK (T183) and we found it enriched, like the phosphorylated MKK7, in the shaft of neurites (see Results Figure 3 A-C p.69). Moreover, it is excluded from the nucleus, suggesting a different, extra-nuclear role for JNKs than the control of cellular stress.

When we knocked down *Mkk7* using small interference RNAs (siRNAs) we observed severe defects in neurite outgrowth in knock down cells compared to the control. In N1E-115 knock down cells, neurites can still sprout, but they can't elongate and the defect is related to the inability to bundle and therefore rigidify microtubules in the neurite shaft. The literature shows an involvement of JNK in the regulation of the cytoskeleton and in particular of the microtubules, via phosphorylation of microtubule associated proteins (MAPs) that can stabilize microtubules. We therefore examined the localization of activated, phosphorylated MAPs and found that pMAP2 and pMAP1B, two known downstream effectors of JNKs, are also localized in the shaft of neurites (see Results Figure 3 G,H p69).

Thus, MKK7 allows neurite extension in N1E-115 cells and, most likely, it does it through the activation of the JNK pathway and the action of MAPs.

Is a specific JNK signaling network involved in the control of neurite extension?

The studies that try to assign cytoskeleton-stabilizing functions to JNK are quite nebulous. Which of the JNKs does what? Which upstream MAPKKK acts on MKKs? And which MAP is involved in which process? We tried to define if a specific JNK signaling network can be directly responsible for a successful neurite elongation in our cell system and, for this purpose, we used a systemic approach. We reconstructed *in silico* the possible cytoskeleton-regulating JNK network using the Ingenuity Pathway software, taking advantage of the previous published N1E-115 proteome (see Results Figure 7 A p.77) (Pertz, Wang et al. 2008). We first verified the localization of the components of the network by immunofluorescence, using available antibodies. We found that, in addition to phosphorylated MKK7, mono-phosphorylated JNK (T183), pMAP1B and pMAP2, the upstream kinase DLK is extremely enriched in the neurite shaft. Also the analysis of the proteome confirms this data, by showing an 8 times enrichment of the protein in the neurite compared to the cell body.

Interestingly, we found that the double phosphorylated form of JNK (T183 and Y185) is located in growth cones together with the activated, phosphorylated MKK4 (pMKK4), the scaffold proteins JIP1 and JIP3 and with the phosphorylated microtubule destabilizer Stathmin1, suggesting the existence of two distinct branches of the JNK pathway with distinct functions. This last evidence confirms the observation of a subcellular localization of pJNK T183-Y185 in the growth cones of hippocampal neurons during axonal guidance (Oliva, Atkins et al. 2006).

We continued our exploration of the JNK network using an siRNA approach. We knocked down each component of the network and analyzed the phenotypes, in terms of neurite outgrowth, protrusion-retraction dynamics and microtubules stability. We found that DLK, MKK7, JNK1 and MAP1B phenocopy each other in all three analyzed aspects (see Results Figure 7B-D p.77). This results are consisting with previously reported findings: 1) DLK regulates microtubule stabilization during neuronal outgrowth (Hirai, Banba et al. 2011); 2) DLK preferentially phosphorylates MKK7 (versus MKK4) in vitro (Merritt, Mata et al. 1999); MKK7 preferentially phosphorylate T183 (versus Y185) in JNKs (Lawler, Fleming et al. 1998); 4) DLK regulates microtubule stability through JNK1 (Hirai, Banba et al. 2011); 5) JNK1 has specifically been linked to microtubule regulation through MAP phosphorylation in the brain (Chang, Jones et al. 2003). In addition FRET experiments confirmed this findings by showing an enhanced activity of a JNK probe in the neurite shaft during neurite extension.

In our work we formally demonstrated that one specific branch of the JNK signaling pathway is involved in the stabilization of the microtubules, which is essential for neurite extension. This function is achieved by the formation of a space restricted signaling module in the neurite shaft. A second parallel signaling module consisting of MKK4, other JNK isoforms (namely JNK2) and Stahmin1 is excluded from this process and could be involved in the guidance of the neurite, due to its specific activity in the growth cone.

Is the local translation of MKK7 mRNA required for the function of the DLK-JNK1-MKK7-MAP1B axes in the neurite shaft?

To address this question we performed a functional study of the locally synthesized MKK7. We tried to rescue the *Mkk7* knock down phenotype with the co-transfection of different siRNA resistant constructs and MKK7 siRNAs. We used vectors carrying GFP alone, GFP fused to the coding sequence of MKK7 or GFP-MKK7 with one or the other 3'UTRs of MKK7 that allow the correct localization of the transcript and therefore the local translation of the messenger. We observed that only when locally synthesized (with the GFP-MKK7/3'-UTR), MKK7 was able to fully rescue the phenotype, confirming the importance of the local production of the protein (see Results Figure 5 p.73).

From these experiments we can conclude that the local translation of MKK7 is essential for the localization of the DLK-JNK1-MKK7-MAP1B signaling module correctly in the neurite shaft, allowing it to stabilize the microtubules and guarantee an efficient extension of the neurites.

Are the findings limited to the N1E-115 neuroblastoma cell line?

We asked ourselves if our findings are limited to N1E-115 cells or if the described mechanism could also occur in primary neurons. To address this question we performed immunofluorescence experiments in E-18 mouse hippocampal primary neurons in culture as well as *in situ* hybridization. We chose these cells in agreement with the Allen brain atlas that shows high expression of MKK7 in the hippocampus and because of the wide use of hippocampal primary neurons in the study of neuronal differentiation and axonal guidance. We performed our experiments in day *in vitro* 1 neurons, thus during the early stages of neuronal differentiation, before the axon/dendrites specification step. Consistently with the observations in N1E-115 cells, also in primary neurons the DLK-MKK7-JNK1-MAP1B signaling module localizes in the neurite shaft suggesting that the explored mechanism can well be occurring in neurons as well. As a further confirmation, also in neurons the double-phosphorylated fraction of JNK localizes to the growth cones, as already described in

previous studies (Oliva, Atkins et al. 2006). In addition, *Mkk7* RNA granules can be seen in the growth cones of mouse primary neurons (see Results Figure 8 p.79).

In conclusion, this study allowed to first identify a specific spatio-temporal JNK signaling module that is necessary for an efficient neurite outgrowth. The network has to be correctly localized in the neurite shaft in order to ensure the stabilization of the microtubules and the local translation of the mRNA encoding for MKK7 is necessary for this purpose. Furthermore, the JNK signaling network is sequestered form the nucleus where it is required for the transcriptional regulation of genes that are involved in the control of apoptosis.

8. Discussion and Outlook

8. Discussion and Outlook

In our work we demonstrated that local translation of the mRNA encoding the MAP kinase kinase MKK7 occurs in the growth cone. This allows to activate a specific JNK signaling module that it is necessary for the MAP1B-dependent stabilization of microtubules during neurite elongation. This novel finding raises intriguing questions and opens the doors to further investigations.

How is MKK7 mRNA transported to the growth cone?

One first, important step that can help answering this question is the identification of determinants in the mRNA encoding for MKK7, such as binding sites and secondary structures. The specific subcellular localization of transcripts is driven, with very few exceptions, by *cis*-elements that are present in the 3'-UTR (Kislauskis and Singer 1992). RNA binding proteins, such as Staufen, FMRP, SYNCRIP, Pur-α can interact with the messengers and with other proteins inducing the formation of dense RNA-granules that can be loaded on motors (kinesin, myosins and dyneins) and transported along the cytoskeleton. In our study we confirmed that MKK7 3'-UTR is essential for targeting the messenger to the growth cone. Nevertheless, a preliminary bio-informatic analysis didn't allow us to detect any known *cis*-element in this region. The identification of new determinants might allow to determine which RNA-binding proteins are involved in the transport and the control of translation, including motors, translational repressor and eventually components of the translational machinery. Experimental approaches will be then needed for the validation of bio-informatic findings.

How is local MKK7 mRNA translation induced in the growth cone?

Our work suggests that cell-geometry could be implicated in the control of translation in a cell autonomous manner. We propose that a growth cone can be seen as a platform for translation, a physical support where this process can occur. Our data show that the contact of cells with a correct extracellular matrix together with serum-starvation is sufficient to induce local synthesis of MKK7, without any additional stimulus, such as NGF or BDNF, in N1E-115 cells. Our hypothesis is therefore that integrins, molecules that are the most responsible for geometry changes, could switch on local translation. This idea is supported by the evidence that ribosomes, RNA binding proteins and mRNAs localize to adhesion complexes (Chicurel, Singer et al. 1998) and that β-actin mRNA translation is induced by Src-dependent phosphorylation of the translational repressor ZBP-1 at the adhesion sites (Huttelmaier, Zenklusen et al. 2005). One intriguing possibility is suggested by Flanagan's group studies: they showed that DCC, a Netrin receptor, co-localizes with ribosomes in

growth cones, sequestering them and keeping them in an inactivated state. Binding of Netrin-1 induces a conformational change of the receptor, allowing the release of ribosomes and therefore the possibility to synthesize proteins (Tcherkezian, Brittis et al. 2010). Integrins could similarly sequester ribosomes and release them upon a matrix-dependent conformational change.

What are the functions of the identified JNK-signaling pathways?

In addition to the DLK-MKK7-JNK1-MAP1B signaling module, our data suggest the existence of a second pathway that includes MKK4, the dually phosphorylated JNK (pJNKT183-Y185), Stathmin and JIP1/3. All of these proteins share a same discrete localization patter in the growth cone, rather than at the base of the neurite. The knock down of these components didn't lead to any defects in terms of neurite outgrowth, microtubule stability in the neurite shaft or protrusion-retraction dynamics, suggesting a different involvement in the regulation of neuronal differentiation. Interestingly, Banker's group visualized the double phosphorylated form of JNK in the growth cone of developing hippocampal neurons and assigned to this form of activated JNK a role in axon specification, but not in dendritogenesis (Oliva, Atkins et al. 2006). Our hypothesis is therefore that the second signaling module that we identified could be specifically involved in a second phase of development, during the axon-specification process. Further studies in primary neurons are therefore needed in order to better characterize the two different signaling networks at different stages of differentiation.

Our work lacks information about JNK3. In our screen we observed that the knock down of *jnk3* doesn't lead to any obvious defect. This result is surprising, considering the high enrichment of this JNK in the brain and its involvement in neuritogenesis in DRG neurons (Barnat, Enslen et al. 2010). Once more it is confirmed that JNKs have distinct functions in different cells and in different cell contexts.

How is the identified JNK signaling module kept in place?

Our work demonstrates that a specific JNK signaling module is localized at the base of neurites. It is not clear which mechanism allows to keep it in place, preventing activated molecule to diffuse towards the soma.

Already 40 years ago Conradi demonstrated the existence in motoneurons of a physical barrier, the so-called axonal initiation segment (or axon hillock), that can separate the axonal compartment from the soma (Conradi 1966). This initial portion of the axon has the main function to allow the propagation of action potentials from the soma throughout the axon towards the synapses. Nevertheless, other structural functions have been assigned to it: the particular structure of the hillock that resembles a membrane cytoskeleton, made of Ankyrin

G (AnkG), Amphyphysin II and actin, limits the diffusion of proteins from the axon to the soma and *vice versa* in rat primary neurons (Winckler, Forscher et al. 1999). The idea that also in our system this filter could play a major role derives from the observation of immunofluorescence staining of the studied proteins. pMKK7, like pJNK (T183), DLK and MAP1B are visible in dense structures that could well be oligomers or signalosomes. Our hypothesis is that a physical barrier could limit the transit of such structures towards the cell body and could allow to keep them in the neurite shaft. Nevertheless, the analysis of the distribution of AnkG in our cell line together with knock down experiments of *AnkG* could not demonstrate this hypothesis, but further, more specific investigations are needed.

Alternatively, the signaling module could be kept in place in the neurite shaft by another barrier, made of septins (Xie, Vessey et al. 2007). Interestingly, proteomics analysis of N1E-115 cells reveals a high enrichment of some Septin family members in the neurite (Pertz, Wang et al. 2008).

we observed that some proteins that belong to this family are enriched in the neurite Eventually an active phosphatase that can inactivate the components of the pathway could be localized at the neck of the neurite, just inside the soma. In our work we individuated some candidates that could play this role; nevertheless, knock down of these phosphoteses didn't show any obvious result in terms of neurite outgrowth, a read-out that is maybe not ideal for studying this function at the neurite neck.

What is the role of DLK?

Depending on the cellular context, DLK regulates neurite outgrowth (Hirai, Banba et al. 2011), but also axon regeneration (Yan D 2009) as well as degeneration upon neuronal injury (Miller, Press et al. 2009), (Sengupta Ghosh, Wang et al. 2011), (Xiong, Wang et al. 2010). In the latter context, DLK regulates both Wallerian degeneration (Miller, Press et al. 2009) and retrograde shuttling of JNK signaling complexes to the nucleus (Sengupta Ghosh, Wang et al. 2011), (Xiong, Wang et al. 2010). Consistently with a cell autonomous switch, an interesting possibility is that growth cone elimination through injury, which should lead to a loss of MKK7 local translation, might allow DLK to be coupled with distinct JNK signaling complexes that regulate the latter functions. In this context, the regeneration function of DLK is known to occur through MKK4 (Yan D 2009). Local translation of MKK7 mRNA would therefore be the key mechanism that leads DLK toward the promotion of neurite extension rather than the induction of Wallerian degeneration or neuronal regeneration after injury, through MKK4.

Are other neurite-enriched mRNAs also locally translated? And for which purpose?

In a genome-wide screen we identified 80 mRNAs that are enriched in neurites compared to cell bodies. They encode a number of proteins that have local functions in the neurite (e.g. motors, trafficking proteins, cytoskeletal proteins and secreted factors), but also signaling proteins, anti-apoptotic factors (Nol3 and CFLAR) and even transcription factors (ZEB1, ZC3H13, MAFF, KANK2, ZBTB12). The growth cone can be once more the platform for local translation and provide the synthesis of proteins that will be used directly at the site or retrogradely transported to the cell body and/or to the nucleus where they can exert their functions (activate transcription or control apoptosis). An example of local translation and retrograde transport of the protein has been provided by Jaffrey's group. The authors showed that the mRNA encoding for the transcription factor CREB can be locally translated in growth cones, phosphorylated and retrogradely transported to the nucleus, where it induces the transcription of pro-surviving genes (Cox, Hengst et al. 2008).

9. References

9. Reference

Aakalu, G., W. B. Smith, et al. (2001). "Dynamic Visualization of Local Protein Synthesis in Hippocampal Neurons." Neuron 30(2): 489-502.

Abe, N. and V. Cavalli (2008). "Nerve injury signaling." Curr Opin Neurobiol 18(3): 276-283.

Ackmann, M., H. Wiech, et al. (2000). "Nonsaturable Binding Indicates Clustering of Tau on the Microtubule Surface in a Paired Helical Filament-like Conformation." Journal of Biological Chemistry 275(39): 30335-30343.

Adereth, Y., V. Dammai, et al. (2005). "RNA-dependent integrin [alpha]3 protein localization regulated by the Muscleblind-like protein MLP1." Nat Cell Biol 7(12): 1240-1247.

Ainger, K., D. Avossa, et al. (1993). "Transport and localization of exogenous myelin basic protein mRNA microinjected into oligodendrocytes." The Journal of Cell Biology 123(2): 431-441.

Alonso, A., J. Sasin, et al. (2004). "Protein Tyrosine Phosphatases in the Human Genome." Cell 117(6): 699-711.

Amos, L. A. and J. Löwe (1999). "How Taxol® stabilises microtubule structure." Chemistry & Biology 6(3): R65-R69.

Amos, L. A. and D. Schlieper (2005). Microtubules and Maps. Advances in Protein Chemistry. M. S. John and A. D. P. David, Academic Press. Volume 71: 257-298.

An, J. J., K. Gharami, et al. (2008). "Distinct Role of Long 3'-UTR BDNF mRNA in Spine Morphology and Synaptic Plasticity in Hippocampal Neurons." Cell 134(1): 175-187.

Andreassi, C., C. Zimmermann, et al. (2010). "An NGF-responsive element targets myo-inositol monophosphatase-1 mRNA to sympathetic neuron axons." Nat Neurosci 13(3): 291-301.

Baas, P. W. and D. W. Buster (2004). "Slow axonal transport and the genesis of neuronal morphology." Journal of Neurobiology 58(1): 3-17.

Bardwell, A. J., E. Frankson, et al. (2009). "Selectivity of Docking Sites in MAPK Kinases." Journal of Biological Chemistry 284(19): 13165-13173.

Barnat, M., H. Enslen, et al. (2010). "Distinct Roles of c-Jun N-Terminal Kinase Isoforms in Neurite Initiation and Elongation during Axonal Regeneration." The Journal of Neuroscience 30(23): 7804-7816.

Barrett, L. E., J. Y. Sul, et al. (2006). "Region-directed phototransfection reveals the functional significance of a dendritically synthesized transcription factor." Nat Methods 3(6): 455-460.

Baud, V., Z.-G. Liu, et al. (1999). "Signaling by proinflammatory cytokines: oligomerization of TRAF2 and TRAF6 is sufficient for JNK and IKK activation and target gene induction via an amino-terminal effector domain." Genes & Development 13(10): 1297-1308.

Becker, E., U. Huynh-Do, et al. (2000). "Nck-Interacting Ste20 Kinase Couples Eph Receptors to c-Jun N-Terminal Kinase and Integrin Activation." Mol. Cell. Biol. 20(5): 1537-1545.

Besse, F. and A. Ephrussi (2008). "Translational control of localized mRNAs: restricting protein synthesis in space and time." Nat Rev Mol Cell Biol 9(12): 971-980.

Bettinger, B. T. and D. C. Amberg (2007). "The MEK kinases MEKK4/Ssk2p facilitate complexity in the stress signaling responses of diverse systems." Journal of Cellular Biochemistry 101(1): 34-43.

Bingol, B. and E. M. Schuman (2006). "Activity-dependent dynamics and sequestration of proteasomes in dendritic spines." Nature 441(7097): 1144-1148.

Björkblom, B., J. C. Vainio, et al. (2008). "All JNKs Can Kill, but Nuclear Localization Is Critical for Neuronal Death." Journal of Biological Chemistry 283(28): 19704-19713.

Boggs, J. (2006). "Myelin basic protein: a multifunctional protein." Cellular and Molecular Life Sciences 63(17): 1945-1961.

Bogoyevitch, M. A. and B. Kobe (2006). "Uses for JNK: the Many and Varied Substrates of the c-Jun N-Terminal Kinases." Microbiol. Mol. Biol. Rev. 70(4): 1061-1095.

Bosc, C., A. Andrieux, et al. (2003). "STOP Proteins†." Biochemistry 42(42): 12125-12132.

Bradshaw, K. D., N. J. Emptage, et al. (2003). "A role for dendritic protein synthesis in hippocampal late LTP." European Journal of Neuroscience 18(11): 3150-3152.

Brecht, S., R. Kirchhof, et al. (2005). "Specific pathophysiological functions of JNK isoforms in the brain." European Journal of Neuroscience 21(2): 363-377.

Campbell, D. S. and C. E. Holt (2001). "Chemotropic Responses of Retinal Growth Cones Mediated by Rapid Local Protein Synthesis and Degradation." Neuron 32(6): 1013-1026.

Cantiello, H. F. (1997). "Role of actin filament organization in cell volume and ion channel regulation." Journal of Experimental Zoology 279(5): 425-435.

Carlsson, A. E. (2010). "Actin Dynamics: From Nanoscale to Microscale." Annu Rev Biophys 39: 91–110.

Carson, J. H., H. Cui, et al. (2001). "The balance of power in RNA trafficking." Current Opinion in Neurobiology 11(5): 558-563.

Cassimeris L, S. C. (2001). "Regulation of microtubule-associated proteins." Int Rev Cytol 210: 163-226.

Cavalli, V., P. Kujala, et al. (2005). "Sunday Driver links axonal transport to damage signaling." The Journal of Cell Biology 168(5): 775-787.

Chang, L., Y. Jones, et al. (2003). "JNK1 Is Required for Maintenance of Neuronal Microtubules and Controls Phosphorylation of Microtubule-Associated Proteins." Developmental Cell 4(4): 521-533.

Cheeseman, I. M. and A. Desai (2008). "Molecular architecture of the kinetochore-microtubule interface." Nat Rev Mol Cell Biol 9(1): 33-46.

Chekulaeva, M., M. W. Hentze, et al. (2006). "Bruno Acts as a Dual Repressor of oskar Translation, Promoting mRNA Oligomerization and Formation of Silencing Particles." Cell 124(3): 521-533.

Chen, J., Y. Kanai, et al. (1992). "Projection domains of MAP2 and tau determine spacings between microtubules in dendrites and axons." Nature 360(6405): 674-677.

Chicurel, M. E., R. H. Singer, et al. (1998). "Integrin binding and mechanical tension induce movement of mRNA and ribosomes to focal adhesions." Nature 392(6677): 730-733.

Chicurel, M. E., R. H. Singer, et al. (1998). "Integrin binding and mechanical tension induce movement of mRNA and ribosomes to focal adhesions." Nature 392(6677): 730-733.

Chong, K. W., A. Y. Lee, et al. (2006). "pH dependent high transfection efficiency of mouse neuroblastomas using TransFectin." J Neurosci Methods 158(1): 56-63.

Coffey, E. T., V. Hongisto, et al. (2000). "Dual roles for c-Jun N-terminal kinase in developmental and stress responses in cerebellar granule neurons." J Neurosci 20(20): 7602-7613.

Conradi, S. (1966). "Ultrastructural specialization of the initial axon segment of cat lumbar motoneurons. Preliminary observations." Acta Soc Med Ups 71(5): 281-284.

Cooper, G. M. (2000). "Intermediate Filaments." The Cell, A Molecular Approach 2nd edition.

Cooper, J. A. and D. A. Schafer (2000). "Control of actin assembly and disassembly at filament ends." Current Opinion in Cell Biology 12(1): 97-103.

Coso, O. A., M. Chiariello, et al. (1995). "The small GTP-binding proteins Rac1 and Cdc42regulate the activity of the JNK/SAPK signaling pathway." Cell 81(7): 1137-1146.

Cox, L. J., U. Hengst, et al. (2008). "Intra-axonal translation and retrograde trafficking of CREB promotes neuronal survival." Nat Cell Biol 10(2): 149-159.

Cunningham, S. C., E. Gallmeier, et al. (2006). "Targeted Deletion of MKK4 in Cancer Cells: A Detrimental Phenotype Manifests as Decreased Experimental Metastasis and Suggests a Counterweight to the Evolution of Tumor-Suppressor Loss." Cancer Research 66(11): 5560-5564.

Dahanukar, A., J. A. Walker, et al. (1999). "Smaug, a Novel RNA-Binding Protein that Operates a Translational Switch in Drosophila." Molecular Cell 4(2): 209-218.

Dajas-Bailador, F., E. V. Jones, et al. (2008). "The JIP1 scaffold protein regulates axonal development in cortical neurons." Curr Biol 18(3): 221-226.

David J, K. (1999). "Functions of gelsolin: motility, signaling, apoptosis, cancer." Current Opinion in Cell Biology 11(1): 103-108.

Davis, R. (2000). "Signal Transduction by the JNK Group of MAP Kinases." Cell 103(2): 239-252.

de Hoog, C. L., L. J. Foster, et al. (2004). "RNA and RNA binding proteins participate in early stages of cell spreading through spreading initiation centers." Cell 117(5): 649-662.

Dehmelt, L. and S. Halpain (2004). "Actin and microtubules in neurite initiation: Are MAPs the missing link?" Journal of Neurobiology 58(1): 18-33.

Deng, Y., R. H. Singer, et al. (2008). "Translation of ASH1 mRNA is repressed by Puf6p–Fun12p/eIF5B interaction and released by CK2 phosphorylation." Genes & Development 22(8): 1037-1050.

Desai, A., S. Verma, et al. (1999). "Kin I Kinesins Are Microtubule-Destabilizing Enzymes." Cell 96(1): 69-78.

Dhanasekaran, D. N., K. Kashef, et al. (2007). "Scaffold proteins of MAP-kinase modules." Oncogene 26(22): 3185-3202.

Di Paolo, G., V. Pellier, et al. (1996). "The phosphoprotein stathmin is essential for nerve growth factor-stimulated differentiation." The Journal of Cell Biology 133(6): 1383-1390.

Du, T.-G., M. Schmid, et al. (2007). "Why cells move messages: The biological functions of mRNA localization." Seminars in Cell & Developmental Biology 18(2): 171-177.

Eliscovich, C., I. Peset, et al. (2008). "Spindle-localized CPE-mediated translation controls meiotic chromosome segregation." Nat Cell Biol 10(7): 858-865.

Elvira, G., S. Wasiak, et al. (2006). "Characterization of an RNA Granule from Developing Brain." Molecular & Cellular Proteomics 5(4): 635-651.

Eminel, S., L. Roemer, et al. (2008). "c-Jun N-terminal kinases trigger both degeneration and neurite outgrowth in primary hippocampal and cortical neurons." Journal of Neurochemistry 104(4): 957-969.

Eto, K., T. Kawauchi, et al. (2010). "Role of dual leucine zipper-bearing kinase (DLK/MUK/ZPK) in axonal growth." Neuroscience Research 66(1): 37-45.

Fan, M. and T. C. Chambers (2001). "Role of mitogen-activated protein kinases in the response of tumor cells to chemotherapy." Drug Resistance Updates 4(4): 253-267.

Fanara, P., B. Oback, et al. (1999). "Identification of MINUS, a small polypeptide that functions as a microtubule nucleation suppressor." EMBO J 18(3): 565-577.

Fivaz, M. and T. Meyer (2003). "Specific localization and timing in neuronal signal transduction mediated by protein-lipid interactions." Neuron 40(2): 319-330.

Fleming, Y., C. G. Armstrong, et al. (2000). "Synergistic activation of stress-activated protein kinase 1/c-Jun N-terminal kinase (SAPK1/JNK) isoforms by mitogen-activated protein kinase kinase 4 (MKK4) and MKK7." Biochem J 352 Pt 1: 145-154.

Fosbrink, M., N. N. Aye-Han, et al. (2010). "Visualization of JNK activity dynamics with a genetically encoded fluorescent biosensor." Proc Natl Acad Sci U S A 107(12): 5459-5464.

Friocourt, G., P. Marcorelles, et al. (2011). "Role of cytoskeletal abnormalities in the neuropathology and pathophysiology of type I lissencephaly." Acta Neuropathologica 121(2): 149-170.

G.R Fanger, T. K. S. a. G. L. J. (2000). "Control of MAPK signaling by Ste20- and Ste11-like kinases." Signaling Networks and Cell Cycle Control, Humana Press: 183–211.

Ganiatsas, S., L. Kwee, et al. (1998). "SEK1 deficiency reveals mitogen-activated protein kinase cascade crossregulation and leads to abnormal hepatogenesis." Proceedings of the National Academy of Sciences 95(12): 6881-6886.

Gardiol, A., C. Racca, et al. (1999). "Dendritic and Postsynaptic Protein Synthetic Machinery." The Journal of Neuroscience 19(1): 168-179.

Gdalyahu, A., I. Ghosh, et al. (2004). "DCX, a new mediator of the JNK pathway." EMBO J 23(4): 823-832.

Gigant, B., P. A. Curmi, et al. (2000). "The 4 Å X-Ray Structure of a Tubulin:Stathmin-like Domain Complex." Cell 102(6): 809-816.

Glanzer, J., K. Y. Miyashiro, et al. (2005). "RNA splicing capability of live neuronal dendrites." Proceedings of the National Academy of Sciences of the United States of America 102(46): 16859-16864.

González-Billault, C., M. Engelke, et al. (2002). "Participation of structural microtubule-associated proteins (MAPs) in the development of neuronal polarity." Journal of Neuroscience Research 67(6): 713-719.

Grenningloh, G., S. Soehrman, et al. (2004). "Role of the microtubule destabilizing proteins SCG10 and stathmin in neuronal growth." Journal of Neurobiology 58(1): 60-69.

Grooms, S. Y., K.-M. Noh, et al. (2006). "Activity Bidirectionally Regulates AMPA Receptor mRNA Abundance in Dendrites of Hippocampal Neurons." The Journal of Neuroscience 26(32): 8339-8351.

Gumy, L. F., G. S. H. Yeo, et al. (2011). "Transcriptome analysis of embryonic and adult sensory axons reveals changes in mRNA repertoire localization." RNA 17(1): 85-98.

Guo, C. and A. J. Whitmarsh (2008). "The β-Arrestin-2 Scaffold Protein Promotes c-Jun N-terminal Kinase-3 Activation by Binding to Its Nonconserved N Terminus." Journal of Biological Chemistry 283(23): 15903-15911.

Haeusgen, W., T. Herdegen, et al. (2010). "Specific regulation of JNK signalling by the novel rat MKK7γ1 isoform." Cellular Signalling 22(11): 1761-1772.

Haeusgen, W., T. Herdegen, et al. (2011). "The bottleneck of JNK signaling: Molecular and functional characteristics of MKK4 and MKK7." European Journal of Cell Biology 90(6-7): 536-544.

Hanz, S., E. Perlson, et al. (2003). "Axoplasmic Importins Enable Retrograde Injury Signaling in Lesioned Nerve." Neuron 40(6): 1095-1104.

Harada, A., K. Oguchi, et al. (1994). "Altered microtubule organization in small-calibre axons of mice lacking tau protein." Nature 369(6480): 488-491.

Harada, A., J. Teng, et al. (2002). "MAP2 is required for dendrite elongation, PKA anchoring in dendrites, and proper PKA signal transduction." The Journal of Cell Biology 158(3): 541-549.

Harper, S. J., Lo Grasso, P. (2001). "Inhibitors of the JNK signaling pathway." Drugs of the Future 26(10): 957.

Heald, R. and E. Nogales (2002). "Microtubule dynamics." Journal of Cell Science 115(1): 3-4.

Hermann H, H. R. (1998). "Sub-cellular biochemistry - Intermediate filaments." Plenum Press.

Hill, M. and P. Gunning (1993). "Beta and gamma actin mRNAs are differentially located within myoblasts." The Journal of Cell Biology 122(4): 825-832.

Hirai, S., Y. Banba, et al. (2011). "Axon formation in neocortical neurons depends on stage-specific regulation of microtubule stability by the dual leucine zipper kinase-c-Jun N-terminal kinase pathway." J Neurosci 31(17): 6468-6480.

Ho, D. T., A. J. Bardwell, et al. (2006). "Interacting JNK-docking Sites in MKK7 Promote Binding and Activation of JNK Mitogen-activated Protein Kinases." Journal of Biological Chemistry 281(19): 13169-13179.

Hodgson, L., O. Pertz, et al. (2008). "Design and optimization of genetically encoded fluorescent biosensors: GTPase biosensors." Methods Cell Biol 85: 63-81.

Holland, P. M., M. Suzanne, et al. (1997). "MKK7 Is A Stress-activated Mitogen-activated Protein Kinase Kinase Functionally Related to hemipterous." Journal of Biological Chemistry 272(40): 24994-24998.

Holt, C. E. and S. L. Bullock (2009). "Subcellular mRNA localization in animal cells and why it matters." Science 326(5957): 1212-1216.

Huang, C., K. Jacobson, et al. (2004). "MAP kinases and cell migration." Journal of Cell Science 117(20): 4619-4628.

Huber, K. M., M. S. Kayser, et al. (2000). "Role for Rapid Dendritic Protein Synthesis in Hippocampal mGluR-Dependent Long-Term Depression." Science 288(5469): 1254-1256.

Hughes, J. R., S. L. Bullock, et al. (2004). "inscuteable mRNA Localization Is Dynein-Dependent and Regulates Apicobasal Polarity and Spindle Length in Drosophila Neuroblasts." Current Biology 14(21): 1950-1956.

Husson, C., F.-X. Cantrelle, et al. (2010). "Multifunctionality of the β-thymosin/WH2 module: G-actin sequestration, actin filament growth, nucleation, and severing." Annals of the New York Academy of Sciences 1194(1): 44-52.

Huttelmaier, S., D. Zenklusen, et al. (2005). "Spatial regulation of beta-actin translation by Src-dependent phosphorylation of ZBP1." Nature 438(7067): 512-515.

Ingber, D. E. (1993). "Cellular tensegrity: defining new rules of biological design that govern the cytoskeleton." Journal of Cell Science 104(3): 613-627.

Inoue, Y. H., M. S. Savoian, et al. (2004). "Mutations in orbit/mast reveal that the central spindle is comprised of two microtubule populations, those that initiate cleavage and those that propagate furrow ingression." The Journal of Cell Biology 166(1): 49-60.

Ip, Y. T. and R. J. Davis (1998). "Signal transduction by the c-Jun N-terminal kinase (JNK) — from inflammation to development." Current Opinion in Cell Biology 10(2): 205-219.

Jaffe, A. B., A. Hall, et al. (2005). "Association of CNK1 with Rho Guanine Nucleotide Exchange Factors Controls Signaling Specificity Downstream of Rho." Current Biology 15(5): 405-412.

Johnson, G. L. and K. Nakamura (2007). "The c-jun kinase/stress-activated pathway: Regulation, function and role in human disease." Biochimica et Biophysica Acta (BBA) - Molecular Cell Research 1773(8): 1341-1348.

Jung, H., C. M. O'Hare, et al. (2011). "Translational regulation in growth cones." Current Opinion in Genetics & Development 21(4): 458-464.

Kanai, Y., N. Dohmae, et al. (2004). "Kinesin Transports RNA: Isolation and Characterization of an RNA-Transporting Granule." Neuron 43(4): 513-525.

Kang, H., L. Z. Jia, et al. (1996). "Determinants of BDNF-induced hippocampal synaptic plasticity: role of the Trk B receptor and the kinetics of neurotrophin delivery." Learning & Memory 3(2-3): 188-196.

Kar, S., J. Fan, et al. (2003). "Repeat motifs of tau bind to the insides of microtubules in the absence of taxol." EMBO J 22(1): 70-77.

Kar, S., G. J. Florence, et al. (2003). "Discodermolide interferes with the binding of tau protein to microtubules." FEBS Letters 539(1-3): 34-36.

Kavallaris, M. (2010). "Microtubules and resistance to tubulin-binding agents." Nat Rev Cancer 10(3): 194-204.

Kawauchi, T., K. Chihama, et al. (2003). "The in vivo roles of STEF/Tiam1, Rac1 and JNK in cortical neuronal migration." EMBO J 22(16): 4190-4201.

Kawauchi, T., K. Chihama, et al. (2005). "MAP1B phosphorylation is differentially regulated by Cdk5/p35, Cdk5/p25, and JNK." Biochemical and Biophysical Research Communications 331(1): 50-55.

Kelkar, N., S. Gupta, et al. (2000). "Interaction of a Mitogen-Activated Protein Kinase Signaling Module with the Neuronal Protein JIP3." Mol. Cell. Biol. 20(3): 1030-1043.

Kiebler, M. A. and G. J. Bassell (2006). "Neuronal RNA granules: movers and makers." Neuron 51(6): 685-690.

Kiebler, M. A. and G. J. Bassell (2006). "Neuronal RNA Granules: Movers and Makers." Neuron 51(6): 685-690.

Kim, M. H., T. Cierpicki, et al. (2003). "The DCX-domain tandems of doublecortin and doublecortin-like kinase." Nat Struct Mol Biol 10(5): 324-333.

Kishimoto, H., K. Nakagawa, et al. (2003). "Different Properties of SEK1 and MKK7 in Dual Phosphorylation of Stress-induced Activated Protein Kinase SAPK/JNK in Embryonic Stem Cells." Journal of Biological Chemistry 278(19): 16595-16601.

Kislauskis, E. H., Z. Li, et al. (1993). "Isoform-specific 3'-untranslated sequences sort alpha-cardiac and beta-cytoplasmic actin messenger RNAs to different cytoplasmic compartments." The Journal of Cell Biology 123(1): 165-172.

Kislauskis, E. H. and R. H. Singer (1992). "Determinants of mRNA localization." Current Opinion in Cell Biology 4(6): 975-978.

Kislauskis, E. H., X. Zhu, et al. (1994). "Sequences responsible for intracellular localization of beta-actin messenger RNA also affect cell phenotype." The Journal of Cell Biology 127(2): 441-451.

Kopp, E., R. Medzhitov, et al. (1999). "ECSIT is an evolutionarily conserved intermediate in the Toll/IL-1 signal transduction pathway." Genes & Development 13(16): 2059-2071.

Kreis, J. S. a. T. E. (1991). "Motor protein independent binding of endocytic carrier vesicles to microtubules in vitro." J. Biol. Chem 266: 18141–18148.

Kress, T. L., Y. J. Yoon, et al. (2004). "Nuclear RNP complex assembly initiates cytoplasmic RNA localization." The Journal of Cell Biology 165(2): 203-211.

Krichevsky, A. M. and K. S. Kosik (2001). "Neuronal RNA Granules: A Link between RNA Localization and Stimulation-Dependent Translation." Neuron 32(4): 683-696.

Kuan, C.-Y., D. D. Yang, et al. (1999). "The Jnk1 and Jnk2 Protein Kinases Are Required for Regional Specific Apoptosis during Early Brain Development." Neuron 22(4): 667-676.

Kukekov, N. V., Z. Xu, et al. (2006). "Direct Interaction of the Molecular Scaffolds POSH and JIP Is Required for Apoptotic Activation of JNKs." Journal of Biological Chemistry 281(22): 15517-15524.

Kuwako, K.-i., K. Kakumoto, et al. (2010). "Neural RNA-Binding Protein Musashi1 Controls Midline Crossing of Precerebellar Neurons through Posttranscriptional Regulation of Robo3/Rig-1 Expression." Neuron 67(3): 407-421.

Kyriakis, J. M. and J. Avruch (1990). "pp54 microtubule-associated protein 2 kinase. A novel serine/threonine protein kinase regulated by phosphorylation and stimulated by poly-L-lysine." Journal of Biological Chemistry 265(28): 17355-17363.

Lau, A. G., H. A. Irier, et al. (2010). "Distinct 3′UTRs differentially regulate activity-dependent translation of brain-derived neurotrophic factor (BDNF)." Proceedings of the National Academy of Sciences 107(36): 15945-15950.

Lawler, S., Y. Fleming, et al. (1998). "Synergistic activation of SAPK1/JNK1 by two MAP kinase kinases in vitro." Current Biology 8(25): 1387-1391.

Lécuyer, E., H. Yoshida, et al. (2007). "Global Analysis of mRNA Localization Reveals a Prominent Role in Organizing Cellular Architecture and Function." Cell 131(1): 174-187.

Lee, C. M., D. Onésime, et al. (2002). "JLP: A scaffolding protein that tethers JNK/p38MAPK signaling modules and transcription factors." Proceedings of the National Academy of Sciences 99(22): 14189-14194.

Lee JK, H. W., Lee YD, Han PL. (1999). "Dynamic expression of SEK1 suggests multiple roles of the gene during embryogenesis and in adult brain of mice." Brain Res Mol Brain Res 20(66): 133-140.

Leung, K. M., F. P. van Horck, et al. (2006). "Asymmetrical beta-actin mRNA translation in growth cones mediates attractive turning to netrin-1." Nat Neurosci 9(10): 1247-1256.

Li, C., G. j. Bassell, et al. (2009). "Fragile X mental retardation protein is involved in protein synthesis-dependent collapse of growth cones induced by Semaphorin-3A." Frontiers in Neural Circuits 3.

Li, S., J. Finley, et al. (2002). "Crystal Structure of the Cytoskeleton-associated Protein Glycine-rich (CAP-Gly) Domain." Journal of Biological Chemistry 277(50): 48596-48601.

Lin, A. C. and C. E. Holt (2007). "Local translation and directional steering in axons." EMBO J 26(16): 3729-3736.

Lin, A. C. and C. E. Holt (2008). "Function and regulation of local axonal translation." Current Opinion in Neurobiology 18(1): 60-68.

Lin, D., T. V. Pestova, et al. (2008). "Translational Control by a Small RNA: Dendritic BC1 RNA Targets the Eukaryotic Initiation Factor 4A Helicase Mechanism." Mol. Cell. Biol. 28(9): 3008-3019.

Lindwall, C., L. Dahlin, et al. (2004). "Inhibition of c-Jun phosphorylation reduces axonal outgrowth of adult rat nodose ganglia and dorsal root ganglia sensory neurons." Molecular and Cellular Neuroscience 27(3): 267-279.

Lindwall, C. and M. Kanje (2005). "Retrograde axonal transport of JNK signaling molecules influence injury induced nuclear changes in p-c-Jun and ATF3 in adult rat sensory neurons." Molecular and Cellular Neuroscience 29(2): 269-282.

Liu, Q.-R., L. Lu, et al. (2006). "Rodent BDNF genes, novel promoters, novel splice variants, and regulation by cocaine." Brain Research 1067(1): 1-12.

Lomaga, M. A., W.-C. Yeh, et al. (1999). "TRAF6 deficiency results in osteopetrosis and defective interleukin-1, CD40, and LPS signaling." Genes & Development 13(8): 1015-1024.

Marillat, V., C. Sabatier, et al. (2004). "The Slit Receptor Rig-1/Robo3 Controls Midline Crossing by Hindbrain Precerebellar Neurons and Axons." Neuron 43(1): 69-79.

Mark W Kieran1, S. K., Brenda Vail1, Leonard I Zon1 and Bruce J Mayer (1999). "Concentration-dependent positive and negative regulation of a MAP kinase by a MAP kinase kinase." Oncogene 18(48): 6647-6657.

Martin, K. C., A. Casadio, et al. (1997). "Synapse-Specific, Long-Term Facilitation of Aplysia Sensory to Motor Synapses: A Function for Local Protein Synthesis in Memory Storage." Cell 91(7): 927-938.

Martin, K. C. and A. Ephrussi (2009). "mRNA Localization: Gene Expression in the Spatial Dimension." Cell 136(4): 719-730.

Martin, K. C. and R. S. Zukin (2006). "RNA trafficking and local protein synthesis in dendrites: an overview." J Neurosci 26(27): 7131-7134.

McNally, K. P., D. Buster, et al. (2002). "Katanin-mediated microtubule severing can be regulated by multiple mechanisms." Cell Motility and the Cytoskeleton 53(4): 337-349.

Merianda, T. T., A. C. Lin, et al. (2009). "A functional equivalent of endoplasmic reticulum and Golgi in axons for secretion of locally synthesized proteins." Molecular and Cellular Neuroscience 40(2): 128-142.

Merritt, S. E., M. Mata, et al. (1999). "The mixed lineage kinase DLK utilizes MKK7 and not MKK4 as substrate." J Biol Chem 274(15): 10195-10202.

Merritt, S. E., M. Mata, et al. (1999). "The Mixed Lineage Kinase DLK Utilizes MKK7 and Not MKK4 as Substrate." Journal of Biological Chemistry 274(15): 10195-10202.

Michael, C. (2001). "Protein phosphatase 5 in signal transduction." Trends in Endocrinology & Metabolism 12(1): 28-32.

Mili, S., K. Moissoglu, et al. (2008). "Genome-wide screen reveals APC-associated RNAs enriched in cell protrusions." Nature 453(7191): 115-119.

Miller, B. R., C. Press, et al. (2009). "A dual leucine kinase-dependent axon self-destruction program promotes Wallerian degeneration." Nat Neurosci 12(4): 387-389.

Miller, S., M. Yasuda, et al. (2002). "Disruption of Dendritic Translation of CaMKIIα Impairs Stabilization of Synaptic Plasticity and Memory Consolidation." Neuron 36(3): 507-519.

Minden, A., A. Lin, et al. (1995). "Selective activation of the JNK signaling cascadeand c-Jun transcriptional activity by the small GTPases Rac and Cdc42Hs." Cell 81(7): 1147-1157.

Mitchison, T. and M. Kirschner (1984). "Dynamic instability of microtubule growth." Nature 312(5991): 237-242.

Miyamoto, K., V. Pasque, et al. (2011). "Nuclear actin polymerization is required for transcriptional reprogramming of Oct4 by oocytes." Genes & Development 25(9): 946-958.

Mooney, L. M. and A. J. Whitmarsh (2004). "Docking Interactions in the c-Jun N-terminal Kinase Pathway." Journal of Biological Chemistry 279(12): 11843-11852.

Nakagawa, K., M. Sugahara, et al. (2010). "Filamin associates with stress signalling kinases MKK7 and MKK4 and regulates JNK activation." Biochemical Journal 427(2): 237-245.

Nakamura, A., K. Sato, et al. (2004). "Drosophila Cup Is an eIF4E Binding Protein that Associates with Bruno and Regulates oskar mRNA Translation in Oogenesis." Developmental Cell 6(1): 69-78.

Newbern, J., A. Taylor, et al. (2007). "c-Jun N-terminal kinase signaling regulates events associated with both health and degeneration in motoneurons." Neuroscience 147(3): 680-692.

Ng, D. C., T. T. Zhao, et al. (2010). "c-Jun N-terminal kinase phosphorylation of stathmin confers protection against cellular stress." J Biol Chem 285(37): 29001-29013.

Nguyen, P., T. Abel, et al. (1994). "Requirement of a critical period of transcription for induction of a late phase of LTP." Science 265(5175): 1104-1107.

Nie, D., A. Di Nardo, et al. (2010). "Tsc2-Rheb signaling regulates EphA-mediated axon guidance." Nat Neurosci 13(2): 163-172.

Nishina, H., T. Wada, et al. (2004). "Physiological Roles of SAPK/JNK Signaling Pathway." Journal of Biochemistry 136(2): 123-126.

Nishitoh, H., M. Saitoh, et al. (1998). "ASK1 Is Essential for JNK/SAPK Activation by TRAF2." Molecular Cell 2(3): 389-395.

Nogales, E., M. Whittaker, et al. (1999). "High-Resolution Model of the Microtubule." Cell 96(1): 79-88.

Okabe, M., T. Imai, et al. (2001). "Translational repression determines a neuronal potential in Drosophila asymmetric cell division." Nature 411(6833): 94-98.

Oliva, A. A., C. M. Atkins, et al. (2006). "Activated c-Jun N-Terminal Kinase Is Required for Axon Formation." The Journal of Neuroscience 26(37): 9462-9470.

Ostroff, L. E., J. C. Fiala, et al. (2002). "Polyribosomes Redistribute from Dendritic Shafts into Spines with Enlarged Synapses during LTP in Developing Rat Hippocampal Slices." Neuron 35(3): 535-545.

Oyang, E. L., B. C. Davidson, et al. (2011). "Functional Characterization of the Dendritically Localized mRNA Neuronatin in Hippocampal Neurons." PLoS One 6(9): e24879.

Paquin, N., M. Ménade, et al. (2007). "Local Activation of Yeast ASH1 mRNA Translation through Phosphorylation of Khd1p by the Casein Kinase Yck1p." Molecular Cell 26(6): 795-809.

Peng, J., M. J. Kim, et al. (2004). "Semiquantitative Proteomic Analysis of Rat Forebrain Postsynaptic Density Fractions by Mass Spectrometry." Journal of Biological Chemistry 279(20): 21003-21011.

Perlson, E., S. Hanz, et al. (2005). "Vimentin-Dependent Spatial Translocation of an Activated MAP Kinase in Injured Nerve." Neuron 45(5): 715-726.

Pertz, O. C., Y. Wang, et al. (2008). "Spatial mapping of the neurite and soma proteomes reveals a functional Cdc42/Rac regulatory network." Proc Natl Acad Sci U S A 105(6): 1931-1936.

Pierce, J. P., K. van Leyen, et al. (2000). "Translocation machinery for synthesis of integral membrane and secretory proteins in dendritic spines." Nat Neurosci 3(4): 311-313.

Pierre, G. (2002). "Nuclear Envelope: Torn Apart at Mitosis." Current Biology 12(7): R242-R244.

Piper, M., R. Anderson, et al. (2006). "Signaling Mechanisms Underlying Slit2-Induced Collapse of Xenopus Retinal Growth Cones." Neuron 49(2): 215-228.

Pulverer, B. J., J. M. Kyriakis, et al. (1991). "Phosphorylation of c-jun mediated by MAP kinases." Nature 353(6345): 670-674.

Raman, M., W. Chen, et al. (2007). "Differential regulation and properties of MAPKs." Oncogene 26(22): 3100-3112.

Ravelli, R. B. G., B. Gigant, et al. (2004). "Insight into tubulin regulation from a complex with colchicine and a stathmin-like domain." Nature 428(6979): 198-202.

Reinhard, C., B. Shamoon, et al. (1997). "Tumor necrosis factor [alpha]-induced activation of c-jun N-terminal kinase is mediated by TRAF2." EMBO J 16(5): 1080-1092.

Rincón, M., A. Whitmarsh, et al. (1998). "The JNK Pathway Regulates the In Vivo Deletion of Immature CD4+CD8+ Thymocytes." The Journal of Experimental Medicine 188(10): 1817-1830.

Robert G, O. (2007). "Intermediate filaments: A historical perspective." Experimental Cell Research 313(10): 1981-1994.

Rook, M. S., M. Lu, et al. (2000). "CaMKIIα 3′ Untranslated Region-Directed mRNA Translocation in Living Neurons: Visualization by GFP Linkage." The Journal of Neuroscience 20(17): 6385-6393.

S A Endow, S. J. K., L L Satterwhite, M D Rose, V P Skeen, and E D Salmon (1994). "Yeast Kar3 is a minus-end microtubule motor protein that destabilizes microtubules preferentially at the minus ends." embo journal 13(11): 2708–2713.

S Gupta, T. B., A J Whitmarsh, J Cavanagh, H K Sluss, B Dérijard, and R J Davis (1996). "Selective interaction of JNK protein kinase isoforms with transcription factors." EMBO J 15(11): 2760–2770.

Sabapathy, K., W. Jochum, et al. (1999). "Defective neural tube morphogenesis and altered apoptosis in the absence of both JNK1 and JNK2." Mechanisms of Development 89(1-2): 115-124.

-Nido, et al. (2000). "Phosphorylation of microtubule-associated protein 2 (MAP2) and its relevance for the regulation of the neuronal cytoskeleton function." Progress in Neurobiology 61(2): 133-168.

Sapir, T., D. Horesh, et al. (2000). "Doublecortin mutations cluster in evolutionarily conserved functional domains." Human Molecular Genetics 9(5): 703-712.

Sasaki, Y., K. Welshhans, et al. (2010). "Phosphorylation of Zipcode Binding Protein 1 Is Required for Brain-Derived Neurotrophic Factor Signaling of Local β-Actin Synthesis and Growth Cone Turning." The Journal of Neuroscience 30(28): 9349-9358.

Sato, S., H. Sanjo, et al. (2005). "Essential function for the kinase TAK1 in innate and adaptive immune responses." Nat Immunol 6(11): 1087-1095.

Schaeffer, H. J. and M. J. Weber (1999). "Mitogen-Activated Protein Kinases: Specific Messages from Ubiquitous Messengers." Mol. Cell. Biol. 19(4): 2435-2444.

Schratt, G. M., F. Tuebing, et al. (2006). "A brain-specific microRNA regulates dendritic spine development." Nature 439(7074): 283-289.

Schuman, E. M. (1999). "mRNA Trafficking and Local Protein Synthesis at the Synapse." Neuron 23(4): 645-648.

Sengupta Ghosh, A., B. Wang, et al. (2011). "DLK induces developmental neuronal degeneration via selective regulation of proapoptotic JNK activity." J Cell Biol 194(5): 751-764.

Skup, M. (2008). "Dendrites as separate compartment – local protein synthesis." Acta Neurobiol Exp 68: 305–321.

Song, L., J. Li, et al. (2006). "IKKβ programs to turn on the GADD45α–MKK4–JNK apoptotic cascade specifically via p50 NF-κB in arsenite response." The Journal of Cell Biology 175(4): 607-617.

Steward, O. and E. M. Schuman (2003). "Compartmentalized Synthesis and Degradation of Proteins in Neurons." Neuron 40(2): 347-359.

Steward, O. and P. F. Worley (2001). "Selective Targeting of Newly Synthesized Arc mRNA to Active Synapses Requires NMDA Receptor Activation." Neuron 30(1): 227-240.

Sun, Y., T. Yang, et al. (2007). "The JNK Pathway and Neuronal Migration." Journal of Genetics and Genomics 34(11): 957-965.

Sung, Y. J., D. T. W. Chiu, et al. (2006). "Activation and retrograde transport of protein kinase G in rat nociceptive neurons after nerve injury and inflammation." Neuroscience 141(2): 697-709.

Sutton, M. A. and E. M. Schuman (2006). "Dendritic Protein Synthesis, Synaptic Plasticity, and Memory." Cell 127(1): 49-58.

Swat, W., K. Fujikawa, et al. (1998). "SEK1/MKK4 Is Required for Maintenance of a Normal Peripheral Lymphoid Compartment but Not for Lymphocyte Development." Immunity 8(5): 625-634.

Takei, Y., J. Teng, et al. (2000). "Defects in Axonal Elongation and Neuronal Migration in Mice with Disrupted tau and map1b Genes." The Journal of Cell Biology 150(5): 989-1000.

Takekawa, M., K. Tatebayashi, et al. (2005). "Conserved Docking Site Is Essential for Activation of Mammalian MAP Kinase Kinases by Specific MAP Kinase Kinase Kinases." Molecular Cell 18(3): 295-306.

Takemura, R., S. Okabe, et al. (1995). "Polarity orientation and assembly process of microtubule bundles in nocodazole-treated, MAP2c-transfected COS cells." Molecular Biology of the Cell 6(8): 981-996.

Tararuk, T., N. Östman, et al. (2006). "JNK1 phosphorylation of SCG10 determines microtubule dynamics and axodendritic length." The Journal of Cell Biology 173(2): 265-277.

Taylor, A. M., N. C. Berchtold, et al. (2009). "Axonal mRNA in Uninjured and Regenerating Cortical Mammalian Axons." The Journal of Neuroscience 29(15): 4697-4707.

Tcherkezian, J., P. A. Brittis, et al. (2010). "Transmembrane Receptor DCC Associates with Protein Synthesis Machinery and Regulates Translation." Cell 141(4): 632-644.

Teng, J., Y. Takei, et al. (2001). "Synergistic effects of MAP2 and MAP1B knockout in neuronal migration, dendritic outgrowth, and microtubule organization." The Journal of Cell Biology 155(1): 65-76.

Tiedge, H. and J. Brosius (1996). "Translational Machinery in Dendrites of Hippocampal Neurons in Culture." The Journal of Neuroscience 16(22): 7171-7181.

Timmusk, T., K. Palm, et al. (1993). "Multiple promoters direct tissue-specific expression of the rat BDNF gene." Neuron 10(3): 475-489.

Tiruchinapalli, D. M., Y. Oleynikov, et al. (2003). "Activity-Dependent Trafficking and Dynamic Localization of Zipcode Binding Protein 1 and β-Actin mRNA in Dendrites and Spines of Hippocampal Neurons." The Journal of Neuroscience 23(8): 3251-3261.

Tögel, M., G. Wiche, et al. (1998). "Novel Features of the Light Chain of Microtubule-associated Protein MAP1B: Microtubule Stabilization, Self Interaction, Actin Filament Binding, and Regulation by the Heavy Chain." The Journal of Cell Biology 143(3): 695-707.

Tournier, C., C. Dong, et al. (2001). "MKK7 is an essential component of the JNK signal transduction pathway activated by proinflammatory cytokines." Genes & Development 15(11): 1419-1426.

Tournier, C., P. Hess, et al. (2000). "Requirement of JNK for Stress- Induced Activation of the Cytochrome c-Mediated Death Pathway." Science 288(5467): 870-874.

Tournier, C., A. J. Whitmarsh, et al. (1997). "Mitogen-activated protein kinase kinase 7 is an activator of the c-Jun NH2-terminal kinase." Proc Natl Acad Sci U S A 94(14): 7337-7342.

Tournier, C., A. J. Whitmarsh, et al. (1999). "The MKK7 Gene Encodes a Group of c-Jun NH2-Terminal Kinase Kinases." Mol. Cell. Biol. 19(2): 1569-1581.

Trapp, B. D., T. Moench, et al. (1987). "Spatial segregation of mRNA encoding myelin-specific proteins." Proceedings of the National Academy of Sciences 84(21): 7773-7777.

V Doye, S. L. G., T Dobransky, H Chneiweiss, L Beretta, and A Sobel (1992). "Expression of transfected stathmin cDNA reveals novel phosphorylated forms associated with developmental and functional cell regulation" Biochem J. 287(2): 549–554.

Vaillant, A. R., R. Müller, et al. (1998). "Characterization of the Microtubule-binding Domain of Microtubule-associated Protein 1A and Its Effects on Microtubule Dynamics." Journal of Biological Chemistry 273(22): 13973-13981.

Vessey, J. P., P. Macchi, et al. (2008). "A loss of function allele for murine Staufen1 leads to impairment of dendritic Staufen1-RNP delivery and dendritic spine morphogenesis." Proc Natl Acad Sci U S A 105(42): 16374-16379.

Virdee, K., A. J. Bannister, et al. (1997). "Comparison Between the Timing of JNK activation, c-Jun Phosphorylation, and Onset of Death Commitment in Sympathetic Neurones." Journal of Neurochemistry 69(2): 550-561.

Wada, T., N. Joza, et al. (2004). "MKK7 couples stress signalling to G2/M cell-cycle progression and cellular senescence." Nat Cell Biol 6(3): 215-226.

Waetzig, V., Y. Zhao, et al. (2006). "The bright side of JNKs-Multitalented mediators in neuronal sprouting, brain development and nerve fiber regeneration." Prog Neurobiol 80(2): 84-97.

Wan, Y. Y., H. Chi, et al. (2006). "The kinase TAK1 integrates antigen and cytokine receptor signaling for T cell development, survival and function." Nat Immunol 7(8): 851-858.

Wang, C., A. Cormier, et al. (2007). "Insight into the GTPase Activity of Tubulin from Complexes with Stathmin-like Domains†." Biochemistry 46(37): 10595-10602.

Wang, E. T., R. Sandberg, et al. (2008). "Alternative isoform regulation in human tissue transcriptomes." Nature 456(7221): 470-476.

Wang, H., A. Iacoangeli, et al. (2002). "Dendritic BC1 RNA: Functional Role in Regulation of Translation Initiation." The Journal of Neuroscience 22(23): 10232-10241.

Wang, L., Y. Pan, et al. (2004). "Evidence of MKK4 pro-oncogenic activity in breast and pancreatic tumors." Oncogene 23(35): 5978-5985.

Wang, X., A. Destrument, et al. (2007). "Physiological roles of MKK4 and MKK7: Insights from animal models." Biochimica et Biophysica Acta (BBA) - Molecular Cell Research 1773(8): 1349-1357.

Wang, X., B. Nadarajah, et al. (2007). "Targeted Deletion of the Mitogen-Activated Protein Kinase Kinase 4 Gene in the Nervous System Causes Severe Brain Developmental Defects and Premature Death." Mol. Cell. Biol. 27(22): 7935-7946.

Welshhans, K. and G. J. Bassell (2011). "Netrin-1-induced local beta-actin synthesis and growth cone guidance requires zipcode binding protein 1." J Neurosci 31(27): 9800-9813.

Weston, C. R. and R. J. Davis (2007). "The JNK signal transduction pathway." Curr Opin Cell Biol 19(2): 142-149.

Whitmarsh, A. J., J. Cavanagh, et al. (1998). "A Mammalian Scaffold Complex That Selectively Mediates MAP Kinase Activation." Science 281(5383): 1671-1674.

Winckler, B., P. Forscher, et al. (1999). "A diffusion barrier maintains distribution of membrane proteins in polarized neurons." Nature 397(6721): 698-701.

Wu, K. Y., U. Hengst, et al. (2005). "Local translation of RhoA regulates growth cone collapse." Nature 436(7053): 1020-1024.

Xie X, G. Y., Fox T, Coll JT, Fleming MA, Markland W, Caron PR, Wilson KP, Su MS (1998). "Crystal structure of JNK3: a kinase implicated in neuronal apoptosis." structure 6(8): 983-991.

Xie, Y., J. P. Vessey, et al. (2007). "The GTP-Binding Protein Septin 7 Is Critical for Dendrite Branching and Dendritic-Spine Morphology." Current Biology 17(20): 1746-1751.

Xiong, X., X. Wang, et al. (2010). "Protein turnover of the Wallenda/DLK kinase regulates a retrograde response to axonal injury." J Cell Biol 191(1): 211-223.

Xu, J., J. F. Casella, et al. (1999). "Effect of capping protein, CapZ, on the length of actin filaments and mechanical properties of actin filament networks." Cell Motility and the Cytoskeleton 42(1): 73-81.

Xu, Z., N. V. Kukekov, et al. (2003). "POSH acts as a scaffold for a multiprotein complex that mediates JNK activation in apoptosis." EMBO J 22(2): 252-261.

Y R Chen, T. H. T. (2000). "The c-Jun N-terminal kinase pathway and apoptotic signaling (review)." International Journal of Oncology.

Yamada, S. D., J. A. Hickson, et al. (2002). "Mitogen-activated Protein Kinase Kinase 4 (MKK4) Acts as a Metastasis Suppressor Gene in Human Ovarian Carcinoma." Cancer Research 62(22): 6717-6723.

Yan, D., Z. Wu, et al. (2009). "The DLK-1 kinase promotes mRNA stability and local translation in C. elegans synapses and axon regeneration." Cell 138(5): 1005-1018.

Yan D, W. Z., Chisholm AD, Jin Y (2009). "The DLK-1 kinase promotes mRNA stability and local translation in C. elegans synapses and axon regeneration." Cell 138(5): 1005-1018.

Yang, D., C. Tournier, et al. (1997). "Targeted disruption of the MKK4 gene causes embryonic death, inhibition of c-Jun NH2-terminal kinase activation, and defects in AP-1 transcriptional activity." Proceedings of the National Academy of Sciences 94(7): 3004-3009.

Yang, J., M. Boerm, et al. (2000). "Mekk3 is essential for early embryonic cardiovascular development." Nat Genet 24(3): 309-313.

Yang, J., L. New, et al. (1998). "Molecular cloning and characterization of a human protein kinase that specifically activates c-Jun N-terminal kinase." Gene 212(1): 95-102.

Yasuda, J., A. J. Whitmarsh, et al. (1999). "The JIP Group of Mitogen-Activated Protein Kinase Scaffold Proteins." Mol. Cell. Biol. 19(10): 7245-7254.

Yoshimura, A., R. Fujii, et al. (2006). "Myosin-Va Facilitates the Accumulation of mRNA/Protein Complex in Dendritic Spines." Current Biology 16(23): 2345-2351.

Yujiri, T., M. Ware, et al. (2000). "MEK kinase 1 gene disruption alters cell migration and c-Jun NH2-terminal kinase regulation but does not cause a measurable defect in NF-κB activation." Proceedings of the National Academy of Sciences 97(13): 7272-7277.

Zaessinger, S., I. Busseau, et al. (2006). "Oskar allows nanos mRNA translation in Drosophila embryos by preventing its deadenylation by Smaug/CCR4." Development 133(22): 4573-4583.

Zhang, H. L., T. Eom, et al. (2001). "Neurotrophin-Induced Transport of a β-Actin mRNP Complex Increases β-Actin Levels and Stimulates Growth Cone Motility." Neuron 31(2): 261-275.

Zhengui Xia, M. D., Joel Raingeaud, Roger J. Davis, Michael E. Greenberg (1995). "Opposing Effects of ERK and JNK-p38 MAP Kinases on Apoptosis." science 270(5240): 1326-1331.

Zivraj, K. H., Y. C. Tung, et al. (2010). "Subcellular profiling reveals distinct and developmentally regulated repertoire of growth cone mRNAs." J Neurosci 30(46): 15464-15478.

10. Acknowledgments

10. Acknowledgments

I would like to thank my Supervisor, Prof. Olivier Pertz, for giving me the opportunity to accomplish my PhD in his lab and for the support for my private carrier. Thank you Olivier!

Special thanks go to Michel, for his help, right from the beginning of this adventure, for the nice time spent together in the lab, at Cargo, at Hirschy,,,,, at the Gleiss 13. I hope we will keep in touch!

Thanks to all the members of my lab, for being how they are, for the support and for the smiles.

I would like to acknowledge Prof. Markus Rüegg and Prof. Gerhard Christofori as members of my thesis committee.

A very special thank to Simone, for making my last and most difficult years of PhD sweet and painless. Thank you so so much for your patience, for you support and for your love! It's also thanks to you that I managed to reach the end.

Grazie alla mia famiglia, per l'affetto e la vicinanza e per avermi sempre capito e sostenuto. E un bacione alle mie nipotine, che con la loro presenza mi hanno fatto sorridere. Grazie Mamma, Patric, Chiara, Nicole e Martina.

And finally, thanks to my Dad, perchè anche se non ci sei piu, sento che sei sempre qui con me. Mi hai dato la forza, il coraggio e l'ambizione. Rimani sempre con me!

I thank you all, Ladies and Gentlemen!

11. Appendix

11. Appendix

Assessment of Rho GTPase signaling during neurite outgrowth

Daniel Feltrin and Olivier Pertz

Summary

Rho GTPases are key regulators of the cytoskeleton during the process of neurite outgrowth. Based on overexpression of dominant-positive and negative Rho GTPase constructs, the classic view is that Rac1 and Cdc42 are important for neurite elongation whereas RhoA regulates neurite retraction in response to collapsing agents. However, recent work has suggested a much finer control of spatio-temporal Rho GTPase signaling in this process. Understanding this complexity level necessitates a panel more sensitive tools than previously used. Here, we discuss a novel assay that enables the biochemical fractionation of the neurite from the soma of differentiating N1E-115 neuronal-like cells. This allows for spatio-temporal characterization of a large number of protein components, interactions and post-translational modifications using classic biochemical but also proteomics approaches. We also provide protocols for siRNA-mediated knockdown of genes and sensitive assays that allow quantitative analysis of the neurite outgrowth process.

Keywords: Neurite outgrowth, effector pulldown assays, immunofluorescence, timelapse imaging

1. INTRODUCTION

Proper functioning of the nervous system requires connections between neurons and their targets. This requires undifferentiated cells to extend cylindrical extensions in a process called neurite outgrowth (da Silva and Dotti 2002). This process is a three step event. First, the round shape of the cell is broken down and a filopodia-like extension is generated. Second, the extension elongates and it is transformed into a proper neurite. Finally, the neurite differentiates into an axon or a dendrite. Recently, genetic and biochemical approaches have been applied to identify and characterize molecular components involved in this process. A wealth of evidence has suggested that cytoskeletal (actin and microtubules), adhesion and trafficking dynamics play central roles in neurite outgrowth initiation and elongation. Thus, integrated approaches are necessary for an adequate understanding of neurite outgrowth and there is a need for tools that allow large scale identification and characterization of components important for this morphogenetic event. Here, we present a method that allows the large scale purification of neurites from the soma of differentiating neuronal cells, and thus allows simple spatio-temporal measurements of the subcellular localization (neurite/soma) of protein components, protein-protein interactions, signaling activities and post-translational modifications using classic biochemical techniques (Pertz, Wang et al. 2008). This assay takes advantage of N1E-115 neuroblastoma cells but can in principle also be extended to other cell types. An example that will be discussed in the present article are Rho GTPase activation effector pulldown assays of the neurite and soma fractions which reveal that Rac1 and Cdc42 activation is virtually confined to the extending neurite. We also have combined this assay with large scale quantitative proteomics to decipher the neurite and soma proteomes of N1E-115 cells. Using a bioinformatic approach, we have identified a potential neurite-localized Rho GTPase interactome that comprises several Guanine nucleotide exchange factors (GEFs), GTPase activating proteins (GAPs) and downstream effectors (Pertz, Wang et al. 2008). This suggests that Rac1 and Cdc42 activation in the neurite is the result of a complex signaling network. To understand the molecular significance of this complexity, we took a RNA interference approach to knockdown individually a subset of Rac1 and Cdc42 specific GEFs and GAPs that are enriched in the neurite. Surprisingly, whereas expression of dominant negative alleles of Rac1 and Cdc42 lead to potent phenotypes such as complete loss of neurite outgrowth, siRNA-mediated knockdown of the GEFs and GAPs only affect neurite outgrowth in a very mild manner (e.g. loss of neurite outgrowth is never observed). In fact, we observe a large variety of more subtle phenotypes, affecting diverses functions such as: filopodium stability and morphology, initiation of neurite outgrowth, neurite elongation and neurite pathfinding. These complex phenotypes can only be understood with more sensitive

assays such as high resolution imaging of the cytoskeleton and time-lapse experiments that evaluate the fine morphodynamic behavior of neurite outgrowth. These results point to a much more complex regulation of Rho GTPase signaling during neurite outgrowth than previously anticipated, and suggest a signaling modularity in which different GEFs and GAPs regulate distinct biochemical pools of Rac 1 and Cdc42 with different functions. These results are compatible with insights obtained using fluorescent Rho GTPase activation biosensors, which have revealed multiple subcellular pools of active GTPases with distinct functions operating simultaneously within one cell (Nalbant, Hodgson et al. 2004; Pertz, Hodgson et al. 2006; Pertz 2010). In this article, we present some of the experimental approaches that were necessary to understand the complexity of spatio-temporal Rho GTPase signaling during neurite outgrowth. These includes protocols for siRNA transfection into N1E-115 cells, their neuronal differentiation, immunofluorescence techniques to visualize their actin and microtubule cytoskeleton, automated image analysis of neurite length and protocols for phase timelapse microscopy to harness the fine morphodynamics of the neurite outgrowth process.

2. MATERIALS

Prepare all the solutions using ultrapure water, and analytical grade reagents. Use sterile mediums and reagents for the cell culture procedures.

2.1. CELL CULTURE

1. N1E-115 neuroblastoma cells (American Tissue Culture Collection).
2. Culture medium: Dulbecco's Modified Eagle Medium (Sigma Aldrich Chemie GmbH, Germany), supplemented with 1% of Penicillin-Streptomycin (Sigma Aldrich Chemie GmbH, Germany), 2% of L-Glutamine (Sigma Aldrich Chemie GmbH, Germany) and 10% of Fetal Bovine Serum (Sigma Aldrich Chemie GmbH, Germany)
3. Differentiation medium: Neurobasal medium (GIBCO, Invitrogen Auckland, NZ), supplemented with 1% of Penicillin-Streptomycin and 2% of L-Glutamine.
4. Phosphate Buffered Saline (PBS): 13.7mM Sodium Chloride, 0.27 mM Potassium Chloride, 10 mM Sodium Hydrogen Phosphate (Na_2HPO_4), 0.2 mM Potassium Hydrogen Phosphate (KH_2PO_4). Autoclave.
5. PUCK'S saline solution: 0.17 mM Disodium Hydrogen Phosphate, 0.22 mM Potassium Dihydrogen Phosphate, 20 mM Hepes, 138 mM Sodium Chloride, 5.4 mM Calcium Chloride, 5.5 mM Glucose and 58.4 mM Sucrose. Autoclave.

2.2. MICROPOROUS TRANSWELL FILTER SYSTEM

1. Transwell Permeable Supports. Use polycarbonate membranes with 3.0 µm pore size (Costar, Corning Inc., NY, USA). For imaging, use 6.5 mm diameter (12 inserts/24 well plate). For biochemical neurite purification, use 24 mm diameter (6 inserts/ 6 well plate) (see **Note 1**).
2. Laminin from Engelbreth-Holm-Swarm murine sarcoma basement membrane (Sigma Aldrich Chemie GmbH, Germany).
3. HPLC grade Methanol (Scharlab SL, Spain).
4. Cotton swabs.
5. Syringe needles (Microlance3, Becton Dickinson, Dublin Ireland).

2.3. LYSIS BUFFERS AND RHO GTPASE PULLDOWN

1. Native lysis buffer: 150 mM Sodium Chloride, 1.0% NP-40 or Triton X-100, 0.5% sodium deoxycholate, 0.1% Sodium Dodecyl Sulphate (SDS), 50 mM Tris, ph 8.0.

2. Denaturing lysis buffer: 1% SDS, 2mM Vanadate,1mM Phenylmethanesulfonyl Fluoride (PMSF), 1 tablet Proteases Inhibitor Cocktail/10 ml of buffer (Roche Diagnostics GmbH, Mannheim, Germany), pH 7.
3. Denaturing lysis buffer for proteomics analysis: 4 mM Tris ph 7.5, 8 M Urea, 0.1% RapiGest (Waters Corporation, Milford, MA, USA), 1 mM Vanadate, 1 PhosSTOP Phosphatase Inhibitor Cocktail Tablet / 10 ml buffer (ROCHE Diagnostics GmbH, Mannheim, Germany) (see **Note 2**).
4. Spin columns (Pierce, Thermo Fisher Scientific, Rockford, Illinois, USA)
5. GST-Pak or GST-Rhotekin pulldown kits (Millipore Chemicon, Billerica, Massachusetts, USA).

2.4. siRNA reagents

1. Pure DMEM medium (Sigma Aldrich Chemie GmbH, Germany)
2. ON-TARGETplus SMARTpool siRNAs (Dharmacon, Thermo Fisher Scientific, , Rockford, Illinois, USA). (see **Note 3**).
3. DharmaFECT 2 Transfection Reagent (Dharmacon, Thermo Fisher Scientific, , Rockford, Illinois, USA)

2.5. IMMUNOFLUORESCENCE

1. BRB80 buffer: 80 mM PIPES pH 6.8, 1mM $MgCl_2$, 1 mM EGTA.
2. Fixing solution: 1X BRB80, 0.25% glutaraldehyde (Sigma Aldrich Chemie GmbH, Germany).
3. Permeabilization solution: 1X BRB80, 0.25% glutaraldehyde, 0.1% Triton X-100.
4. Antibody buffer: PBS, 2%BSA (Sigma Aldrich Chemie GmbH, Germany), 0.1% Triton X-100.
5. Glutaraldehyde Autofluorescence Limiting buffer: PBS, 0.2% Sodium Borohydride (Sigma Aldrich Chemie GmbH, Germany) (see **note 4**).
6. ProLong Gold antifade reagent (Invitrogen, Eugene, Oregon, USA).
7. Tubulin antibody (Monoclonal Anti-α-Tubulin Clone DM 1A, developed in mouse (Sigma Aldrich Chemie GmbH, Germany) , Alexa Fluor 488 phalloidun (Invitrogen, Eugene, Oregon, USA). Secondary antibody: Alexa Fluor 546 goat anti-mouse IgG /H+L (Invitrogen, Eugene, Oregon, USA).

2.6. NEURITE OUTGROWTH ANALYSIS AND TIMELAPSE EXPERIMENTS

1. Coverslips (Menzel-Gläser Gmbh, Saarbrückener, Germany).
2. Glass-bottom plates (Mattech Co, Ashland, MA, USA)
3. Neurobasal medium supplemented with 25 mM of Hepes.
4. Epifluorescence microscope.
5. Metamorph Imaging Software (Molecular Devices, Downington, PA, USA).

3. METHODS

3.1. N1E-115 CELL CULTURE AND DIFFERENTIATION

1. Grow N1E-115 cells in DMEM culture medium, in 10 cm dishes at a density that never exceeds 70% of confluence, at 37°C and 5% CO_2.
2. For passaging, wash the cells in a 10 cm dish once with warm PBS, aspirate PBS, incubate cells in 2 ml warm PUCKS's saline solution at 37°C for 3-5 minutes, add 8 mL of DMEM culture medium and mechanically detach the cells by gently rinsing the plate and transfer the medium containing the cells in a 15 ml tube. Centrifuge the cells and remove supernatant. Resuspend cell pellet in DMEM culture medium. Typically passage 1/5 three times a week.
3. For neuronal differentiation, serum-starve a 50% confluent 10 cm dish of N1E-115 cells by aspirating the DMEM culture medium, rinsing the dish once with 10 mL of sterile PBS, aspirating again and adding to the cells 10 mL of Neurobasal differentiation medium (see **Note 5**). Typical morphologies of undifferentiated and differentiated cells are shown in Fig.1.

3.2. NEURITE AND SOMA PURIFICATION ON MICROPOROUS TRANSWELL FILTERS

1. Grow approximately 15×10^6 N1E-115 cells and differentiate them by serum starvation in Neurobasal differentiation medium overnight (see **Note 6**).
2. Dilute the laminin in sterile PBS to a final concentration of 10 µg/mL.
3. Place the filters upside-down on the lid of the 6 well plate where the filters are stored and pipette on top 500 µL of the solution containing laminin on the bottom of the filters. We typically use 12 filters (e.g. two 6-well plates) in one experiment. Two filters will be used for soma purification and ten filters for neurite purification (see **Note 7**).
4. Incubate at 37°C for 2 h or over night at 4°C. This should be performed in an as sterile as possible environment.
5. Aspirate the solution from the bottom of the filters and place them back in the 6 well plate where you previously added 2 ml of Neurobasal medium in the bottom chamber (e.g. well).
6. Detach cells using PUCK's saline solution as explained in 3.1.2. Count the cells and resuspend the cells at a concentration of 10^6 cells per ml in Neurobasal differentiation medium.
7. Dispense 1.2 ml of this cell solution (1.2×10^6 cells) on the top of the filter.

8. Incubate at 37°C for 24 hours in the cell culture incubator.
9. Cool down PBS in a beaker and pour 2 ml methanol/well in a 6-well plate on ice before starting the experiment.
10. Remove the 6 well-plate from the incubator and place it on ice for 10 minutes.
11. Holding the filter with a pincette, wash the filter by carefully dipping them in the PBS containing beaker and transfer the filter to the methanol containing 6-well plate.
12. Add 2 mL of Methanol to the top of the filters for cell fixation (see **Note 8**).
13. Incubate at 4°C for 20 minutes.
14. Remove the filters from the plate and dry them upside-down.
15. Make one cotton swab slightly wet with some PBS. For soma purification, scrape the bottom of the filters with the swab. For neurite purification, scrape the top of the filter with the swab. Cut the filters at the edges using a syringe needle. Pool the respective neurite and soma filters in separate spin columns where you previously pipeted 200-300 µL of Lysis buffer. Schematics of the procedure is found in Fig.2A.
16. For lysis in denaturing buffer, boil the spin column at 100°C for 5 minutes. Centrifuge the spin column and recover lysate in the bottom tube. Measure protein concentration using your favorite assay and supplement with Laemmli buffer. You can use your lysate for Western blot analysis to compare abundance of your favorite protein in equivalent amounts of neurite and soma lysate (see **Note 9**).
17. For lysis in denaturing buffer for proteomics analysis, do not boil but incubate filters with lysis buffer for 5 minutes at room temperature. Centrifuge spin columns and recover lysate in the bottom tube. Measure protein concentration using your favorite assay and use in your favorite proteomics experiment.
18. For lysis in native buffer, omit the methanol fixation step. Perform all the steps at 4°C. Centrifuge the spin columns and recover the soluble fraction of the cell lysate in the bottom tube. A second lysate clarification step (centrifugation) might be necessary to get rid of the particulate fraction. Measure protein concentration using your favorite assay.
19. For GST-PAK pulldown of active Rac1 or Cdc42, use 100 µg of neurite and soma lysates. Perform the pulldown according to Manufacturer's instructions (see **Note 10**). Typical result of Rac1 and Cdc42 effector pulldown assays are shown in Fig.2B.

3.3. TRANSFECTION OF SIRNAS IN N1E-115 CELLS

1. **Day 1: cell plating.** Plate 2×10^5 cells per well in a 6-well plate in DMEM culture medium (see **Note 11**).
2. **Day 2: transfection.** In a 1.5 mL tube pipet 100 µL of pure DMEM. Add to the medium 100 pmol of siRNA (5 µL of a 20 µM concentrated stock solution). Tube A (see **Note 12**).
3. In another tube pipet 100 µL of pure DMEM per well. Add to the medium 6 µL of DharmaFECT 2 transfection Reagent. TUBE B.
4. Pipet the solution of tube A to tube B and mix gently (no vortex).
5. Incubate for 20 minutes at room temperature.
6. Aspirate the medium from the cells in the 6 well plate and rinse once with 1 mL of sterile PBS.
7. Aspirate PBS and pipet 1 mL of DMEM culture medium (see **Note 13**)
8. Add the transfection mix drop wise to the wells.
9. **Day 3: medium change.** Aspirate the medium from the cells.
10. Rinse once with 1 mL of sterile PBS.
11. Aspirate the PBS and pipet 2 ml of DMEM culture medium.
12. **Day 4: cell starving and differentiation.** Aspirate the complete DMEM from the cells.
13. Rinse once with 1mL of sterile PBS and aspirate it.
14. Pipet 2 mL of Neurobasal differentiation medium to the cells.
15. **Day 5: cell plating for assays.** Coat 16 mm coverslips or 12 well glass bottom plates with 10 µg/mL laminin for 2 h at 37°C or at 4°C over night (see **Note 14**).
16. Aspirate the Neurobasal differentiation medium from the 6 well-plate that contains the serum-starved cells. Rinse the cells once with 1 mL of sterile PBS and aspirate it. Detach the cells using 1 ml of PUCK's saline solution by incubating at 37°C for 3-5 minutes. Resuspend in a given volume of neurobasal differentiation medium and count the cells. Centrifuge the cells, aspirate the supernatant and resuspend the cells in an appropriate volume.
17. Plate 4×10^4 cells per well (or per coverslip). The remainder of the cells can be used for other assays.
18. Place cells in the incubator for 3 hours for the timelapse assay or for 16-24 hours for the neurite outgrowth analysis.

3.4 EVALUATION OF NEURITE OUTGROWTH RESPONSES

i. F-ACTIN / TUBULIN IMMUNOSTAINING

1. This protocol starts with cells that were allowed to extend neurites for 16-24 hours (see **Note 15**).
2. Fill another 12 well-plate with 1 mL of PBS.
3. Carefully transfer the coverslips to the plate with PBS to wash them.
4. Fix the cells by transferring the coverslips in the fixing solution for 45 seconds.
5. Transfer the coverslips to the permeabilization solution and incubate for 10 minutes.
6. Wash twice for 10 minutes with PBS.
7. Transfer the coverslips to the 0.2% Sodium Borohydride solution. Incubate for 20 minutes.
8. Wash twice for 10 minutes with PBS.
9. Incubate for 10 minutes with the antibody buffer.
10. Prepare the dilution of the primary antibody: dilute the antibody against tubulin 1:500 in antibody buffer.
11. Transfer the coverslips to a parafilm and pipette 100 µL of the antibody buffer with the primary antibody to the surface of each coverslip.
12. Incubate at RT for 30 minutes.
13. Transfer back to the 12 well-plate and wash three times for 10 minutes with PBS.
14. Prepare the secondary antibody, diluting it 1:1000 in the Antibody buffer. Dilute also the DAPI 1:1000 (of a 1 mg/mL concentrated stock solution) in the same buffer for the staining of the nuclei. (Add here eventually also a fluorescent conjugated Phalloidin for the staining of f-actin, diluting 1000 times a 2 mg/mL concentrated solution).
15. Transfer the coverslips to the parafilm and pipette 100 µL of the Antibody buffer with secondary antibody and DAPI (and eventually Phalloidin) to the surface of each coverslip.
16. Incubate at RT and in the dark for 20 minutes.
17. Wash three times with PBS (always protect from the light).
18. Prepare the slides to be mounted by pipetting one drop of Prolong Gold antifade Reagent per coverslips (typically each slides can host two coverslips).
19. Gently mount the slides by putting the coverslips upside down on the drop of Prolong Gold antifade Reagent.

20. Leave the mounted slides dry over night in the dark.

ii. NEURITE OUTGROWTH ANALYSIS AND HIGH RESOLUTION IMAGING

1. Using a 10x air objective acquire multiple tubulin and DAPI pictures (multiple fields of view) (see **Note 16**). We typically use the "Scan slide" module of the Metamorph software that allow to stitch multiple fields of view in one image (see Fig. 2A).
2. Perform neurite outgrowth analysis using the metamorph neurite outgrowth plugin. The module will use the DAPI image for the recognition of the cell bodies and the tubulin image for segmentation of the neurite. The plugin will ask for a panel of parameters that can be measured manually in metamorph (cell body width, fluorescence intensity and area; neurite minimum and maximum width and fluorescence intensity). Once these parameters are determined, we test them and compare the original and the segmented images. The parameters are then fine tuned for optimal results and all images can then be analyzed.
3. The software will provide binary images of the nuclei and of the neurites (Fig. 2B) as well as numerical results of including total neurite outgrowth, area of the cell bodies, number of neurites per cell body, neurite branching, … These numerical results can then be exported to Excel or other software for statistical analysis and graph representations. Typical results of this procedure are shown in Fig.3.
4. For high resolution analysis, we use high numerical aperture oil immersion lenses. Typical results are shown in Fig. 4.

iii. TIMELAPSE ANALYSIS

1. After 3 hours of incubation in a cell incubator, which allows for spreading and initial neurite outgrowth, the dynamics of the neurite outgrowth process can be analyzed using phase contrast timelapse experiments (see **Note 17**).
2. Gently aspirate the medium from the wells using a pipette. Do not aspirate using a vacuum line (see **Note 18**).
3. Pipet very gently fresh neurobasal medium supplemented with 20 mM Hepes, filling up the well completely (see **Note 19**).
4. Quickly place the lid avoiding air bubbles.

5. Run a 16 hours timelapse experiment at the microscope using a multidimensional acquisition program (for example use the multi dimensional acquisition module of Metamorph, that allows to save several positions, using several wavelengths). We typically perform multistage experiments that allow timelapse capture of multiple positions across multiple wells (e.g. multiple siRNA experiments). Use a microscope equipped with a temperature-controlling box, that keeps the temperature fixed at 37°C. It's also possible to perfuse the box with 5% CO_2 (in this case Hepes is dispensible) (see **Note 20**).
6. Timelapse movies are then visually inspected using metamorph software for evaluation of neurite outgrowth morphodynamic phenotypes.

4. NOTES

1. Some of the Costar transwell filters are leaky. Be careful to test different batches of transwell filters before purchasing them. For that purpose, put 2 ml H_2O in the lower chamber (for 24 mm filters in 6-well plates) and check if it can leak into the upper chamber. The 3 mm pore filter is adequate for N1E-115 Neuroblastoma cells which have a soma diameter of roughly 35 mm. Smaller pore sizes might apply for other cell lines or primary neurons that are typically smaller.
2. Detergents such as SDS are typically not tolerated by mass spectrometry machines. This is the best denaturing buffer we have tested so far for this application. Furthermore it is compatible with subsequent trypsin digestion when diluted.
3. A wide variety of siRNA reagents from different manufacturers function in N1E-115 cells. Dharmafect 2 is our favorite transfection reagent because of low toxicity and potency (100 % transfection efficiency and siRNA being detected in the cells for the whole duration of the experiment).
4. This buffer has to be freshly prepared for each experiment. Bubbles should observed in the solution. Be careful, this is toxic !
5. Additional supplements such a B12 as commonly used for culture of primary neurons are not needed. Serum-free DMEM can also be used for differentiation but is less potent than Neurobasal medium.
6. Rather than starving cells on the filter, we find that a cycle of neuronal differentiation through serum starvation in Neurobasal differentiation medium and subsequent replating on the filter allows for very robust neurite outgrowth necessary for efficient neurite purification. For cell number, a 50 % confluent dish typically yields 10^6 cells. In one experiment, 15-20 10 cm dishes are typically used. 15 cm dishes can also be used to lower the amount of plates to handle.
7. For neurite purification, one filter typically yields 20-30 µg of cell lysate depending on the cell lysis buffer. For soma purification, 300 µg cell lysate are typically obtained. This allows to generate 200-300 µg neurite and 600 µg soma lysate in one experiment.
8. Methanol fixation allows to freeze the signaling state of the cell, and therefore to avoid the upregulation of stress signaling pathways during the neurite or soma scraping procedure. This is at the expense of the loss of membrane components during the fixation. This procedure is compatible

with evaluation of phosphorylation events using phosphor-specific antibodies and western blot analysis. However this is not compatible with native conditions necessary for activation pulldown assays or co-immunoprecipitation experiments.

9. Once neurite and soma lysates have been separated, equal lysate amounts can be loaded on a gel and probed using western blot. With the assumption that protein density (amount of protein per cell volume) is constant within a cell, this allows to measure relative protein density in each respective subcellular domain (neurite and soma). Classic quality controls for correct loading are done with Erk2 and phospho-Erk antibodies. Total Erk is equally abundant in neurite and soma lysates, whereas phospho-Erk is highly enriched in the neurite. It is important to mention that many proteins are found in the detergent insoluble fraction in the neurite and might show different degrees of enrichment depending if a denaturing or native lysis buffer is used. Thus phospho-ERK signal in the neurite is typically lost when the neurite has been lyzed in a native buffer.

10. Using this procedure, we were successful in detecting robust pools of active Rac1 and Cdc42 in the neurite fraction (see Figure 2B). However, this might still be a under-estimate since a large pool of Rac1 and Cdc42 are observed in the particulate fraction. We were not able to detect any RhoA activation in the neurite because all RhoA was found in the particulate fraction and therefore is resilient to solubilization by native lysis buffers.

11. 2×10^5 cells / well allows to perform a series of experiments such as timelapse analysis, immunofluorescence and quantitative RT-PCR to test siRNA mediated knockdown efficacy. If knockdown efficacy has to be tested using western blot, we advise to transfect a second well.

12. We use Dharmacon smart pool plus siRNAs. This typically allows for 70 % of knockdown efficiency at the mRNA level and for 90-95 % knockdown efficiency at protein level. We use a non-targeting siRNA smart pool as control.

13. Transfection is performed in DMEM culture medium. The presence of serum allows the cells to remain in the undifferentiated state and increases cell survival. Transfection in serum free differentiation medium leads to poor cell survival.

14. At this stage of the procedure, cells should be inspected and neurites should be observed if differentiation has occurred.

15. The immunofluorescence procedure presented here allows for excellent preservation of the actin and tubulin cytoskeleton. This procedure can be extended to other proteins. However, in this case, one has to keep in mind that glutaraldehyde can lead to loss of antigenicity of certain epitopes. Furthermore, a commonly observed artifact is a dim fluorescence signal in the nucleus.

16. Because there is no need for high spatial resolution to get a global picture of neurite outgrowth, we typically work by binning the images 3x3. This allows better signal to noise (which is not limiting here), but also allows to drastically reduce the image size. This then allows to perform automated image analysis much faster with simple computers.

17. We find that cells are highly sensitive to stress such as light in the initial spreading and neurite outgrowth phase. Once cells are adherent, they get light resistant and can be timelapsed.

18. N1E-115 cells on a laminin-coated coverslip are extremely loosely adherent. They adhere through some extent through their soma but mostly through their growth cones. Any strong shear stress will therefore immediately lead to their detachment.

19. After a certain amount of time, the Neurobasal medium deteriorates leading to cell death. Once we open a new Neurobasal bottle, we aliquot it and store it in 50 ml tubes.

20. While glass bottom multiwall plates are preferable, phase contrast timelapse imaging can also be performed using classic plastic dishes with excellent picture quality. We typically use 10x or 20x long working distance, phase contrast objective to obtain 10 or 3 cells per field of view.

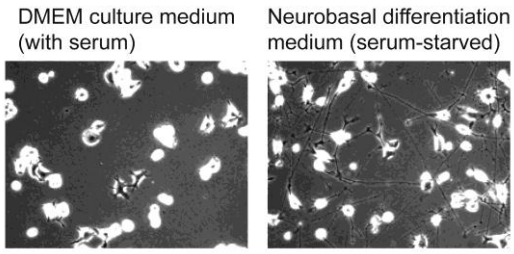

Fig. 1

Fig.1. Phase contrast pictures of non differentiated and differentiated N1E-115 cells.

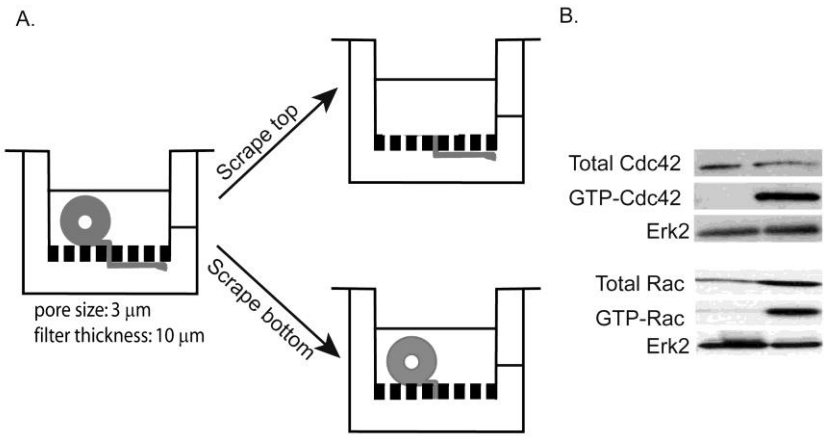

Fig. 2

Fig.2. Neurite purification procedure. (A) Schematics of the procedure. Note that bottom of the transwell filters are coated with laminin. (B) Typical western blot result of an effector pulldown assays of Rac1 and Cdc42 activity in neurite and soma fraction. While Rac1 and Cdc42 are more or less equally distributed in neurite and soma fractions, active pools of Rac1 and Cdc42 are solely restricted to the neurite. Erk2 is equally distributed in neurite and soma fractions and serves as loading control.

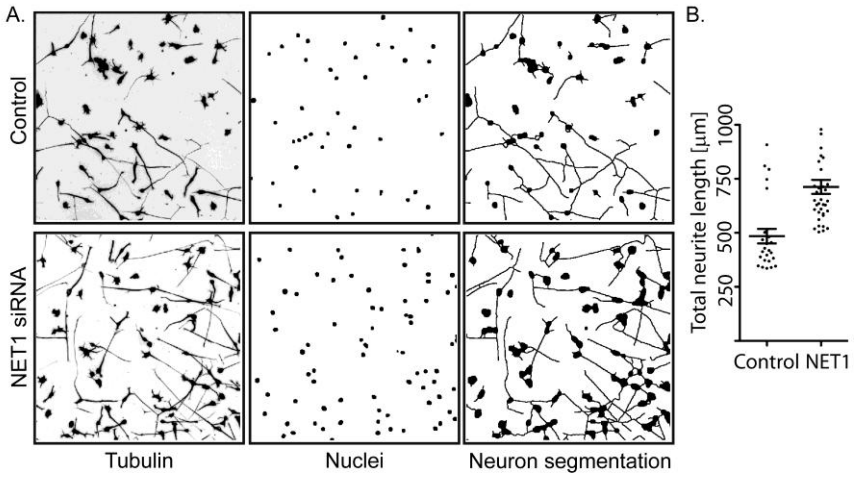

Fig. 3

Fig.3. Neurite outgrowth measurements. (A) Fluorescent micrographs of control and Net1 siRNA transfected cells, that were replated on a laminin-coated coverslip and stained for tubulin (left panel). Net1 is a GEF for RhoA. Image is represented with an inverted contrast. Middle and right panels display segmented binary images of the DAPI (nuclei) and tubulin (neurites) channels as analyzed using the neurite outgrowth algorithm. (B) Graph of total neurite length on a per cell basis measurements from segmented images in (A).

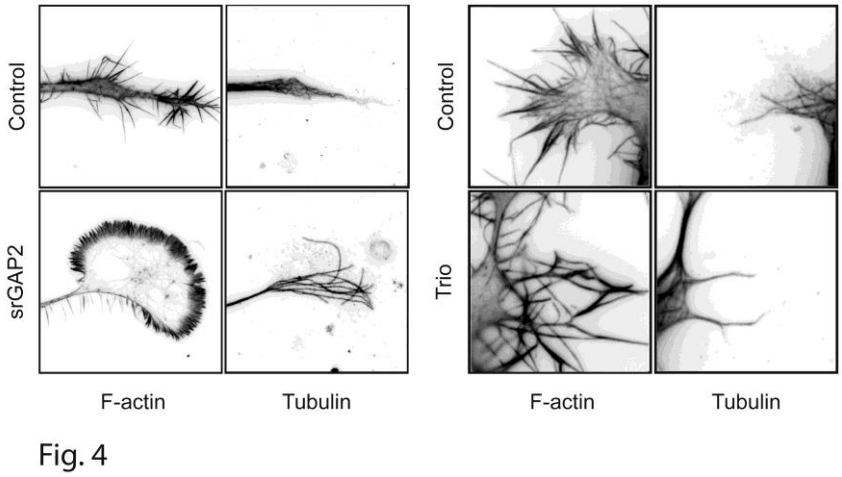

Fig. 4

Fig.4. High resolution micrographs of F-actin and tubulin stained control or knockdown cells. Images were acquired with a 63x high NA objective and are represented with inverted contrast. Note large filopodia arrays leading to spread growth cone in srGAP2 knockdown cells (GAP for Rac1). Note aberrant, intertwined filopodia found at the periphery of TRIO knockdown cells (GEF for Rac1 and RhoA).

REFERENCES

1. da Silva JS, Dotti CG (2002) Breaking the neuronal sphere: regulation of the actin cytoskeleton in neuritogenesis. Nat Rev Neurosci 3: 694-704.
2. Pertz OC, Wang Y, Yang F, Wang W, Gay LJ, et al. (2008) Spatial mapping of the neurite and soma proteomes reveals a functional Cdc42/Rac regulatory network. Proc Natl Acad Sci U S A 105: 1931-1936.
3. Nalbant P, Hodgson L, Kraynov V, Toutchkine A, Hahn KM (2004) Activation of endogenous Cdc42 visualized in living cells. Science 305: 1615-1619.
4. Pertz O (2010) Spatio-temporal Rho GTPase signaling - where are we now? J Cell Sci 123: 1841-1850.
5. Pertz O, Hodgson L, Klemke RL, Hahn KM (2006) Spatiotemporal dynamics of RhoA activity in migrating cells. Nature 440: 1069-1072.

12. Curriculum Vitae

CURRICULUM VITAE

Daniel Feltrin

D.O.B. : 17/09/1982, in Vipiteno (BZ) ITALY

Address: Wasgenring 103, CH-4055 Basel, Switzerland

E-mail: daniel.feltrin@unibas.ch

Phone: +41 (0)79 67 100 12

Nationality: Italian

Swiss Driving License B

Swiss Living Permit B (until April 2013)

EDUCATION:

2008 – December 2011

Center for Biomedicine, Institute of Biochemistry and Genetics, University of Basel

PhD program in Neurobiology

Graduated with merit (6/6 Summa cum Laude)

Research project: Local mRNA translation in the regulation of neurite outgrowth

Supervisor: Prof. Olivier Pertz

2010 – Expected: March 2012

University Hospital Basel, Clinical Trial Unit, Advanced Studies

University professional in "Clinical Trial Practice and Management"

Postgraduate education programme for clinical research professionals

2005 - 2007 **School of Pharmacy, University of Milan**

Laurea specialistica in Pharmaceutical Biotechnologies

Graduated cum Laude (110/110) with merit

Course electives: Bioinformatics, Advanced Topics in Molecular Genetics, Molecular Biology, Pharmacolgy, Advanced Biochemical and Biotechnological Techniques.

Research project title*:* "The somatostatin system, a potential innovative target in cancer research: studies in models of prostate carcinoma and of neuroendocrine tumor"

Supervisor: Prof. Paolo Magni

Coordinator: Dr. Massimiliano Ruscica

2001 - 2005 **School of Pharmacy, University of Milan**

BSc in Pharmaceutical Biotechnologies

Graduated with 97out of 110

Thesis project: "Reference method for glicated hemoglobin (HbA1c) measurement by mass spectrometry" (Obtained 10/11)

Supervisor: Prof. Donatella Caruso

1996 - 2001 **Liceo Classico P.Virgilio, Vipiteno (BZ), Italy**

Graduated with 95/100 (excellent)

WORKING EXPERIENCES:

2011,

December- **Covance Inc., Allschwil, Switzerland**

Clinical Research Associate Assistant (CRAA)

2008, April- **University of Basel, Center for Biomedicine, Insitute of Biochemistry and Genetics, Basel, Switzerland**

PhD Student in the Neurobiology field. Field of interest: Local mRNA-translation in developing neurons.

2011,

June 6th-10th **Quintiles Drug Research Unit at Guy's Hospital, London, UK**
Work shadowing week, according to the schedule of the "Clinical Trial Practice and Management" postgraduate education programme for clinical research professionals

2010,

Sep 13th-17th **Inselspital Bern, Poliklinik für Infektiologie, Bern, Switzerland**

Work shadowing week, according to the schedule of the "Clinical Trial Practice and Management" postgraduate education programme for clinical research professionals

2007, Sep-

2008, Mar **Queen Mary University of London, Barts and the London School of Medicine and Dentistry, London, UK**

Centre for Endocrinology

Research Assistant at the Centre for Molecular Endocrinology

2007,

Mar - Sep. **School of Pharmacy, University of Milan,**

Department of Endocrinology, Centre of Excellence on Neurodegenerative, Diseases, Milan, Italy

Research Assistant in the Centre for Molecular Endocrinology

Research activity in collaboration with Novartis Pharmaceutical Co. aiming to identify the mechanisms of action of somatostatin and its analogues in vitro on tumor cell lines.

Research activity in collaboration with Ipsen Co.

2006 - 2007 **School of Pharmacy, University of Milan**

Department of Endocrinology, Centre of Excellence on Neurodegenerative Diseases, Milan, Italy

Graduate student.

Completed a 12-month research project which required extensive analysis of data

Managed my time effectively between seminars and research

Attended weekly lab meetings and journal clubs

2004 **School of Pharmacy, University of Milan**

Department of Pharmacology, Milan, Italy

Graduate student

Assistant and trainee

Completed a 4-month research project which required extensive analysis of data

Managed my time effectively between seminars and research

Attended weekly lab meetings and journal clubs

Languages: **Italian** (native language)

German (C1) very good (Bilingual Certificate B (Italian/German) of the Autonome Provinz Bozen/Provincia Autonoma di Bolzano)

English (B2) fluent (Trinity College London Certificate grade 8)

IT Skills: Excellent use of MS Word, MS Excel and MS PowerPoint, Statistical software (Origin, Prism), Analysis software (Metamorph, Partek)

PUBLICATIONS:

- **Feltrin D**, Fusco L, Martin K, Letzelter M, Fluri E,Witte H,Scheiffele P and Pertz O, GROWTH CONE *MKK7* MRNA TRANSLATION REGULATES MAP1B-DEPENDENT MICROTUBULE BUNDLING TO CONTROL NEURITE ELONGATION, 2011, Plos Biology (Under review)
- **Feltrin D**, Pertz O, ASSESSMENT OF RHO GTPASE SIGNALING DURING NEURITE OUTGROWTH, 2011, Methods in Molecular Biology, Humana Press, USA
- Jang KJ, Suh KY, **Feltrin D**, Jeon NL, Pertz O, TWO DISTINCT FILOPODIA POPULATIONS AT THE GROWTH CONE ALLOW TO SNESE NANOTOPOGRAPHICAL EXTRACELLULAR MATRIX CUES TO GUIDE NEURITE OUTGROWTH, 2010, PlosOne
- Ruscica M, Arvigo M, Gatto F, Dozio E, **Feltrin D**, Culler MD, Minuto F, Motta M, Ferone D, Magni P, REGULATION OF PROSTATE CANCER CELL PROLIFERATION BY SOMATOSTATIN RECEPTOR ACTIVATION, 2009, Mol Cell Endocrinology
- Christ-Crain M, Kola B, Lolli F, Fekete C, **Feltrin D**, Seboek D, Wittman G, Ajodha S, Harvey-White J, Kunos G, Mueller B, Pralong F, Aubert G, Arnaldi G, Giacchetti G, Boscaro M, Grossman AB and Korbonits M, AMP-ACTIVETED PROTEIN KINASE MEDIATES GLUCOCORTICOID-INDUCED METABOLIC CHANGES: A NOVEL MECHANISM IN CUSHING'S SYNDROME, 2008, Faseb J
- Dozio E, Ruscica M, **Feltrin D**, Motta M and Magni P, CHOLINERGIC REGULATION OF NEUROPEPTIDE Y SINTHESIS AND RELEASE IN HUMAN NEUROBLATOMA CELLS, 2007, Peptides

GRANTS AND AWARDS:

2007 Sovvenzione Ingenio, funded by the European Community and the Regione Lombardia, Italy. 6000 €

2007 Project Unipharma Graduates III (Project Leonardo da Vinci), funded by the European Community and the Neopolis Foundation, Italy.

2001-2004 Three-year Studentship by the Italian Government

ATTENDANCE AT COURSES AND CONFERENCES

Feltrin D, Fluri E, Pertz O, "Local translation of MKK7 mRNA allows JNK-dependent neurite outgrowth"

- Abstarct accepted for **Flash communication** and Poster presentation at "EMBO conference on spatial dynamics of intracellular comunication", SPATIAL 2011, EMBO Conference Series, Engelberg (Switzerland), 5th-19th May 2011

Feltrin D, Fluri E, Pertz O, "MAP2K7 local translation allows JNK-dependent neurite outgrowth"

- Abstract accepted for poster presentation at BioValley Life Science Week 2010, Basel, October 2010

Feltrin D, Fluri E, Pertz O, "MAP2K7 local translation allows JNK-dependent neurite outgrowth"

- Abstract accepted for poster presentation at "The cytoskeleton in Development and Pathology", Djurönäset, Stockholm Archipelago, Sweden, 19th-24th June 2010

"Partek Data Analysis Workshop" featuring Partek Genomics Suite Software, University of Basel, Biozentrum, 23rd-25th February 2010

Feltrin D, Fluri E, Pertz O, "Local mRNA Translation During neurite Outgrowth"

- Abstract accepted for poster presentation at BioValley Life Science Week 2009, Basel, October 2009

"Advanced Biomicroscopy" course, 7th-11th September 2009, FMI, Basel

Lim C T, Kola B, **Feltrin D**, Perez-Tilve D, Grossman A B, Tschöp M H, Korbonits M "The Effects of Ghrelin and Cannabinoids on AMP-Activated Protein Kinase (AMPK) Activity in Wild Type and Growth Hormone-Secretagogue Receptor (GHS-R) Knock-Out Animals"

- Abstract published in *Endocrine Abstracts* Volume 19 (*Endocrine Abstracts* ***19*** O22, 2009)

- Abstract accepted for poster presentation by FASEB Summer Research Conference 2008 on 'AMPK: In Sickness and Health From Molecule to Man' in Snekkersten, Denmark, August 2008

- Abstract accepted for poster presentation on William Harvey Research Day, organized by William Harvey Research Institute, Barts and The London 2008 November 2008

"Strumenti e metodiche per la gestione e la valorizzazione dei risultati della ricerca accademica ed industriale" course, Milan, November 2007

Radioactivity safety course, London, Queen Mary University, October 2007

Società Italiana di Endocrinologia meeting, Verona 13rd-17th June 2007

Workshop on Chemoprevention in Oncology "Pharmacological Prevention in Oncology", Gruppo Multimedica, Sesto San Giovanni (MI), Italy, 11th-12th June 2007

INTERESTS, ACTIVITIES & OTHER INFORMATIONS

I love sport, and I enjoy playing football, beach volley and squash. Cycling is my passion and jogging my stress reliever.

I have travelled extensively and I enjoy sightseeing. I enjoy getting in touch with people of other countries and cultures.